Geometric Blow-Up for Folded Limit Cycle Manifolds in Three Time-Scale Systems

S. Jelbart[1] · C. Kuehn[1] · S.-V. Kuntz[1]

Abstract

Geometric singular perturbation theory provides a powerful mathematical framework for the analysis of 'stationary' multiple time-scale systems which possess a *critical manifold*, i.e. a smooth manifold of steady states for the limiting fast subsystem, particularly when combined with a method of desingularisation known as *blow-up*. The theory for 'oscillatory' multiple time-scale systems which possess a limit cycle manifold instead of (or in addition to) a critical manifold is less developed, particularly in the non-normally hyperbolic regime. We use the blow-up method to analyse the global oscillatory transition near a regular folded limit cycle manifold in a class of three time-scale 'semi-oscillatory' systems with two small parameters. The systems considered behave like oscillatory systems as the smallest perturbation parameter tends to zero, and stationary systems as both perturbation parameters tend to zero. The additional time-scale structure is crucial for the applicability of the blow-up method, which cannot be applied directly to the two time-scale oscillatory counterpart of the problem. Our methods allow us to describe the asymptotics and strong contractivity of all solutions which traverse a neighbourhood of the global singularity. Our main results cover a range of different cases with respect to the relative time-scale of the angular dynamics and the parameter drift. We demonstrate the applicability of our results for systems with periodic forcing in the slow equation, in particular for a class of Liénard equations. Finally, we consider a toy model used to study tipping phenomena in climate systems with periodic forcing in the fast equation, which violates the conditions of our main results, in order to demonstrate the applicability of classical (two time-scale) theory for problems of this kind.

Keywords Geometric singular perturbation theory · Global fast–slow systems · Three time-scale systems · Geometric blow-up · Limit cycle bifurcations

✉ S.-V. Kuntz
saraviola.kuntz@ma.tum.de

[1] Department of Mathematics, Technical University of Munich, 85748 Garching, Germany

Mathematics Subject Classification 34D15 · 34E10 · 34E13 · 34E15 · 34E20 · 34C45 · 34C27

1 Introduction

Many physical and applied systems featuring multiple time-scale dynamics can be mathematically modelled by singularly perturbed systems of ordinary differential equations in the standard form

$$
\begin{aligned}
x' &= f(x, y, \varepsilon), \\
y' &= \varepsilon g(x, y, \varepsilon),
\end{aligned}
\tag{1}
$$

where $x \in \mathbb{R}^m$, $y \in \mathbb{R}^n$, $(\cdot)' = \mathrm{d}/\mathrm{d}t$, $0 < \varepsilon \ll 1$ is a small perturbation parameter and the functions $f, g : \mathbb{R}^m \times \mathbb{R}^n \times [0, \varepsilon_0] \to \mathbb{R}^m \times \mathbb{R}^n$ are at least C^1-smooth. If the limiting system obtained from (1) when $\varepsilon \to 0$ possesses a *critical manifold*, i.e. if the set of equilibria $S = \{(x, y) : f(x, y, 0) = 0\}$ forms an n-dimensional submanifold of the phase space $\mathbb{R}^m \times \mathbb{R}^n$, then system (1) can be analysed using a mathematical framework known as *geometric singular perturbation theory (GSPT)* (Fenichel 1979; Jones 1995; Kuehn 2015; Wechselberger 2020). Typical GSPT analyses consist of two parts, depending on whether S is *normally hyperbolic*, i.e. depending on whether the linearisation with respect to the fast variables $D_x f|_S$ when $\varepsilon = 0$ is hyperbolic.

The local dynamics near normally hyperbolic submanifolds of S can be accurately described using *Fenichel–Tikhonov theory* (Fenichel 1979; Tikhonov 1952) (see also Jones 1995; Kuehn 2015; Wechselberger 2020; Wiggins 1994), which ensures that solutions are well approximated by regular perturbations of singular trajectories constructed as concatenations of trajectory segments from the distinct limiting problems which arise when $\varepsilon \to 0$ in system (1) on the fast and slow time-scales t and $\tau = \varepsilon t$, respectively. However, Fenichel–Tikhonov theory breaks down in the non-normally hyperbolic regime. The dynamics near non-normally hyperbolic points or submanifolds of S, which generically correspond to bifurcations in the layer problem $(1)|_{\varepsilon=0}$, can be studied using various techniques. A particularly powerful approach is the so-called *blow-up method*, which was pioneered for fast–slow systems in Dumortier and Roussarie (1996) and later in Krupa and Szmolyan (2001a), Krupa and Szmolyan (2001b), Krupa and Szmolyan (2001c). In these works and many others (see Jardón-Kojakhmetov and Kuehn 2021 for a recent survey), the authors showed that the loss of hyperbolicity at a non-normally hyperbolic point or submanifold Q can often be 'resolved' after lifting the problem to a higher-dimensional space in which Q is blown-up to a higher-dimensional manifold $\mathcal{Q}$. Following a suitable *desingularisation*, which amounts to a singular transformation of time, a non-trivial vector field with improved hyperbolicity properties can be identified on $\mathcal{Q}$. This allows one to study the dynamics in the non-normally hyperbolic regime using classical dynamical systems methods like regular perturbation and centre manifold theory. We refer to Kosiuk and Szmolyan (2009), Kosiuk and Szmolyan (2011), Kosiuk and Szmolyan (2016), Kristiansen and Szmolyan (2021), Krupa and Szmolyan (2001a), Krupa and Szmolyan (2001b), Krupa and Szmolyan (2001c), Kuehn and Szmolyan (2015), Szmolyan and Wechselberger

(2001), Szmolyan and Wechselberger (2004) for seminal works in both applied and theoretical contexts, based on this combination of Fenichel–Tikhonov theory and the blow-up method.

The mathematical theory and methods described above are local in the sense that they apply specifically to fast–slow systems possessing an n-dimensional critical manifold S. A corresponding global theory in which the layer problem $(1)|_{\varepsilon=0}$ possesses a limit cycle manifold in place of (or in addition to) a critical manifold is less developed. Following Il'yashenko (1997), we shall refer to the former class as *stationary* fast–slow systems and the latter class as *oscillatory* fast–slow systems. A program for the development of a global GSPT which is general enough to encompass oscillatory fast–slow systems was initiated by Guckenheimer (1996); however, a number of key analytical and methodological obstacles to its development remain.

One such obstacle concerns the development of Fenichel–Tikhonov theory for oscillatory fast–slow systems. A number of authors have made important contributions in this direction. Anosova showed that normally hyperbolic limit cycle manifolds in oscillatory fast–slow systems of form (1) persist as $O(\varepsilon)$-close locally invariant manifolds for the perturbed system (Anosova 1999, 2002), similarly to the persistence of a normally hyperbolic critical manifold in Fenichel–Tikhonov theory. For oscillatory fast–slow systems with one slow variable, the persistence and contractivity properties of the centre-stable/unstable manifolds have been described in detail in Jelbart and Kuehn (2023) using properties of the Poincaré map and a discrete GSPT framework developed therein. This study also yielded an asymptotic formula for the slow drift along the manifold, which agrees with the formula predicted by classical averaging theory (Pontryagin and Rodygin 1960).

Global theory for oscillatory fast–slow systems in the non-normally hyperbolic regime is less developed, despite the ubiquity of fast–slow extensions of global bifurcations in applications, for example in biochemical models exhibiting *bursting* (Bertram et al. 1995; Ermentrout and Terman 2010; Guckenheimer et al. 2005; Rinzel 1987). Notable exceptions include the study of a dynamic saddle-node of cycles bifurcation in a variant of the FitzHugh–Nagumo equations in Kirillov and Nekorkin (2015), and the rigorous topological classification of so-called *torus canards* in Vo (2017), which occur near folded cycle bifurcations in the layer problem in oscillatory fast–slow systems (Vo 2017). See e.g. Baspinar et al. (2021), Benes et al. (2011), Desroches et al. (2012), Kramer et al. (2008), Roberts et al. (2015)) for more (predominantly numerical) important work on torus canards. The results in Vo (2017) were obtained using averaging theory, Floquet theory and (stationary) GSPT. Indirect contributions to the non-normally hyperbolic theory for oscillatory fast–slow systems have also been made via the study of non-normally hyperbolic singularities in fast–slow maps, since these can be used to infer dynamical properties of corresponding limit cycle bifurcations (or fast–slow extensions thereof) in one greater dimension. The slow passage through a flip/period-doubling bifurcation (and even through an entire period-doubling cascade) was treated in Baesens (1991, 1995), and further results on the slow passage through discrete transcritical, pitchfork and Neimark–Sacker/torus-type bifurcations have been derived using non-standard analysis; we refer to the review paper (Fruchard and Schäfke 2009) and the references therein.

In general, the development of mathematical methods for handling non-hyperbolic dynamics in oscillatory fast–slow systems is complicated by the fact that local techniques like the blow-up method rely upon near-equilibrium properties possessed by stationary but not oscillatory fast–slow systems. The desingularisation step in blow-up analyses, for example, relies upon a formal division of the blown-up vector field by zero. This step is crucial for obtaining a desingularised vector field with improved hyperbolicity properties, but it is only well-defined if the original (blown-up) vector field is in equilibrium wherever it is formally divided by zero. For oscillatory fast–slow systems of form (1), a 'typical' non-normally hyperbolic cycle has non-equilibrium dynamics, so it cannot be desingularised and the blow-up method does not apply.

The aim of this work is to show that stationary methods (in particular the blow-up method) which may not apply for oscillatory fast–slow systems, may be applicable in the study of oscillatory multiple time-scale systems with at least three distinct time-scales. Specifically, we consider systems of the form

$$
\begin{aligned}
r' &= f(r, \theta, y, \varepsilon_1, \varepsilon_2), \\
\theta' &= \varepsilon_1 g(r, \theta, y, \varepsilon_1, \varepsilon_2), \\
y' &= \varepsilon_2 h(r, \theta, y, \varepsilon_1, \varepsilon_2),
\end{aligned}
\tag{2}
$$

where $(r, \theta, y) \in \mathbb{R}_{\geq 0} \times \mathbb{R}/\mathbb{Z} \times \mathbb{R}$ are cylindrical coordinates, $0 < \varepsilon_1, \varepsilon_2 \ll 1$ are singular perturbation parameters, and $f, g, h : \mathbb{R}_{\geq 0} \times \mathbb{R}/\mathbb{Z} \times \mathbb{R} \times [0, \varepsilon_{1,0}] \times [0, \varepsilon_{2,0}] \to \mathbb{R}$ are sufficiently smooth for our purposes. Depending upon the relative magnitude of ε_1 and ε_2, system (2) has either two or three distinct time-scales. Although we present results on a range of different cases, we are primarily interested in the case

$$
0 < \varepsilon_2 \ll \varepsilon_1 \ll 1,
\tag{3}
$$

which defines a class of three time-scale *semi-oscillatory* systems that are in a certain sense 'in between' the classes of stationary and oscillatory fast–slow systems described above. Heuristically, this is because under suitable assumptions (to be outlined in detail in Sect. 2), system (2) is an oscillatory fast–slow system with respect to the limit $\varepsilon_1 > 0, \ \varepsilon_2 \to 0$, and a stationary fast–slow system with respect to the double singular limit $(\varepsilon_1, \varepsilon_2) \to (0, 0)$ (Kuehn et al. 2022). It is worthy to note that multiple time-scale systems with more than two time-scales appear frequently in applications. The long-term dynamics of a forced van der Pol oscillator with three time-scales was studied as early as 1947 in Cartwright and Littlewood (1947). A theoretical basis for normally hyperbolic theory for stationary multiple time-scale systems with three or more time-scales has appeared more recently in e.g. Cardin et al. (2014), Cardin and Teixeira (2017), Kruff and Walcher (2019), Lizarraga et al. (2021). Progress has also been made in the non-normally hyperbolic setting, particularly via the study of three time-scale applications and 'prototypical systems' inspired by applications; we refer to De Maesschalck et al. (2014), Desroches and Kirk (2018), Jalics et al. (2010), Kaklamanos and Popović (2022), Kaklamanos et al. (2022), Kaklamanos et al. (2023), Krupa et al. (2008), Letson et al. (2017), Nan et al. (2015).

We present a detailed analysis of the 'jump-type' transition near a non-normally hyperbolic cycle of regular fold type using geometric blow-up. More precisely, we assume that the limiting system $(2)_{\varepsilon_1 > 0, \varepsilon_2 = 0}$ undergoes a type of folded cycle bifurcation under variation in y which is common in applications with periodic forcing in the slow equation. This global bifurcation is closely related to (and can in many ways be seen as an oscillatory analogue to) the regular fold or jump point in stationary fast–slow systems, which has been studied in $\mathbb{R}^2$ and $\mathbb{R}^3$ in particular using blow-up techniques in Krupa and Szmolyan (2001a), Szmolyan and Wechselberger (2004); see also Mishchenko et al. (1975) for a detailed treatment of the planar case using classical asymptotic methods. After deriving a prototypical system by imposing a number of defining assumptions on system (2), we show that the blow-up method can be applied, even though a rigorous reduction to the stationary setting is not possible due to angular coupling. The formal division by zero which is necessary to obtain a desingularised vector field with improved hyperbolicity properties is possible if the time-scale associated to the rotation is sufficiently slow relative to the fast radial dynamics, i.e. if ε_1 is sufficiently small.

The blow-up analysis allows for the detailed characterisation of the transition map induced by the flow, including the asymptotic and contractivity properties of the transition undergone by solutions traversing the neighbourhood of the global singularity. If $\varepsilon_2/\varepsilon_1 \sim 1$ or $\varepsilon_2/\varepsilon_1 \gg 1$ (so that (3) is not satisfied), then system (2) is a stationary fast–slow system. In this case, the local dynamics can (for the most part) be described in detail using the results established for two time-scale systems in Krupa and Szmolyan (2001a), Mishchenko et al. (1975), Szmolyan and Wechselberger (2004), after Taylor expansion about a given jump point. However, these results do not apply directly to the scaling regimes we consider which satisfy (3), i.e. they do not apply in the semi-oscillatory case. One important reason for this is that the singularity is 'global' in the angular coordinate θ. Consequently, it does not suffice to blow-up at a single point on the non-hyperbolic cycle. Rather, it is necessary to blow-up the entire non-hyperbolic cycle to a 'torus of spheres' $S^1 \times S^2$. A similar approach is adopted in the geometric analysis of the periodically forced van der Pol equation in Burke et al. (2016); however, in our case, the leading-order equations derived on the blown-up sphere may depend upon the angular variable θ, which remains non-local. As a consequence, the local dynamics cannot be analysed with a straightforward adaptation of the arguments used to study the dynamics near a regular fold point/curve in Krupa and Szmolyan (2001a), Szmolyan and Wechselberger (2004). Rather, new arguments are needed. We derive results for two different scaling regimes defined by $(\varepsilon_1, \varepsilon_2) = (\varepsilon^\alpha, \varepsilon^3)$, where $\alpha \in \{1, 2\}$ and $0 < \varepsilon \ll 1$. In each case, the size of the leading-order term in the asymptotics for the parameter drift in y is shown to agree with the known results for the stationary regular fold point (Krupa and Szmolyan 2001a; Szmolyan and Wechselberger 2004). In contrast to the classical fold, however, the leading-order coefficient is shown to depend on θ, and we provide an explicit formula for this dependence in the case $\alpha = 2$. We also provide asymptotics for the angular coordinate θ as a function of the initial conditions and small parameters, and an asymptotic estimate for the number of rotations about the y-axis over the course of the transition. The results obtained are shown to depend on the relative magnitude of ε_1 and ε_2 (i.e. on α), with the main qual-

itative difference pertaining to the asymptotic estimates for θ and the corresponding number of rotations.

Finally, we apply our results in order to derive detailed asymptotic information near folded limit cycle manifolds of periodically forced Liénard equations, and we consider a simple model proposed in Zhu et al. (2015) as a toy model for the study of tipping phenomena in climate systems. Our main results do not apply directly to the latter problem, due to periodic forcing in the fast equation. Rather, we aim to demonstrate with a partial but illustrative geometric analysis that problems of this kind can be treated using classical approaches based on established results for two time-scale systems.

The manuscript is structured as follows. In Sect. 2 we introduce defining assumptions and present the prototypical system for which our main results are stated. The singular dynamics and geometry, which differ in different scalings, are presented in Sect. 2.1. The main results are presented and described in Sect. 3, and the blow-up analysis and proof of the main results are presented in Sect. 4. The applications are treated in Sect. 5. Specifically, in Sect. 5.1 we apply our main results to periodically forced Liénard equations, and in Sect. 5.2 we consider the toy model for the study of tipping phenomena from Zhu et al. (2015) which cannot be treated directly with the results from Sect. 3. We conclude with a summary and outlook in Sect. 6.

2 Assumptions and Setting

We consider C^k-smooth multiple time-scale systems in the general form (2), restated here for convenience:

$$
\begin{aligned}
r' &= f(r, \theta, y, \varepsilon_1, \varepsilon_2), \\
\theta' &= \varepsilon_1 g(r, \theta, y, \varepsilon_1, \varepsilon_2), \\
y' &= \varepsilon_2 h(r, \theta, y, \varepsilon_1, \varepsilon_2),
\end{aligned}
\tag{4}
$$

where $k \in \mathbb{N}$ will be assumed to be 'sufficiently large' throughout, $(\cdot)' = \mathrm{d}/\mathrm{d}t$, the variables are given in cylindrical coordinates $(r, \theta, y) \in \mathbb{R}_{\geq 0} \times \mathbb{R}/\mathbb{Z} \times \mathbb{R}$, and $\varepsilon_1, \varepsilon_2$ are singular perturbation parameters satisfying $0 < \varepsilon_1, \varepsilon_2 \ll 1$. Note also that smoothness implies that f, g, h are 1-periodic in θ. System (4) evolves on either two or three time-scales, depending on whether the ratio $\varepsilon_1/\varepsilon_2$ is asymptotically large, constant or small. The setup and defining assumptions presented below are primarily motivated by the case $0 < \varepsilon_2 \ll \varepsilon_1 \ll 1$, for which system (4) in a certain sense 'intermediate' between stationary and oscillatory fast–slow systems. We shall refer to this as the *semi-oscillatory* case. Since we also consider other possibilities, however, we leave the exact relation between ε_1 and ε_2 unspecified for now. It suffices to observe that the forward evolution of a generic initial condition is characterised by radial motion on the fast time-scale t, angular motion on a time-scale $\tau_{\varepsilon_1} = \varepsilon_1 t$, and vertical 'parameter drift' on a time-scale $\tau_{\varepsilon_2} = \varepsilon_2 t$.

In the following we impose a number of defining conditions in terms of the limiting oscillatory fast–slow system obtained in the singular limit $\varepsilon_1 > 0$, $\varepsilon_2 \to 0$, i.e. on

$$
\begin{aligned}
r' &= f(r, \theta, y, \varepsilon_1, 0), \\
\theta' &= \varepsilon_1 g(r, \theta, y, \varepsilon_1, 0), \\
y' &= 0.
\end{aligned}
\tag{5}
$$

We remark that the singular limit $\varepsilon_1 > 0$, $\varepsilon_2 \to 0$ is only 'natural' in the semi-oscillatory case, i.e. if $\varepsilon_1/\varepsilon_2 \gg 1$ so that the rotation is fast relative to the parameter drift.

Assumption 1 (*Existence of a limit cycle for $\varepsilon_1 > 0$, $\varepsilon_2 \to 0$*). There exist a constant $\varepsilon_{1,0} > 0$ and a constant $v > 0$ such that system (5) has a circular limit cycle

$$
S_0^c = \{(v, \theta, 0) : \theta \in \mathbb{R}/\mathbb{Z}\}.
$$

More precisely, we assume that

$$
f(v, \theta, 0, \varepsilon_1, 0) = 0, \qquad g(v, \theta, 0, \varepsilon_1, 0) \neq 0,
\tag{6}
$$

for all $\theta \in \mathbb{R}/\mathbb{Z}$ and $\varepsilon_1 \in (0, \varepsilon_{1,0})$.

Remark 2.1 The assumption that the limit cycle S_0^c is circular and in particular the zero condition on f in (6), is natural in applications with small-amplitude external periodic forcing (amplitudes of $\mathcal{O}(\varepsilon_2)$ or smaller). However, it rules out applications with 'large' periodic forcing in the fast equation for r. One reason for imposing such a restriction is that problems of the latter kind can often be treated using classical theory for two time-scale systems. This is demonstrated for a particular application in Sect. 5.2.

We shall be interested in the dynamics in a neighbourhood of S_0^c. This motivates the introduction of the signed radius variable

$$
\tilde{r} := r - v,
$$

in which case $S_0^c = \{(\tilde{r}, \theta, y) : \tilde{r} = 0, \theta \in \mathbb{R}/\mathbb{Z}, y = 0\}$. We assume without loss of generality that

$$
g(v, \theta, 0, \varepsilon_1, 0) > 0,
$$

divide the right-hand side of system (4) by $g(\tilde{r} + v, \theta, y, \varepsilon_1, \varepsilon_2)$, i.e. we apply a time-dependent transformation satisfying $\mathrm{d}\tilde{t} = g(r, \theta, y, \varepsilon_1, \varepsilon_2)\mathrm{d}t$ (which is positive in a sufficiently small toroidal or tubular neighbourhood $\mathcal{V}$ of S_0^c), and rewrite the system in $(\tilde{r}, \theta, y)$-coordinates in order to obtain

$$
\begin{aligned}
\tilde{r}' &= F(\tilde{r}, \theta, y, \varepsilon_1, \varepsilon_2), \\
\theta' &= \varepsilon_1, \\
y' &= \varepsilon_2 H(\tilde{r}, \theta, y, \varepsilon_1, \varepsilon_2),
\end{aligned}
\tag{7}
$$

where by a slight abuse of notation the dash now denotes differentiation with respect to $\tilde{t}$, and

$$F(\tilde{r},\theta,y,\varepsilon_1,\varepsilon_2):=\frac{f(\tilde{r}+v,\theta,y,\varepsilon_1,\varepsilon_2)}{g(\tilde{r}+v,\theta,y,\varepsilon_1,\varepsilon_2)}, \quad H(\tilde{r},\theta,y,\varepsilon_1,\varepsilon_2):=\frac{h(\tilde{r}+v,\theta,y,\varepsilon_1,\varepsilon_2)}{g(\tilde{r}+v,\theta,y,\varepsilon_1,\varepsilon_2)}.$$

Remark 2.2 In the derivation of system (7) and in many of the proofs below we make use of transformations of time which are formulated in terms of differentials, e.g. $\mathrm{d}\tilde{t} = g(r,\theta,y,\varepsilon_1,\varepsilon_2)\mathrm{d}t$. Strictly speaking, such an 'transformation' only defines $\tilde{t}$ as a unique function of t up to an additive constant. Since we are interested in the behaviour of solutions to autonomous ODEs, which are invariant under time translation, this additive constant can be set to zero without loss of generality.

We are interested in three time-scale systems (7) which feature a regular fast–slow fold of limit cycles with respect to the partial singular limit $\varepsilon_1 > 0$, $\varepsilon_2 \to 0$. Necessary and sufficient conditions for this to occur can be given in terms of the Poincaré map induced on the transversal section Δ obtained by intersecting the toroidal/tubular neighbourhood $\mathcal{V} \supset S_0^c$ with the half-plane defined by $\theta = 0$ (decreasing the size of $\mathcal{V}$ if necessary).

Proposition 2.3 *System* (7) *with* $\varepsilon_1 \in (0,\varepsilon_{1,0})$ *fixed and* $0 < \varepsilon_2 \ll 1$ *induces a Poincaré map* $P : \Delta \to \Delta$ *given by*

$$\begin{aligned}
P(\tilde{r}, y, \varepsilon_1, \varepsilon_2) &= \begin{pmatrix} P_{\tilde{r}}(\tilde{r}, y, \varepsilon_1, \varepsilon_2) \\ P_y(\tilde{r}, y, \varepsilon_1, \varepsilon_2) \end{pmatrix} \\
&= \begin{pmatrix} \tilde{r} \\ y \end{pmatrix} + \varepsilon_1^{-1} \begin{pmatrix} \int_0^1 F(\tilde{r}(\theta),\theta,y(\theta),\varepsilon_1,0)\,\mathrm{d}\theta + O(\varepsilon_2) \\ \varepsilon_2 \int_0^1 H(\tilde{r}(\theta),\theta,y(\theta),\varepsilon_1,0)\,\mathrm{d}\theta + O(\varepsilon_2^2) \end{pmatrix}. \quad (8)
\end{aligned}$$

Proof Since

$$\frac{\mathrm{d}\tilde{r}}{\mathrm{d}\theta} = \varepsilon_1^{-1}F(\tilde{r},\theta,y,\varepsilon_1,\varepsilon_2), \qquad \frac{\mathrm{d}y}{\mathrm{d}\theta} = \varepsilon_1^{-1}\varepsilon_2 H(\tilde{r},\theta,y,\varepsilon_1,\varepsilon_2),$$

we have

$$\begin{aligned}
P(\tilde{r}, y, \varepsilon_1, \varepsilon_2) &= \begin{pmatrix} P_{\tilde{r}}(\tilde{r}, y, \varepsilon_1, \varepsilon_2) \\ P_y(\tilde{r}, y, \varepsilon_1, \varepsilon_2) \end{pmatrix} \\
&= \begin{pmatrix} \tilde{r} \\ y \end{pmatrix} + \varepsilon_1^{-1} \begin{pmatrix} \int_0^1 F(\tilde{r}(\theta),\theta,y(\theta),\varepsilon_1,\varepsilon_2)\,\mathrm{d}\theta \\ \varepsilon_2 \int_0^1 H(\tilde{r}(\theta),\theta,y(\theta),\varepsilon_1,\varepsilon_2)\,\mathrm{d}\theta \end{pmatrix}.
\end{aligned}$$

The result follows after Taylor expanding about $\varepsilon_2 = 0$.   □

The defining conditions for S_0^c to be a regular fast–slow fold of cycles are as follows:

$$P_{\tilde{r}}(0,0,\varepsilon_1,0) = 0, \qquad \frac{\partial P_{\tilde{r}}}{\partial \tilde{r}}(0,0,\varepsilon_1,0) = 1, \qquad (9)$$

together with

$$\frac{\partial^2 P_{\tilde{r}}}{\partial \tilde{r}^2}(0, 0, \varepsilon_1, 0) \neq 0, \qquad \frac{\partial P_{\tilde{r}}}{\partial y}(0, 0, \varepsilon_1, 0) \neq 0,$$

$$\int_0^1 H(\tilde{r}(\theta), \theta, y(\theta), \varepsilon_1, 0) \, \mathrm{d}\theta \neq 0, \tag{10}$$

for all $\varepsilon_1 \in (0, \varepsilon_{1,0})$. The conditions in (9)–(10) are in 1-1 correspondence with the defining conditions for a fold bifurcation in the 1D 'layer map' $\tilde{r} \mapsto \tilde{r} + P_{\tilde{r}}(\tilde{r}, y, \varepsilon_1, 0)$ (with y as a bifurcation parameter), see e.g. Kuznetsov (2013, Ch. 4.3), except for the integral condition, which can be viewed as the analogue of the slow regularity condition on the fast–slow regular fold point in planar continuous-time systems in Krupa and Szmolyan (2001a), Kuehn (2015).

Remark 2.4 The defining conditions for a regular fast–slow fold of cycles in (9)–(10) do not depend on the specific form of the Poincaré map in (8). Nevertheless, we have chosen to state Proposition 2.3 prior to the conditions in (9)–(10) in order to clarify the interpretation of the slow regularity condition, i.e. the integral expression in (10), which is not common in the literature. This condition can be viewed as a condition on the 'reduced map'; we refer to Jelbart and Kuehn (2023), Jelbart and Kuehn (2023) for details.

In the following, we shall actually assume stronger conditions that are sufficient but not necessary for a regular fast–slow fold of cycles, instead of those in (9)–(10). Similarly to Assumption 1, these conditions are expected to be satisfied in applications with small-amplitude external periodic forcing; see again Remark 2.1.

Assumption 2 (*Sufficient conditions for S_0^c to be a regular folded cycle*) The following sufficient (but not necessary) conditions for a fast–slow fold of cycles are satisfied by system (7):

$$F(0, \theta, 0, \varepsilon_1, 0) = 0, \qquad \frac{\partial F}{\partial \tilde{r}}(0, \theta, 0, \varepsilon_1, 0) = 0, \tag{11}$$

together with

$$\frac{\partial^2 F}{\partial \tilde{r}^2}(0, \theta, 0, \varepsilon_1, 0) \neq 0, \qquad \frac{\partial F}{\partial y}(0, \theta, 0, \varepsilon_1, 0) \neq 0, \qquad H(0, \theta, 0, \varepsilon_1, 0) \neq 0, \tag{12}$$

for all $\theta \in \mathbb{R}/\mathbb{Z}$ and $\varepsilon_1 \in (0, \varepsilon_{1,0})$.

It is straightforward to verify that the conditions in (11)–(12) are sufficient to ensure that the Poincaré map (8) satisfies the fold conditions (9)–(10). In particular, (11)–(12) are directly analogous to the defining conditions for the (stationary) regular fold point in Krupa and Szmolyan (2001a), except that we require them to hold for θ-dependent functions.

Assumptions 1–2 and the implicit function theorem imply that system (5) has a two-dimensional manifold of regular limit cycles

$$S_0 = \{(r, \theta, y) \in \mathcal{V} : F(\tilde{r}, \theta, y, \varepsilon_1, 0) = 0\},$$

where $\mathcal{V} \subseteq \mathbb{R}_{\geq 0} \times \mathbb{R}/\mathbb{Z} \times \mathbb{R}$ is the toroidal/tubular neighbourhood about S_0^c introduced above. In other words, system (7) (and by a simple computation also system (4)) is an oscillatory fast–slow system with respect to the (partial) singular limit $\varepsilon_1 > 0$, $\varepsilon_2 \to 0$.

The combination of signs taken by the various nonzero terms in (12) determines the orientation of the bifurcation. In the following we assume without loss of generality that

$$\frac{\partial^2 F}{\partial \tilde{r}^2}(0, \theta, 0, \varepsilon_1, 0) > 0, \qquad \frac{\partial F}{\partial y}(0, \theta, 0, \varepsilon_1, 0) < 0, \qquad H(0, \theta, 0, \varepsilon_1, 0) < 0,$$

(13)

which are consistent with a 'jump-type' orientation in forward time; see Figs. 1 and 2. Based on Assumptions 1–2 and these sign conventions, it suffices to work with the simplified system provided in the following result.

Proposition 2.5 *Let Assumptions 1–2 be satisfied and assume that $0 < \varepsilon_1, \varepsilon_2 \ll 1$. In a sufficiently small toroidal/tubular neighbourhood about S_0^c, which we continue to denote by $\mathcal{V}$, system (7) can be written as*

$$\begin{aligned}
\tilde{r}' &= -a(\theta)y + b(\theta)\tilde{r}^2 + \mathcal{R}_r(\tilde{r}, \theta, y, \varepsilon_1, \varepsilon_2), \\
\theta' &= \varepsilon_1, \\
y' &= \varepsilon_2(-c(\theta) + \mathcal{R}_y(\tilde{r}, \theta, y, \varepsilon_1, \varepsilon_2)),
\end{aligned}$$

(14)

where the functions $a(\theta), b(\theta), c(\theta)$ are positive, 1-periodic and smooth, and the higher-order terms satisfy

$$\begin{aligned}
\mathcal{R}_r(\tilde{r}, \theta, y, \varepsilon_1, \varepsilon_2) &= \mathcal{O}(\tilde{r}^3, y^2, \tilde{r}y, \varepsilon_1\tilde{r}^2, \varepsilon_1 y, \varepsilon_2), \\
\mathcal{R}_y(\tilde{r}, \theta, y, \varepsilon_1, \varepsilon_2) &= \mathcal{O}(\tilde{r}, y, \varepsilon_1, \varepsilon_2).
\end{aligned}$$

Proof Consider system (7) under Assumptions 1–2. Taylor expanding about $\tilde{r} = y = \varepsilon_2 = 0$, we obtain

$$\begin{aligned}
\tilde{r}' &= -f_1(\theta, \varepsilon_1)y + f_2(\theta, \varepsilon_1)\tilde{r}^2 + \mathcal{O}(\tilde{r}^3, y^2, \tilde{r}y, \varepsilon_2), \\
\theta' &= \varepsilon_1, \\
y' &= \varepsilon_2(-h_0(\theta, \varepsilon_1) + \mathcal{O}(\tilde{r}, y, \varepsilon_2)),
\end{aligned}$$

where $f_1(\theta, \varepsilon_1)$, $f_2(\theta, \varepsilon_1)$ and $h_0(\theta, \varepsilon_1)$ are smooth, 1-periodic in θ and positive (this follows from the sign conventions in (13)). Expanding $f_1(\theta, \varepsilon_1)$, $f_2(\theta, \varepsilon_1)$ and $h_0(\theta, \varepsilon_1)$ about $\varepsilon_1 = 0$ and setting

$$a(\theta) := f_1(\theta, 0), \qquad b(\theta) := f_2(\theta, 0), \qquad c(\theta) := h_0(\theta, 0),$$

yields system (14). □

System (14) is related to the local normal form for the regular fold point in Krupa and Szmolyan (2001a) by a simple variable rescaling if $\varepsilon_1 = 0$, i.e. if θ is fixed. For $\varepsilon_1 > 0$, however, the dependence on the angular variable appears via the functions $a(\theta), b(\theta), c(\theta)$ and the higher-order terms $\mathcal{R}_r(\tilde{r}, \theta, y, \varepsilon_1, \varepsilon_2)$ and $\mathcal{R}_y(\tilde{r}, \theta, y, \varepsilon_1, \varepsilon_2)$. In what follows, we drop the tilde notation on $\tilde{r}$ and work with system (14) for the remainder of this manuscript.

Remark 2.6 In Proposition 2.5 we assert that the functions $a(\theta), b(\theta)$ and $c(\theta)$ are 'smooth'. A more precise statement would be to say that they are C^k-smooth, since the system obtained after Taylor expansion is precisely as smooth as the original system (7). Since we will not be interested in smoothness per se, we shall adopt a similar terminology throughout for simplicity, i.e. by 'smooth' we shall mean sufficiently smooth for the validity of our methods (e.g. Taylor expansions).

Remark 2.7 The equation for $\tilde{r}$ in system (14) can be further simplified after setting $\widehat{r} = \sqrt{b(\theta)/a(\theta)}\,\tilde{r}$. This leads to

$$\widehat{r}' = \iota(\theta)\left(-y + \widehat{r}^2\right) + \frac{1}{2}\frac{a(\theta)b'(\theta) - a'(\theta)b(\theta)}{\iota(\theta)^2}\varepsilon_1\widehat{r} + h.o.t.,$$

where $a' := \partial a/\partial\theta$, $b' := \partial b/\partial\theta$ and $\iota(\theta) := \sqrt{a(\theta)b(\theta)}$. The 'price' of this simplification, however, is that the $\mathcal{O}(\varepsilon_1\widehat{r})$ term also appears in the leading-order terms in the blow-up analysis in later sections. For this reason, we continue to work with the formulation in (14).

Remark 2.8 If $\varepsilon_1 \sim \varepsilon_2$ or $\varepsilon_1 \ll \varepsilon_2$, then the θ-variable is 'slow enough' to validate the Taylor expansion of system (14) about a fixed point $(0, \theta^*, 0) \in S_0^c$, i.e. in this case, one can also Taylor expand in the angular coordinate θ. This allows for a subsequent transformation into the simpler local normal form near a fold curve in Szmolyan and Wechselberger (2004, Lem. 3), thereby showing that the dynamics in these cases are governed by the well-known result for two time-scale systems in Szmolyan and Wechselberger (2004, Thm. 1). In the semi-oscillatory case of interest with $\varepsilon_2 \ll \varepsilon_1$, however, θ is fast relative to y and varies over the entire domain $\mathbb{R}/\mathbb{Z}$ as solutions approach S_0^c. As a consequence, one cannot Taylor expand the θ coordinate, and transformation to the local normal form in Szmolyan and Wechselberger (2004) is not possible.

Remark 2.9 In order to sketch geometric objects like S_0 in the upcoming figures, we choose the positive, 1-periodic and smooth functions $a(\theta) = 2 + \sin(4\pi\theta)$ and $b(\theta) = 5 + \cos(2\pi\theta - 1)$. For constant functions a and b, the figures including the θ-coordinate would be rotationally symmetric.

2.1 Geometry and Dynamics in the Singular Limit

We turn now to the singular geometry and dynamics of system (14). Taking the double singular limit $(\varepsilon_1, \varepsilon_2) \to (0, 0)$ yields the *layer problem*

$$
\begin{aligned}
r' &= -a(\theta)y + b(\theta)r^2 + \mathcal{R}_r(r, \theta, y, 0, 0), \\
\theta' &= 0, \\
y' &= 0,
\end{aligned}
\tag{15}
$$

which has a two-dimensional *critical manifold*

$$
S_0 := \{(r, \theta, \varphi_0(r, \theta)) : r \in I_r, \theta \in \mathbb{R}/\mathbb{Z}\},
$$

where $I_r := (-r_0, r_0)$ for a small but fixed $r_0 > 0$ and

$$
y = \varphi_0(r, \theta) = \frac{b(\theta)}{a(\theta)}r^2 + \mathcal{O}(r^3)
$$

solves the equation $F(r, \theta, y, 0, 0) = -a(\theta)y + b(\theta)r^2 + \mathcal{R}_r(r, \theta, y, 0, 0) = 0$ locally via the implicit function theorem.

The stability of S_0 with respect to the fast radial dynamics is determined by the unique non-trivial (i.e. not identically zero) eigenvalue of the linearisation, namely

$$
\lambda(r, \theta) = \left. \frac{\partial}{\partial r} \left(-a(\theta)y + b(\theta)r^2 + \mathcal{R}_r(r, \theta, y, 0, 0) \right) \right|_{S_0} = 2b(\theta)r + \mathcal{O}(r^2).
$$

It follows that the critical manifold has the structure $S_0 = S_0^{\mathrm{a}} \cup S_0^{\mathrm{c}} \cup S_0^{\mathrm{r}}$, where

$$
S_0^{\mathrm{a}} = \{(r, \theta, \varphi_0(r, \theta)) \in S_0 : r < 0\}, \qquad S_0^{\mathrm{r}} = \{(r, \theta, \varphi_0(r, \theta)) \in S_0 : r > 0\},
$$

are normally hyperbolic and attracting/repelling, respectively (assuming $r_0 > 0$ is sufficiently small). The circular set $S_0^{\mathrm{c}} = \{(0, \theta, 0) \in S_0\}$, which corresponds to the regular folded cycle in Assumption 2, is non-normally hyperbolic. The situation is sketched in Figs. 1 and 2.

The dynamics and geometry for the layer problem (15) do not depend upon the relative magnitude of ε_1 and ε_2. The reduced dynamics on S_0, however, are expected to differ significantly depending on the size of $\varepsilon_1/\varepsilon_2$. As noted already in Sect. 1, we consider three distinct possibilities:

(C1) Angular dynamics are fast relative to the parameter drift, i.e.
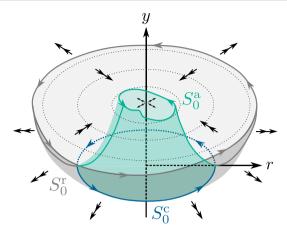
$$
\frac{\varepsilon_1}{\varepsilon_2} \gg 1.
$$

Fig. 1 Singular geometry and dynamics in case (C1). Fast and slow dynamics are depicted (here and throughout) by double and single arrows, respectively. The attracting and repelling normally hyperbolic submanifolds of the critical manifold S_0, denoted by S_0^a and S_0^r, are shown in shaded turquoise and grey, respectively, and sketched for the particular choice of $a(\theta)$ and $b(\theta)$ defined in Remark 2.9. The non-normally hyperbolic folded cycle S_0^c is shown in blue. The reduced flow in case (C1) is periodic, i.e. y is a parameter and S_0 is foliated by limit cycles of period $\tau_{\varepsilon_1} = 1$ (Color figure online)
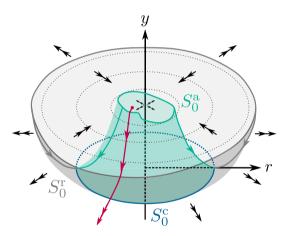

Fig. 2 Singular geometry and dynamics in case (C3) sketched for the particular choice of $a(\theta)$ and $b(\theta)$ in Remark 2.9. The dynamics is distinguished from cases (C1) and (C2) by the reduced flow on S_0. In this case, θ is a parameter and singular orbits (concatenations of solution segments of layer and reduced problem) are contained within constant angle planes $\{\theta = const.\}$. An example of such an orbit is sketched in red (Color figure online)

(C2) Angular dynamics occur on the same time-scale as the parameter drift, i.e. there is a constant $\sigma > 0$ such that

$$\frac{\varepsilon_1}{\varepsilon_2} = \sigma.$$

(C3) Angular dynamics are slow relative to the parameter drift, i.e.

$$\frac{\varepsilon_1}{\varepsilon_2} \ll 1.$$

A different reduced problem is obtained on S_0 in each case. We briefly consider each case in turn.

The Reduced Problem in Case (C1)

In this case we rewrite system (14) on the slow time-scale $\tau_{\varepsilon_1} = \varepsilon_1 t$. This leads to

$$
\begin{aligned}
\varepsilon_1 \dot{r} &= -a(\theta)y + b(\theta)r^2 + \mathcal{R}_r(r, \theta, y, \varepsilon_1, \varepsilon_2), \\
\dot{\theta} &= 1, \\
\dot{y} &= \frac{\varepsilon_2}{\varepsilon_1}(-c(\theta) + \mathcal{R}_y(r, \theta, y, \varepsilon_1, \varepsilon_2)),
\end{aligned}
\tag{16}
$$

where the dot denotes differentiation with respect to the slow time τ_{ε_1}. Since $\varepsilon_1/\varepsilon_2 \gg 1$, we first take $\varepsilon_2 \to 0$, and then $\varepsilon_1 \to 0$ (in that order). This leads to the reduced problem

$$
\begin{aligned}
0 &= -a(\theta)y + b(\theta)r^2 + \mathcal{R}_r(r, \theta, y, 0, 0), \\
\dot{\theta} &= 1, \\
\dot{y} &= 0.
\end{aligned}
\tag{17}
$$

In this case, S_0 is foliated by limit cycles of period $\tau_{\varepsilon_1} = 1$, i.e. $t = 1/\varepsilon_1$. An expression for the vector field on S_0, expressed in the (r, θ)-coordinate chart, can be obtained by differentiating the constraint $y = \varphi_0(r, \theta)$ with respect to τ_{ε_1} and rearranging terms. We obtain

$$
\begin{aligned}
\dot{r} &= \frac{a'(\theta)b(\theta) - a(\theta)b'(\theta)}{2a(\theta)b(\theta)}r + \mathcal{O}(r^2), \\
\dot{\theta} &= 1,
\end{aligned}
$$

where $a' := \partial a/\partial\theta$ and $b' := \partial b/\partial\theta$. This case is sketched in Fig. 1.

The Reduced Problem in Case (C2)

To obtain the reduced problem in case (C2) we may write system (14) on either time-scale τ_{ε_1} or τ_{ε_2}, which are related via $\tau_{\varepsilon_1} = \sigma \tau_{\varepsilon_2}$. Writing the system on the τ_{ε_2} time-scale leads to

$$
\begin{aligned}
\varepsilon_2 \dot{r} &= -a(\theta)y + b(\theta)r^2 + \mathcal{R}_r(r, \theta, y, \varepsilon_1, \varepsilon_2), \\
\dot{\theta} &= \frac{\varepsilon_1}{\varepsilon_2}, \\
\dot{y} &= -c(\theta) + \mathcal{R}_y(r, \theta, y, \varepsilon_1, \varepsilon_2),
\end{aligned}
\tag{18}
$$

where this time, the dot denotes differentiation with respect to the slow time τ_{ε_2}. Taking the double singular limit and using the fact that $\varepsilon_1/\varepsilon_2 = \sigma$ leads to the reduced problem

$$
\begin{aligned}
0 &= -a(\theta)y + b(\theta)r^2 + \mathcal{R}_r(r, \theta, y, 0, 0), \\
\dot{\theta} &= \sigma, \\
\dot{y} &= -c(\theta) + \mathcal{R}_y(r, \theta, y, 0, 0).
\end{aligned}
\tag{19}
$$

In contrast to the limiting equations (17) in case (C1), none of the variables become parameters in system (19). This is natural because in case (C2), system (14) only has two (as opposed to three) time-scales. In the (r, θ)-coordinate chart, the dynamics are determined by

$$
\begin{aligned}
\dot{r} &= -\frac{a(\theta)c(\theta)}{2b(\theta)r} + \mathcal{O}(1), \\
\dot{\theta} &= \sigma.
\end{aligned}
\tag{20}
$$

In particular, solutions reach $r = 0$ (and therefore S_0^c) in finite time.

The Reduced Problem in Case (C3)

In this case we rewrite system (14) on the slow time-scale $\tau_{\varepsilon_2} = \varepsilon_2 t$, thereby obtaining system (18). Since $\varepsilon_1/\varepsilon_2 \ll 1$, we first take $\varepsilon_1 \to 0$, and then $\varepsilon_2 \to 0$ (in that order). This leads to the reduced problem

$$
\begin{aligned}
0 &= -a(\theta)y + b(\theta)r^2 + \mathcal{R}_r(r, \theta, y, 0, 0), \\
\dot{\theta} &= 0, \\
\dot{y} &= -c(\theta) + \mathcal{R}_y(r, \theta, y, 0, 0).
\end{aligned}
\tag{21}
$$

This time, the angular variable θ is the slow variable to be considered as a parameter in system (19). In particular, the dynamics on S_0 can be represented by the 1-parameter family of ODEs

$$
\dot{r} = -\frac{ac}{2br} + \mathcal{O}(1),
$$

where $a = a(\theta)$, $b = b(\theta)$ and $c = c(\theta)$ are constants parameterised by $\theta \in \mathbb{R}/\mathbb{Z}$. Similarly to case (C2), solutions reach S_0^c in finite time. Moreover, singular orbits obtained as concatenations of layer and reduced orbit segments are contained within constant θ planes. As a result, the singular geometry and dynamics in case (C3) is equivalent to the singular geometry and dynamics of the normal form for the planar regular fold point in Krupa and Szmolyan (2001a). This case is sketched in Fig. 2.

For $0 < \varepsilon_1, \varepsilon_2 \ll 1$, Fenichel–Tikhonov theory implies that compact submanifolds of the normally hyperbolic critical manifolds S_0^a and S_0^r persist as $\mathcal{O}(l(\varepsilon_1, \varepsilon_2))$-close locally invariant *slow manifolds* $S_{l(\varepsilon_1,\varepsilon_2)}^a$ and $S_{l(\varepsilon_1,\varepsilon_2)}^r$, respectively (Fenichel
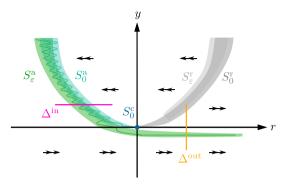
Fig. 3 Projected geometry and dynamics in the (r, y)-plane, as described by Theorem 3.2. The critical manifold and its submanifolds are sketched in colours consistent with earlier figures for the particular choice of $a(\theta)$ and $b(\theta)$ defined in Remark 2.9. The entry, exit sections Δ^{in}, Δ^{out} (magenta, orange) and the (extended) Fenichel slow manifolds S_ε^{a}, S_ε^{r} are also shown as shaded regions in green and light grey, respectively. For S_ε^{a} and S_0^{a} additionally a sample trajectory for a fixed θ initial condition is shown (Color figure online)

Fig. 4 The extension of the attracting slow manifold S_ε^{a} (again in shaded green) as described by Theorem 3.2, in the full (r, θ, y)-space. The entry, exit sections Δ^{in}, Δ^{out} as well as the critical manifold and its submanifolds are also shown, with the same colouring as in Fig. 3 for the particular choice of $a(\theta)$ and $b(\theta)$ in Remark 2.9. The intersection $\pi^{(\alpha)}(S_\varepsilon^{\text{a}} \cap \Delta^{\text{in}}) \subset \Delta^{\text{out}}$ is topologically equivalent to a circle (shown in dark green), and $O(\varepsilon^2)$-close to the plane $\{y = 0\}$ in the Hausdorff distance. The specific behaviour of solutions, which depends on α, is not shown (see however Figs. 5, 6, 7 and 8) (Color figure online)

1979; Jones 1995; Kuehn 2015; Wechselberger 2020; Wiggins 1994), where we write $l(\varepsilon_1, \varepsilon_2) := \max\{\varepsilon_1, \varepsilon_2\}$ in order to keep the discussion general, i.e. so that we need not distinguish between cases (C1), (C2) and (C3). Our goal is to describe the extension of the attracting slow manifold $S_{l(\varepsilon_1, \varepsilon_2)}^{\text{a}}$ through a neighbourhood of the non-hyperbolic cycle S_0^{c} corresponding to the regular folded cycle in system (14).

Remark 2.10 In Cardin and Teixeira (2017), the authors extend GSPT for a class of multiple time-scale systems with $n \geq 3$ time-scales which feature 'nested critical

manifolds'. A requirement for the application of this theory to system (14) is that the reduced problem on S_0 has a one-dimensional critical manifold. This condition is not satisfied in any case (C1), (C2) or (C3) because none of the reduced problems (17), (19) and (21) have equilibria in the neighbourhood of interest (i.e. close to $r = y = 0$).

3 Main Results

We now state and describe our main results. In order to distinguish the different cases (C1), (C2) and (C3), we scale ε_1 and ε_2 by a single small parameter $0 < \varepsilon \ll 1$. Main results are stated and proved for system (14) with $\varepsilon_1 = \varepsilon^\alpha$ and $\varepsilon_2 = \varepsilon^3$, i.e. for the system

$$
\begin{aligned}
r' &= -a(\theta)y + b(\theta)r^2 + \widetilde{\mathcal{R}}_r(r, \theta, y, \varepsilon), \\
\theta' &= \varepsilon^\alpha, \\
y' &= \varepsilon^3(-c(\theta) + \widetilde{\mathcal{R}}_y(r, \theta, y, \varepsilon)),
\end{aligned}
\tag{22}
$$

where the functions $a(\theta), b(\theta), c(\theta)$ are positive, 1-periodic and smooth and the higher-order terms satisfy

$$
\widetilde{\mathcal{R}}_r(r, \theta, y, \varepsilon) = \mathcal{O}(r^3, y^2, ry, \varepsilon^\alpha r^2, \varepsilon^\alpha y, \varepsilon^3), \qquad \widetilde{\mathcal{R}}_y(r, \theta, y, \varepsilon) = \mathcal{O}(r, y, \varepsilon^\alpha, \varepsilon^3).
$$

The different cases (C1), (C2) and (C3) are obtained for different values of the scaling parameter $\alpha \in \mathbb{N}_+$ as follows:

- Case (C1)*: $\alpha = 1$;
- Case (C1): $\alpha = 2$;
- Case (C2): $\alpha = 3$;
- Case (C3): $\alpha \geq 4$.

Note that we have introduced an additional case (C1)*. This case is dynamically distinct from the others, but it is not distinguished in Sect. 2 because the geometry and dynamics in the double singular limit are the same as for case (C1).

Remark 3.1 The choice to write ε^3 instead of ε in the equation for y is made a-posteriori in order to avoid fractional exponents in the proofs. Comparisons with known results for the stationary regular fold point in Krupa and Szmolyan (2001a), Szmolyan and Wechselberger (2004) are possible via the simple relation $\varepsilon_{\mathrm{KSW}} = \varepsilon^3$, where we denote by $\varepsilon_{\mathrm{KSW}}$ the small parameter in Krupa and Szmolyan (2001a) and/or Szmolyan and Wechselberger (2004). Similar observations motivated the use of a cubic exponent for the small parameter in other works involving folded singularities, e.g. in Nipp and Stoffer (2013), Nipp et al. (2009).

Our aim is to describe the forward evolution of initial conditions in an annular entry section

$$
\Delta^{\mathrm{in}} := \left\{ (r, \theta, R^2) : r \in [\beta_-, \beta_+], \theta \in \mathbb{R}/\mathbb{Z} \right\},
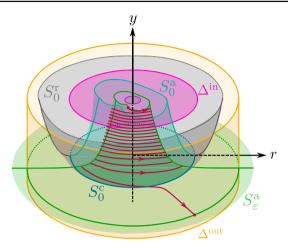\tag{23}
$$

Fig. 5 Case (C1)*. Sketch of the flow of system (22) for $\alpha = 1$. The solution sketched in red makes $N_{\mathrm{rot}}^{(1)}(r, \theta, \varepsilon) = \lfloor \mathcal{O}(\varepsilon^{-2}) \rfloor$ rotations about the y-axis before leaving the neighbourhood close to $S_\varepsilon^{\mathrm{a}} \cap \Delta^{\mathrm{out}}$ at an angle approximated by the expression for $h_\theta^{(1)}(r, \theta, \varepsilon)$ in Theorem 3.2 Assertion (b) (Color figure online)
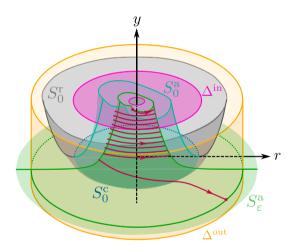

Fig. 6 Case (C1). Sketch of the flow of system (22) for $\alpha = 2$. The solution sketched in red makes $N_{\mathrm{rot}}^{(2)}(r, \theta, \varepsilon) = \lfloor \mathcal{O}(\varepsilon^{-1}) \rfloor$ rotations about the y-axis before leaving the neighbourhood close to $S_\varepsilon^{\mathrm{a}} \cap \Delta^{\mathrm{out}}$ at an angle approximated by the expression for $h_\theta^{(2)}(r, \theta, \varepsilon)$ in Theorem 3.2 Assertion (b) (Color figure online)

where R is a small positive constant and $\beta_- < \beta_+ < 0$ are two negative constants chosen such that $S_0^{\mathrm{a}} \cap \Delta^{\mathrm{in}} \subset \Delta^{\mathrm{in}} \cap \{r \in (\beta_-, \beta_+)\}$. We track solutions of system (22) up to their intersection with the cylindrical exit section

$$\Delta^{\mathrm{out}} := \{(R, \theta, y) : \theta \in \mathbb{R}/\mathbb{Z}, \, y \in [-y_0, y_0]\}, \tag{24}$$
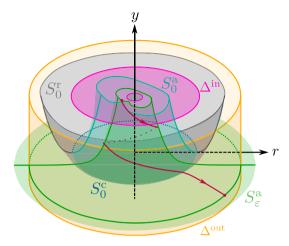
Fig. 7 Case (C2). Sketch of the flow of system (22) for $\alpha = 3$. The solution sketched in red makes $N_{\text{rot}}^{(3)}(r, \theta, \varepsilon) = \lfloor \frac{b(\theta)}{a(\theta)c(\theta)} R + \mathcal{O}(R^2) + \mathcal{O}(\varepsilon^3 \ln \varepsilon) \rfloor$ rotations about the y-axis before leaving the neighbourhood close to $S_\varepsilon^a \cap \Delta^{\text{out}}$ at an angle approximated by the expression for $h_\theta^{(3)}(r, \theta, \varepsilon)$ in Theorem 3.2 Assertion (b) (Color figure online)
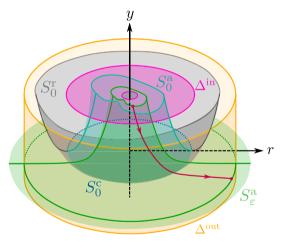

Fig. 8 Case (C3). Sketch of the flow of system (22). The solution sketched in red makes $N_{\text{rot}}^{(\alpha)}(r, \theta, \varepsilon) = 0$ rotations about the y-axis before leaving the neighbourhood close to $S_\varepsilon^a \cap \Delta^{\text{out}}$ at an angle approximated by the expression for $h_\theta^{(\alpha)}(r, \theta, \varepsilon)$ in Theorem 3.2 Assertion (b) ($\alpha \geq 4$) (Color figure online)

for a small positive constant $y_0 > 0$. The critical manifold S_0, the Fenichel slow manifolds (denoted now by S_ε^a and S_ε^r) and the entry/exit sections are visualised in the (r, y)-plane in Fig. 3 and in the three-dimensional space in Fig. 4.

We now state the main result, which characterises the dynamics of the map $\pi^{(\alpha)} : \Delta^{\text{in}} \to \Delta^{\text{out}}$ induced by the flow of system (22) for each $\alpha \in \mathbb{N}_+$, i.e. in all four cases (C1)*, (C1), (C2) and (C3).

Theorem 3.2 *Consider system* (22) *with fixed* $\alpha \in \mathbb{N}_+$. *There exists an* $\varepsilon_0 > 0$ *such that for all* $\varepsilon \in (0, \varepsilon_0]$, *the map* $\pi^{(\alpha)} : \Delta^{\text{in}} \to \Delta^{\text{out}}$ *is well-defined with the following properties*:

(a) *(Extension of* S_ε^a). *There exists a function* $h_y^{(\alpha)} : \mathbb{R}/\mathbb{Z} \times (0, \varepsilon_0] \to \mathbb{R}$ *which is smooth and* 1*-periodic in* θ *such that* $\pi^{(\alpha)}(S_\varepsilon^a \cap \Delta^{\text{in}}) = \{(R, \theta, h_y^{(\alpha)}(\theta, \varepsilon)) : \theta \in \mathbb{R}/\mathbb{Z}\}$ *is a smooth, closed curve*.

(b) *(Asymptotics).* $\pi^{(\alpha)}$ *has the form*

$$\pi^{(\alpha)} : (r, \theta, R^2) \mapsto \left(R, h_\theta^{(\alpha)}(r, \theta, \varepsilon), h_y^{(\alpha)}(h_\theta^{(\alpha)}(r, \theta, \varepsilon), \varepsilon) + h_{\text{rem}}^{(\alpha)}(r, \theta, \varepsilon) \right),$$

where

$$h_y^{(\alpha)}(h_\theta^{(\alpha)}(r, \theta, \varepsilon), \varepsilon) = \mathcal{O}(\varepsilon^2), \qquad h_{\text{rem}}^{(\alpha)}(r, \theta, \varepsilon) = \mathcal{O}\left(e^{-\kappa/\varepsilon^3}\right),$$

and $\kappa > 0$ *is a constant. In particular we have that* $h_\theta(r, \theta, \varepsilon) = \tilde{h}_\theta(r, \theta, \varepsilon)$ mod 1, *where*

$$\tilde{h}_\theta^{(\alpha)}(r, \theta, \varepsilon) = \begin{cases} \theta + \frac{R^2}{c_0}\varepsilon^{-2} + \mathcal{O}(\ln \varepsilon), & \alpha = 1, \\ \theta + \frac{R^2}{c_0}\varepsilon^{-1} + \mathcal{O}(\varepsilon \ln \varepsilon), & \alpha = 2, \\ \psi(\theta) + \mathcal{O}(\varepsilon^3 \ln \varepsilon), & \alpha = 3, \\ \theta + \mathcal{O}(\varepsilon^3 \ln \varepsilon), & \alpha \geq 4, \end{cases} \tag{25}$$

and

$$h_y^{(\alpha)}(\tilde{\theta}, \varepsilon) = \begin{cases} \mathcal{O}(\varepsilon^2), & \alpha = 1, \\ -\left(\frac{c(\tilde{\theta})^2}{a(\tilde{\theta})b(\tilde{\theta})}\right)^{1/3}\Omega_0\varepsilon^2 + \mathcal{O}(\varepsilon^3 \ln \varepsilon), & \alpha \geq 2. \end{cases} \tag{26}$$

Here $c_0 := \int_0^1 c(\theta) \, d\theta > 0$ *is the mean value of* c *over a single period,* $\psi(\theta) = \theta + \frac{b(\theta)}{a(\theta)c(\theta)}R^2 + \mathcal{O}(R^3)$ *is induced by the reduced flow of system* (20) *with* $\sigma = 1$ *up to* $r = 0$, *and the constant* $\Omega_0 > 0$ *is the smallest positive zero of* $J_{-1/3}(2z^{3/2}/3) + J_{1/3}(2z^{3/2}/3)$ *where* $J_{\pm 1/3}$ *are Bessel functions of the first kind*.

(c) *(Strong contraction). The* y-*component of* $\pi^{(\alpha)}(r, \theta, R^2)$ *is a strong contraction with respect to* r. *More precisely,*

$$\frac{\partial}{\partial r}\left(h_y^{(\alpha)}(h_\theta^{(\alpha)}(r, \theta, \varepsilon), \varepsilon) + h_{\text{rem}}^{(\alpha)}(r, \theta, \varepsilon)\right) = \mathcal{O}\left(e^{-\kappa/\varepsilon^3}\right).$$

Theorem 3.2 characterises the asymptotic behaviour of solutions and the extension of the attracting Fenichel slow manifold S_ε^a through a neighbourhood of the regular folded cycle in system (22). The geometry and dynamics for all four cases (C1)*, (C1), (C2) and (C3) are sketched in Figs. 5, 6, 7 and 8, respectively. The proof is broken into two parts, depending on whether or not $\alpha \in \{1, 2\}$. A detailed proof

based on the blow-up method will be given for the cases $\alpha \in \{1, 2\}$ in Sect. 4. Recall that these are the primary cases of interest, since they correspond to semi-oscillatory dynamics. If $\alpha \geq 3$, minor adaptations of the proof for case $\alpha = 2$ can be applied. Moreover, in this case, one can show directly that S_0^c is a closed regular fold curve. From here, Assertions (a)–(c) can be proven directly using established results (or a straightforward adaptation thereof) on the passage past a fold curve in 2-fast 1-slow systems, specifically (Szmolyan and Wechselberger 2004, Thm. 1). We shall therefore omit the details of these cases. Note that for $\alpha \geq 4$ in particular, $h_\theta^{(\alpha)}(r, \theta, \varepsilon) \sim \theta$ as $\varepsilon \to 0$, which implies that the leading-order coefficient in the expansion for $h_y^{(\alpha)}(\theta, \varepsilon)$ is also constant in θ. This is expected, since the dynamics for $\alpha \geq 4$ should resemble the dynamics of the stationary fold point considered in Krupa and Szmolyan (2001a) up to a slight perturbation.

For each $\alpha \in \mathbb{N}_+$, the size of the leading-order term in the asymptotics for the parameter drift in y is also the same as for the stationary regular fold point, at least up to $\mathcal{O}(\varepsilon^3 \ln \varepsilon)$, since

$$h_y^{(\alpha)}(\theta, \varepsilon) = h_y^{(\alpha)}\left(\theta, \varepsilon_{\mathrm{KSW}}^{1/3}\right) = \mathcal{O}\left(\varepsilon_{\mathrm{KSW}}^{2/3}\right) + \mathcal{O}(\varepsilon_{\mathrm{KSW}} \ln \varepsilon_{\mathrm{KSW}}),$$

which agrees with the asymptotic estimates in Krupa and Szmolyan (2001a), Mishchenko et al. (1975), Szmolyan and Wechselberger (2004) (recall from Remark 3.1 that $\varepsilon_{\mathrm{KSW}} = \varepsilon^3$, where $\varepsilon_{\mathrm{KSW}}$ denotes the small parameter in Krupa and Szmolyan (2001a), Szmolyan and Wechselberger (2004)). The strong contraction property in Assertion (c), which does not depend on α, is also the same. These two facts explain the similarity between the dynamics observed in the (r, y)-plane and the dynamics near a stationary regular fold point; c.f. Fig. 3 and Krupa and Szmolyan (2001a, Fig. 2.1). In contrast to the stationary fold, however, the coefficients of $h_y^{(\alpha)}(\theta, \varepsilon)$ depend on θ, and (26) gives the precise form for the leading-order coefficient if $\alpha > 1$, i.e. if $\alpha \in \mathbb{N}_+ \backslash \{1\}$. Moreover, Theorem (3.2) provides detailed asymptotic information about the angular coordinate θ via (25). If $\alpha > 2$ then estimates are sharp as $\varepsilon \to 0$.

Finally, the dynamics in different cases, i.e. for differing values of α, are distinguished via the angular dynamics and in particular, the number of complete rotations about the y-axis during the transition from Δ^{in} to Δ^{out}. We can estimate this number by introducing the function $N_{\mathrm{rot}}^{(\alpha)} : [\beta_-, \beta_+] \times \mathbb{R}/\mathbb{Z} \times (0, \varepsilon_0] \to \mathbb{N}$ via

$$N_{\mathrm{rot}}^{(\alpha)}(r, \theta, \varepsilon) := \left\lfloor \tilde{h}_\theta^{(\alpha)}(r, \theta, \varepsilon) - \theta \right\rfloor.$$

We obtain the following corollary as an immediate consequence of Theorem 3.2.

Corollary 3.3 *Let $\gamma : \mathbb{R} \to \mathbb{R}_{\geq 0} \times \mathbb{R}/\mathbb{Z} \times \mathbb{R}$ be a solution of system* (22) *with initial condition $\gamma(0) = (r, \theta, R) \in \Delta^{\mathrm{in}}$. Then $\gamma(t)$ undergoes*

$$N_{\mathrm{rot}}^{(\alpha)}(r, \theta, \varepsilon) = \begin{cases} \left\lfloor \frac{R^2}{c_0} \varepsilon^{-2} + \mathcal{O}(\ln \varepsilon) \right\rfloor, & \alpha = 1, \\ \left\lfloor \frac{R^2}{c_0} \varepsilon^{-1} + \mathcal{O}(\varepsilon \ln \varepsilon) \right\rfloor, & \alpha = 2, \\ \left\lfloor \frac{b(\theta)}{a(\theta)c(\theta)} R + \mathcal{O}(R^2) + \mathcal{O}(\varepsilon^3 \ln \varepsilon) \right\rfloor, & \alpha = 3, \\ 0, & \alpha \geq 4, \end{cases}$$

complete rotations about the y-axis during its passage to Δ^{out}.

Proof This follows immediately from the asymptotic estimates for $\tilde{h}^{(\alpha)}(r, \theta, \varepsilon)$ in Theorem 3.2 and the definition of $N_{\text{rot}}^{(\alpha)}$.   □

4 Proof of Theorem 3.2

Our aim is to investigate the three time-scale system (22) with $\alpha \in \{1, 2\}$ using the blow-up method developed for fast–slow systems in Dumortier and Roussarie (1996), Krupa and Szmolyan (2001a), Krupa and Szmolyan (2001b), Krupa and Szmolyan (2001c); we refer again to Jardón-Kojakhmetov and Kuehn (2021) for a recent survey. Many aspects of the proof rely in particular on arguments used in the blow-up analysis of the (stationary) regular fold point in Krupa and Szmolyan (2001a). However, many of the calculations are complicated by the fact that the angular variable θ cannot be treated locally. In particular, for $\alpha \in \{1, 2\}$, we cannot simply Taylor expand the equations about a fixed value of θ. Consequently, a local transformation into the local normal form in Szmolyan and Wechselberger (2004) is not possible. A similar feature arises when blowing up the fold cycle in the periodically forced van der Pol equation in the 'intermediate frequency regime' (Burke et al. 2016), except that in our case, there is no decoupling of the angular dynamics in the leading order. We adopt the (now well-established) notational conventions introduced in Krupa and Szmolyan (2001a), Krupa and Szmolyan (2001b), Krupa and Szmolyan (2001c).

The blow-up transformation is defined in Sect. 4.1, as are the three local coordinate charts that we use for calculations. The geometry and dynamics in all three coordinate charts are considered in turn in Sects. 4.2, 4.3 and 4.4. Theorem 3.2 is proved in Sect. 4.5 using the information obtained in local coordinate charts.

4.1 Blow-Up and Local Coordinate Charts

As is standard in blow-up approaches, we consider the extended system obtained from (22) after appending the trivial equation $\varepsilon' = 0$, i.e.

$$
\begin{aligned}
r' &= -a(\theta)y + b(\theta)r^2 + \widetilde{\mathcal{R}}_r(r, \theta, y, \varepsilon), \\
\theta' &= \varepsilon^\alpha, \\
y' &= \varepsilon^3(-c(\theta) + \widetilde{\mathcal{R}}_y(r, \theta, y, \varepsilon)), \\
\varepsilon' &= 0,
\end{aligned}
\tag{27}
$$

where $\alpha \in \{1, 2\}$ is fixed, $\widetilde{\mathcal{R}}_r(r, \theta, y, \varepsilon) = \mathcal{O}(r^3, y^2, ry, \varepsilon^\alpha r^2, \varepsilon^\alpha y, \varepsilon^3)$ and $\widetilde{\mathcal{R}}_y(r, \theta, y, \varepsilon) = \mathcal{O}(r, y, \varepsilon^\alpha)$.

In order to describe the map $\pi^{(\alpha)} : \Delta^{\text{in}} \to \Delta^{\text{out}}$, we introduce extended entry and exit sections

$$
\Delta_\varepsilon^{\text{in}} := \left\{ (r, \theta, R^2, \varepsilon) : r \in [\beta_-, \beta_+], \theta \in \mathbb{R}/\mathbb{Z}, \varepsilon \in [0, \varepsilon_0] \right\},
\tag{28}
$$

and

$$\Delta_\varepsilon^{\text{out}} := \{(R, \theta, y, \varepsilon) : \theta \in \mathbb{R}/\mathbb{Z}, \, y \in [-y_0, y_0], \, \varepsilon \in [0, \varepsilon_0]\}, \tag{29}$$

respectively. The entry, exit sections Δ^{in}, Δ^{out} defined in Sect. 3 (recall Eqs. (23) and (24)) can be viewed as constant ε sections of $\Delta_\varepsilon^{\text{in}}$, $\Delta_\varepsilon^{\text{out}}$, respectively. Based on this simple relationship, we study the map $\pi^{(\alpha)} : \Delta^{\text{in}} \to \Delta^{\text{out}}$ described in Theorem 3.2 via the extended map $\pi_\varepsilon^{(\alpha)} : \Delta_\varepsilon^{\text{in}} \to \Delta_\varepsilon^{\text{out}}$ induced by the flow of initial conditions in $\Delta_\varepsilon^{\text{in}}$ up to $\Delta_\varepsilon^{\text{out}}$ under system (27).

We now define the relevant blow-up transformation. Let $I = [0, \rho_0]$, where $\rho_0 > 0$ is fixed small enough for the validity of local computations, let

$$B_0 := S^2 \times \mathbb{R}/\mathbb{Z} \times [0, \rho_0],$$

and define the (weighted) blow-up transformation via

$$\begin{aligned}
\varphi : B_0 &\to \mathbb{R}_{\geq -\rho_0} \times \mathbb{R}/\mathbb{Z} \times \mathbb{R} \times \mathbb{R}_{\geq 0}, \\
(\bar{r}, \bar{y}, \bar{\varepsilon}, \theta, \rho) &\mapsto (r, \theta, y, \varepsilon) = (\rho\bar{r}, \theta, \rho^2\bar{y}, \rho\bar{\varepsilon}),
\end{aligned} \tag{30}$$

where $(\bar{r}, \bar{y}, \bar{\varepsilon}) \in S^2$. The blow-up map φ is a diffeomorphism for $\rho \in (0, \rho_0]$, but not for $\rho = 0$. In particular, the preimage of the non-hyperbolic cycle S_0^c under φ is a 'torus of spheres' $S^2 \times \mathbb{R}/\mathbb{Z} \times \{0\} \cong S^2 \times S^1$.

For calculational purposes, we introduce local coordinate charts in order to describe the dynamics on

$$B_{\bar{y}}^+ := B_0 \cap \{\bar{y} > 0\}, \qquad B_{\bar{\varepsilon}}^+ := B_0 \cap \{\bar{\varepsilon} > 0\}, \qquad B_{\bar{r}}^+ := B_0 \cap \{\bar{r} > 0\}.$$

Following Krupa and Szmolyan (2001a), we introduce affine projective coordinates via

$$\begin{aligned}
K_1 : \, &B_{\bar{y}}^+ \to \mathbb{R} \times \mathbb{R}/\mathbb{Z} \times \mathbb{R} \times \mathbb{R}, \quad (\bar{r}, \bar{y}, \bar{\varepsilon}, \rho, \theta) \mapsto (r_1, \theta_1, \rho_1, \varepsilon_1) = (\bar{r}\bar{y}^{-\frac{1}{2}}, \theta, \rho\bar{y}^{\frac{1}{2}}, \bar{\varepsilon}\bar{y}^{-\frac{1}{2}}), \\
K_2 : \, &B_{\bar{\varepsilon}}^+ \to \mathbb{R} \times \mathbb{R}/\mathbb{Z} \times \mathbb{R} \times \mathbb{R}, \quad (\bar{r}, \bar{y}, \bar{\varepsilon}, \rho, \theta) \mapsto (r_2, \theta_2, y_2, \rho_2) = (\bar{r}\bar{\varepsilon}^{-1}, \theta, \bar{y}\bar{\varepsilon}^{-2}, \rho\bar{\varepsilon}), \\
K_3 : \, &B_{\bar{r}}^+ \to \mathbb{R} \times \mathbb{R}/\mathbb{Z} \times \mathbb{R} \times \mathbb{R}, \quad (\bar{r}, \bar{y}, \bar{\varepsilon}, \rho, \theta) \mapsto (\rho_3, \theta_3, y_3, \varepsilon_3) = (\rho\bar{r}, \theta, \bar{y}\bar{r}^{-2}, \bar{\varepsilon}\bar{r}^{-1}).
\end{aligned}$$

Here we permit a small abuse of notation by introducing a new variable ε_1, which should not be confused with the small parameter with the same notation in Sects. 1–2. This leads to the following coordinates:

$$\begin{aligned}
K_1 : \, &(r, \theta, y, \varepsilon) = (\rho_1 r_1, \theta_1, \rho_1^2, \rho_1\varepsilon_1), \\
K_2 : \, &(r, \theta, y, \varepsilon) = (\rho_2 r_2, \theta_2, \rho_2^2 y_2, \rho_2), \\
K_3 : \, &(r, \theta, y, \varepsilon) = (\rho_3, \theta_3, \rho_3^2 y_3, \rho_3\varepsilon_3).
\end{aligned} \tag{31}$$

In the analysis, it will be necessary to change coordinates between different charts. The following lemma provides the relevant change of coordinates formulae.

Lemma 4.1 *The change of coordinate maps κ_{ij} from K_i to K_j are diffeomorphisms given by*

$$
\begin{array}{lllll}
\kappa_{12}: & r_2 = r_1\varepsilon_1^{-1}, & \theta_2 = \theta_1, & y_2 = \varepsilon_1^{-2}, & \rho_2 = \rho_1\varepsilon_1, & \text{for } \varepsilon_1 > 0, \\
\kappa_{12}^{-1}: & r_1 = r_2 y_2^{-\frac{1}{2}}, & \theta_1 = \theta_2, & \rho_1 = \rho_2 y_2^{\frac{1}{2}}, & \varepsilon_1 = y_2^{-\frac{1}{2}}, & \text{for } y_2 > 0, \\
\kappa_{23}: & \rho_3 = \rho_2 r_2, & \theta_3 = \theta_2, & y_3 = y_2 r_2^{-2}, & \varepsilon_3 = r_2^{-1}, & \text{for } r_2 > 0, \\
\kappa_{23}^{-1}: & r_2 = \varepsilon_3^{-1}, & \theta_2 = \theta_3, & y_2 = y_3\varepsilon_3^{-2}, & \rho_2 = \rho_3\varepsilon_3, & \text{for } \varepsilon_3 > 0.
\end{array}
\tag{32}
$$

Proof This follows from the local coordinate expressions in (31). □

Remark 4.2 The blow-up transformation (30) has the same form as the blow-up map used to study dynamics near a regular fold curve in $\mathbb{R}^3$ in Szmolyan and Wechselberger (2004), except that the domain of the uncoupled variable θ is $\mathbb{R}/\mathbb{Z}$ instead of $\mathbb{R}$. Note also that since θ is unaffected by (30), it follows that φ can be defined more succinctly in terms of its action on the remaining variables, i.e. via the map

$$
S^2 \times [0, \rho_0] \to \mathbb{R}_{\geq -\rho_0} \times \mathbb{R} \times \mathbb{R}_{\geq 0}, \qquad (\bar{r}, \bar{y}, \bar{\varepsilon}, \rho) \mapsto (r, y, \varepsilon) = (\rho\bar{r}, \rho^2\bar{y}, \rho\bar{\varepsilon}),
$$

which is precisely the blow-up map used to study the regular fold point in Krupa and Szmolyan (2001a) (recall that $\varepsilon_{\mathrm{KSW}} = \varepsilon^3$ by the discussion following the statement of Theorem 3.2).

Remark 4.3 By construction, the blown-up vector field induced by the pushforward of the vector field induced by system (27) under φ is invariant in the hyperplanes $\{\rho = 0\}$ and $\{\bar{\varepsilon} = 0\}$. The former corresponds to blown-up preimage of the non-hyperbolic cycle S_0^c, i.e. the torus of spheres $S^2 \times S^1$. The latter contains the blown-up preimage of the critical manifold S_0. Since $\bar{r}^2 + \bar{y}^2 = 1$ in $\{\bar{\varepsilon} = 0\}$, the preimage of φ in $\{\bar{\varepsilon} = 0\}$ is $S^1 \times \mathbb{R}/\mathbb{Z} \times \mathbb{R}_{\geq 0} \cong S^1 \times S^1 \times \mathbb{R}_{\geq 0}$. Thus, the part of the blown-up singular cycle S_0^c within $\{\bar{\varepsilon} = 0\}$ is a torus.

Remark 4.4 Since $\varepsilon = const.$ in system (27) we have constants of the motion defined by $\varepsilon = \rho_1\varepsilon_1$, $\varepsilon = \rho_2$, $\varepsilon = \rho_3\varepsilon_3$ in charts K_1, K_2, K_3, respectively.

We turn now to the dynamics in charts K_i, $i = 1, 2, 3$.

4.2 Dynamics in the Entry Chart K_1

In chart K_1 we analyse solutions which track the blown-up preimage of the attracting Fenichel slow manifold S_ε^a as they enter a neighbourhood of the non-hyperbolic circle S_0^c.

Lemma 4.5 *Following the positive transformation of time $\rho_1 dt = dt_1$, the desingularised equations in chart K_1 are given by*

$$
\begin{aligned}
r_1' &= -a(\theta_1) + b(\theta_1)r_1^2 + \frac{1}{2}c(\theta_1)\varepsilon_1^3 r_1 + \mathcal{O}(\rho_1), \\
\theta_1' &= \rho_1^{\alpha-1}\varepsilon_1^\alpha, \\
\rho_1' &= -\frac{1}{2}\rho_1\varepsilon_1^3(c(\theta_1) + \mathcal{O}(\rho_1)), \\
\varepsilon_1' &= \frac{1}{2}\varepsilon_1^4(c(\theta_1) + \mathcal{O}(\rho_1)),
\end{aligned}
\tag{33}
$$

where by a slight abuse of notation we now write $(\cdot)' = d/dt_1$.

Proof This follows after direct differentiation of the local coordinate expressions in (31) and subsequent application of the desingularisation $\rho_1 dt = dt_1$. □

The analysis in chart K_1 is restricted to the set

$$
\mathcal{D}_1 := \{(r_1, \theta_1, \rho_1, \varepsilon_1) \in \mathbb{R} \times \mathbb{R}/\mathbb{Z} \times \mathbb{R} \times \mathbb{R} : \ 0 \le \rho_1 \le R, \ 0 \le \varepsilon_1 \le E\},
$$

where R is the constant which defines the entry set Δ^{in} in (23) and $E = \varepsilon_0/R > 0$ due to the relationship $\varepsilon = \rho_1\varepsilon_1$ (recall Remark 4.4). The set $\mathcal{D}_1$ is sketched with other geometric and dynamical objects in chart K_1 in Fig. 9.

System (33) is well-defined within $\{\rho_1 = 0\}$ (recall that $\alpha \in \{1, 2\}$), which corresponds to the part of the blow-up surface in K_1. The subspace $\{\varepsilon_1 = 0\}$ is also invariant and contains two two-dimensional critical manifolds

$$
\begin{aligned}
S_1^a &:= \left\{(r_1, \theta_1, \rho_1, 0) \in \mathcal{D}_1 : r_1 = -\left(\frac{a(\theta_1)}{b(\theta_1)}\right)^{\frac{1}{2}} + \mathcal{O}(\rho_1)\right\}, \\
S_1^r &:= \left\{(r_1, \theta_1, \rho_1, 0) \in \mathcal{D}_1 : r_1 = \left(\frac{a(\theta_1)}{b(\theta_1)}\right)^{\frac{1}{2}} + \mathcal{O}(\rho_1)\right\}.
\end{aligned}
\tag{34}
$$

The manifolds S_1^a and S_1^r correspond to the blown-up preimages of the critical manifolds S_0^a and S_0^r in chart K_1, respectively. Both S_1^a and S_1^r are topologically equivalent to cylindrical segments, and they are normally hyperbolic and attracting resp. repelling up to and including the sets

$$
\begin{aligned}
P_a &:= \left\{\left(-\left(\frac{a(\theta_1)}{b(\theta_1)}\right)^{\frac{1}{2}}, \theta_1, 0, 0\right) : \theta_1 \in \mathbb{R}/\mathbb{Z}\right\}, \\
P_r &:= \left\{\left(\left(\frac{a(\theta_1)}{b(\theta_1)}\right)^{\frac{1}{2}}, \theta_1, 0, 0\right) : \theta_1 \in \mathbb{R}/\mathbb{Z}\right\},
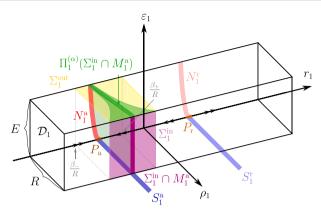\end{aligned}
$$

Fig. 9 Geometry and dynamics within $\mathcal{D}_1$, shown in $(r_1, \rho_1, \varepsilon_1)$-space. Projections of the two-dimensional attracting and repelling critical manifolds $S_1^{\mathrm{a}}, S_1^{\mathrm{r}} \subset \{\varepsilon_1 = 0\}$ (shown in blue and shaded blue) extend up to their intersection with the blow-up surface at $P_{\mathrm{a}}, P_{\mathrm{r}} \subset \{\rho_1 = \varepsilon_1 = 0\}$, respectively. Projections of the two-dimensional centre manifolds $N_1^{\mathrm{a}}, N_1^{\mathrm{r}} \subset \{\rho_1 = 0\}$ emanating from $P_{\mathrm{a}}, P_{\mathrm{r}}$, as described in Lemma 4.6, are sketched in red and shaded red for the case $\alpha = 2$, but they look similar in the case $\alpha = 1$. Entry and exit sections Σ_1^{in} and Σ_1^{out} are shown in shaded magenta and yellow, respectively. The projected three-dimensional centre manifold M_1^{a} and its image under $\Pi_1^{(\alpha)}$ is described by Proposition 4.9. This is shown along with the image $\Pi_1^{(\alpha)}(\Sigma_1^{\mathrm{in}}) \subset \Sigma_1^{\mathrm{out}}$ in green (Color figure online)

which intersect with the blow-up surface; see Figs. 9 and 10. The linearisation of system (33) along P_{a} is

$$
J(P_{\mathrm{a}}) = \begin{pmatrix} -2\sqrt{a(\theta_1)b(\theta_1)} & \big(a(\theta_1)b'(\theta_1) - a'(\theta_1)b(\theta_1)\big)/b(\theta_1) & 0 & 0 \\ 0 & 0 & 0 & 0^{\alpha-1} \\ 0 & 0 & 0 & 0 \\ 0 & 0 & 0 & 0 \end{pmatrix}, \quad (35)
$$

where we write $a' = \partial a/\partial\theta_1$ and $b' = \partial b/\partial\theta_1$, and we write

$$
0^{\alpha-1} = \begin{cases} 1, & \alpha = 1, \\ 0, & \alpha = 2. \end{cases}
$$

In both cases, the set P_{a} is partially hyperbolic with a single non-trivial eigenvalue $-2\sqrt{a(\theta_1)b(\theta_1)} < 0$. The remaining three eigenvalues along P_{a} are identically zero. Thus in the blown-up space (i.e. for system (33)), we have regained partial hyperbolicity. This allows us to extend the attracting centre manifold with base along S_1^{a} up onto the blow-up surface using centre manifold theory.

Lemma 4.6 *Consider system (33) on $\mathcal{D}_1$ with $E, R > 0$ sufficiently small. There exists a three-dimensional centre-stable manifold M_1^{a} such that*

$$
M_1^{\mathrm{a}}|_{\varepsilon_1=0} = S_1^{\mathrm{a}}, \qquad M_1^{\mathrm{a}}|_{\rho_1=0} = N_1^{\mathrm{a}},
$$

where $S_1^a \subset \{\varepsilon_1 = 0\}$ is the two-dimensional attracting critical manifold in (34) *and $N_1^a \subset \{\rho_1 = 0\}$ is a unique two-dimensional centre-stable manifold for the restricted system* (33) $|_{\rho_1=0}$ *emanating from P_a. The manifold M_1^a is given locally as a graph $r_1 = h_{r_1}^{(\alpha)}(\theta_1, \rho_1, \varepsilon_1)$, where*

$$h_{r_1}^{(1)}(\theta_1, \rho_1, \varepsilon_1) = -\left(\frac{a(\theta_1)}{b(\theta_1)}\right)^{\frac{1}{2}} + \frac{a(\theta_1)b'(\theta_1) - a'(\theta_1)b(\theta_1)}{4a(\theta_1)b(\theta_1)}\varepsilon_1 + \mathcal{O}\left(\rho_1, \varepsilon_1^2\right)$$

(36)

and

$$h_{r_1}^{(2)}(\theta_1, \rho_1, \varepsilon_1) = -\left(\frac{a(\theta_1)}{b(\theta_1)}\right)^{\frac{1}{2}} - \frac{c(\theta_1)}{4b(\theta_1)}\varepsilon_1^3 + \mathcal{O}\left(\rho_1, \varepsilon_1^6\right).$$

(37)

In both cases, there exists a constant $\varrho \in (0, \vartheta)$, where $\vartheta := \min_{\theta_1 \in [0,1)} 2\sqrt{a(\theta_1)b(\theta_1)} > 0$, such that initial conditions in Σ_1^{in} are attracted to M_1^a along one-dimensional stable fibers faster than $e^{-\varrho t_1}$.

Proof The existence of a three-dimensional centre manifold M_1^a follows from linearisation (35) and centre manifold theory (Kuznetsov 2013). The fact that M_1^a contains two-dimensional manifolds N_1^a and S_1^a with the properties described follows after direct restriction to the invariant hyperplanes $\{\rho_1 = 0\}$ and $\{\varepsilon_1 = 0\}$, respectively.

The graph representations in (36) and (37) are obtained using the standard approach based on formal matching. More precisely, we substitute a power series ansatz of the form

$$r_1 = h_{r_1}^{(\alpha)}(\theta_1, \rho_1, \varepsilon_1) = \sum_{n=0}^{\infty} \mu_n^{(\alpha)}(\theta_1)\varepsilon_1^n + \mathcal{O}(\rho_1)$$

into the equation for r_1' in system (33) and determine the coefficients $\mu_n^{(\alpha)}(\theta_1)$ by comparing

$$\begin{aligned} r_1' &= \sum_{n=0}^{\infty}\left(\frac{d\mu_n^{(\alpha)}(\theta_1)}{d\theta_1}\theta_1'\varepsilon_1^n + \mu_{n+1}^{(\alpha)}(\theta_1)(n+1)\varepsilon_1^n\varepsilon_1'\right) + \mathcal{O}(\rho_1) \\ &= \sum_{n=0}^{\infty}\left(\frac{d\mu_n^{(\alpha)}(\theta_1)}{d\theta_1}\rho_1^{\alpha-1}\varepsilon_1^{n+\alpha} + \frac{1}{2}\mu_{n+1}^{(\alpha)}(\theta_1)(n+1)\varepsilon^{n+4}\right) + \mathcal{O}(\rho_1), \end{aligned}$$

with

$$r_1' = b(\theta)\left(\sum_{n=0}^{\infty}\mu_n^{(\alpha)}(\theta_1)\varepsilon_1^n\right)^2 - a(\theta_1) + \frac{1}{2}c(\theta_1)\varepsilon_1^3\sum_{n=0}^{\infty}\mu_n^{(\alpha)}(\theta_1)\varepsilon_1^n + \mathcal{O}(\rho_1)$$

$$= b(\theta)\sum_{n=0}^{\infty}\left(\sum_{k=0}^{n}\mu_k^{(\alpha)}(\theta_1)\mu_{n-k}^{(\alpha)}(\theta_1)\right)\varepsilon_1^n - a(\theta_1)$$

$$+ \frac{1}{2}c(\theta_1)\sum_{n=0}^{\infty}\mu_n^{(\alpha)}(\theta_1)\varepsilon_1^{n+3} + \mathcal{O}(\rho_1).$$

Depending on whether $\alpha = 1$ or $\alpha = 2$, the approximations in (36) or (37) are obtained (respectively). The details are omitted for brevity.

The strong contraction along stable fibers at a rate greater than $e^{-\varrho t_1}$ for some $\varrho \in (0, \vartheta)$, where $\vartheta := \min_{\theta_1 \in [0,1)} 2\sqrt{a(\theta_1)b(\theta_1)} > 0$ follows from Fenichel theory (Fenichel 1979, Theorem 9.1) and the fact that the stable leading eigenvalue is $\lambda = -2\sqrt{a(\theta_1)b(\theta_1)}$, recall (35). □

The two-dimensional centre manifold N_1^a is sketched within $\{\rho_1 = 0\}$ in Fig. 11.

Remark 4.7 Similar to Lemma 4.6, there exists a three-dimensional centre-unstable manifold M_1^r at P_r that contains the repelling critical manifold $S_1^r \subset \{\varepsilon_1 = 0\}$ and a repelling centre manifold $N_1^r \subset \{\rho_1 = 0\}$. These objects are shown in Figs. 10 and 11. In $\mathcal{D}_1$, the manifold M_1^r is given as a graph $r_1 = \tilde{h}_{r_1}^{(\alpha)}(\theta_1, \rho_1, \varepsilon_1)$, where

$$\tilde{h}_{r_1}^{(1)}(\theta_1, \rho_1, \varepsilon_1) = \left(\frac{a(\theta_1)}{b(\theta_1)}\right)^{\frac{1}{2}} + \frac{a(\theta_1)b'(\theta_1) - a'(\theta_1)b(\theta_1)}{4a(\theta_1)b(\theta_1)}\varepsilon_1 + \mathcal{O}\left(\rho_1, \varepsilon_1^2\right)$$

and

$$\tilde{h}_{r_1}^{(2)}(\theta_1, \rho_1, \varepsilon_1) = \left(\frac{a(\theta_1)}{b(\theta_1)}\right)^{\frac{1}{2}} - \frac{c(\theta_1)}{4b(\theta_1)}\varepsilon_1^3 + \mathcal{O}(\varepsilon_1^6, \rho_1).$$

In contrast to N_1^a, the manifold N_1^r is not unique. We omit the explicit treatment of the dynamics near M_1^r since it is not relevant to the proof of Theorem 3.2.

Lemma 4.6 can be used to describe the r_1-component of the map $\Pi_1^{(\alpha)} : \Sigma_1^{in} \to \Sigma_1^{out}$ induced by the flow of initial conditions in

$$\Sigma_1^{in} := \{(r_1, \theta_1, R, \varepsilon_1) \in \mathcal{D}_1 : r_1 \in [\beta_-/R, \beta_+/R]\},$$

i.e. the representation of the entry section Δ_ε^{in} defined in (28) in K_1 coordinates, up to the exit section

$$\Sigma_1^{out} := \{(r_1, \theta_1, \rho_1, E) \in \mathcal{D}_1 : r_1 \in [\beta_-/R, \beta_+/R]\}.$$

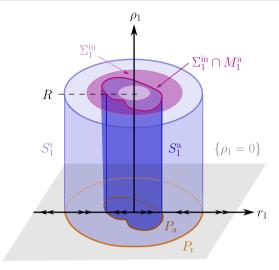**Fig. 10** Geometry and dynamics within the invariant hyperplane $\{\varepsilon_1 = 0\}$, projected into (r_1, θ_1, ρ_1)-space; c.f. Fig. 9 (Color figure online)
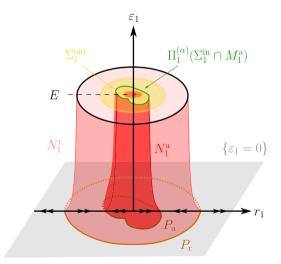

Fig. 11 Geometry and dynamics within the invariant hyperplane $\{\rho_1 = 0\}$, projected into $(r_1, \theta_1, \varepsilon_1)$-space; c.f. Figs. 9 and 10 (Color figure online)

The constants $\beta_- < \beta_+ < 0$ are chosen in such a way that the r_1-coordinate of the centre manifold M_1^a in $\mathcal{D}_1$ is always contained in the interval $(\beta_-/R, \beta_+/R)$, cf. Definition (23) of the entry section Δ^{in}.

The remaining θ_1, ρ_1 and ε_1 components of the map $\Pi_1^{(\alpha)}$ and the transition time taken for solutions with initial conditions in Σ_1^{in} to reach Σ_1^{out} can be estimated directly. To obtain better estimates, we rewrite the positive, 1-periodic smooth function $c(\theta_1)$ as

$$c(\theta_1) = c_0 + c_{\text{rem}}(\theta_1), \tag{38}$$

where $c_0 := \int_0^1 c(\theta_1(t_1)) \, dt_1$ is the mean value of $c(\theta_1)$ over one period and $c_{\text{rem}}(\theta_1) := c(\theta_1) - c_0$ is the smooth, 1-periodic remainder with mean zero. The estimates are provided by the following result.

Lemma 4.8 *Consider an initial condition* $(r_1, \theta_1, \rho_1, \varepsilon_1)(0) = (r_1^*, \theta_1^*, R, \varepsilon_1^*) \in \Sigma_1^{\text{in}}$ *for system (33). Then*

$$\theta_1(t_1) = \theta_1^* + \frac{(R\varepsilon_1^*)^{\alpha-1} \varepsilon_1^{*-2}}{c_0} \left(1 - \left(1 - \frac{3}{2} \varepsilon_1^{*3} \left(\phi(t_1) + t_1 \mathcal{O}(R) \right) \right)^{2/3} \right)$$

$$(1 + \mathcal{O}(R)) \mod 1,$$

$$\rho_1(t_1) = R \left(1 - \frac{3}{2} \varepsilon_1^{*3} \left(\phi(t_1) + t_1 \mathcal{O}(R) \right) \right)^{\frac{1}{3}},$$

$$\varepsilon_1(t_1) = \varepsilon_1^* \left(1 - \frac{3}{2} \varepsilon_1^{*3} \left(\phi(t_1) + t_1 \mathcal{O}(R) \right) \right)^{-\frac{1}{3}},$$

where $\phi(t_1) := \int_0^{t_1} c(\theta_1(s_1)) \, ds_1 = c_0 t_1 + \mathcal{O}(1)$. *The notation* $\mathcal{O}(R)$ *is used to denote (possibly different) remainder terms which satisfy* $|\mathcal{O}(R)| \leq CR$ *for some constant* $C > 0$ *and all* $t_1 \in [0, T_1]$, *where*

$$T_1 = \frac{2}{3c_0} \left(\frac{1}{\varepsilon_1^{*3}} - \frac{1}{E^3} \right) (1 + \mathcal{O}(R)) + \mathcal{O}(1)$$

is the transition time taken for the solution to reach Σ_1^{out}.

Proof. Consider system (33). By keeping track of the higher-order terms when deriving the equation for ε_1' in system (33) one can show that

$$\varepsilon_1' = \frac{1}{2} \varepsilon_1^4 \left(c(\theta_1) - \rho_1 \chi(r_1, \theta_1, \rho_1, \varepsilon_1) \right),$$

where $\chi(r_1, \theta_1, \rho_1, \varepsilon_1) := \rho_1^{-1} \widetilde{\mathcal{R}}_y(\rho_1 r_1, \theta_1, \rho_1^2, \rho_1 \varepsilon_1) = \mathcal{O}(r_1, \rho_1, \varepsilon_1)$. Directly integrating and rearranging a little leads to

$$\varepsilon_1(t_1) = \varepsilon_1^* \left(1 - \frac{3}{2} \varepsilon_1^{*3} \left(\phi(t_1) + t_1 \psi(t_1) \right) \right)^{-\frac{1}{3}},$$

where $\phi(t_1)$ is defined as in the statement of the lemma and

$$t_1 \psi(t_1) = -\int_0^{t_1} \rho_1(s_1) \chi(r_1(s_1), \theta_1(s_1), \rho_1(s_1), \varepsilon_1(s_1)) \, ds_1.$$

The expression for $\rho_1(t_1)$ can be obtained directly from the expression for $\varepsilon_1(t_1)$ using the fact that $\rho_1(t)\varepsilon_1(t) = \varepsilon = R\varepsilon_1^*$ is a constant of the motion; recall Remark 4.4. One can show that $|\psi(t_1)| = \mathcal{O}(R)$ by appealing to the fact that $\chi(r_1(s_1), \theta_1(s_1), \rho_1(s_1), \varepsilon_1(s_1))$ is bounded uniformly for all $s_1 \in [0, T_1]$, since $\rho_1 \in [0, R]$, $\varepsilon_1 \in [0, E]$, $\theta \in \mathbb{R}/\mathbb{Z}$ and $r_1 \in [\beta_-/R, \beta_+/R]$ (the latter follows from the fact that $r_1'|_{r_1=\beta_-/R} > 0$ and $r_1'|_{r_1=\beta_+/R} < 0$). Therefore, there is a constant $C > 0$ such that $|\psi(t_1)| \le CR$ for all $t_1 \in [0, T_1]$, as required.

It remains to estimate $\theta_1(t_1)$ and the transition time T_1. We have that

$$\theta_1' = \rho_1(t_1)^{\alpha-1}\varepsilon_1(t_1)^\alpha = (\varepsilon_1^* R)^{\alpha-1}\varepsilon_1(t_1).$$

The expression for $\theta_1(t_1)$ is obtained by integrating the expression for $\varepsilon_1(t_1)$ and using (38) to estimate

$$\phi(t_1) := \int_0^{t_1} c_0 + c_{\mathrm{rem}}(\theta_1(s_1))\, \mathrm{d}s_1 = c_0 t_1 + \mathcal{O}(1),$$

as $\int_0^1 c_{\mathrm{rem}}(\theta_1(t_1))\, \mathrm{d}t_1 = 0$ and θ_1 is bounded and 1-periodic. To estimate the transition time T_1, the boundary constraint $\varepsilon_1(T_1) = E$ is used; c.f. (Krupa and Szmolyan 2001a, Lemma 2.7). Integrating $\varepsilon_1' = \frac{1}{2}\varepsilon_1^4(c_0 + c_{\mathrm{rem}}(\theta_1) + \mathcal{O}(\rho_1))$ from ε_1^* to E leads to

$$\frac{1}{3}\left(\frac{1}{(\varepsilon_1^*)^3} - \frac{1}{E^3}\right) = \frac{c_0}{2}T_1 + \frac{1}{2}\int_0^{T_1} c_{\mathrm{rem}}(\theta_1(t_1))\, \mathrm{d}t_1 + \frac{1}{2}\int_0^{T_1} \mathcal{O}(\rho_1(t_1))\, \mathrm{d}t_1.$$

By (38), the second term on the right-hand side is $\mathcal{O}(1)$ and the third term can be estimated by $T_1 \mathcal{O}(R)$. Rearranging yields the desired result.   □

Combining Lemmas 4.6 and 4.8 we obtain the following characterisation of the transition map $\Pi_1^{(\alpha)} : \Sigma_1^{\mathrm{in}} \to \Sigma_1^{\mathrm{out}}$, which summarises the dynamics in chart K_1.

Proposition 4.9 *Fix E, $R > 0$ sufficiently small. Then the map $\Pi_1^{(\alpha)} : \Sigma_1^{\mathrm{in}} \to \Sigma_1^{\mathrm{out}}$ is well-defined with the following properties:*

(a) (Asymptotics). *We have*

$$\Pi_1^{(\alpha)}(r_1, \theta_1, R, \varepsilon_1) = \left(\Pi_{1,r_1}^{(\alpha)}(r_1, \theta_1, \varepsilon_1), h_{\theta_1}^{(\alpha)}(r_1, \theta_1, \varepsilon_1), \frac{R}{E}\varepsilon_1, E\right),$$

where

$$\Pi_{1,r_1}^{(\alpha)}(r_1, \theta_1, \varepsilon_1) = h_{r_1}^{(\alpha)}\left(h_{\theta_1}^{(\alpha)}(r_1, \theta_1, \varepsilon_1), \frac{R}{E}\varepsilon_1, E\right) + \mathcal{O}\left(e^{-\tilde{\varrho}/\varepsilon_1^3}\right)$$

where $\tilde{\varrho} = \frac{2\varrho}{3c_0}$, the constant ϱ and the function $h_{r_1}^{(\alpha)}$ are the same as those in Lemma 4.6, and $h_{\theta_1}^{(\alpha)}(r_1, \theta_1, \varepsilon_1) = \tilde{h}_{\theta_1}^{(\alpha)}(r_1, \theta_1, \varepsilon_1) \mod 1$, where

$$\tilde{h}_{\theta_1}^{(\alpha)}(r_1, \theta_1, \varepsilon_1) = \theta_1 + \frac{(R\varepsilon_1)^{\alpha-1}}{c_0}\left(\frac{1}{\varepsilon_1{}^2} + \mathcal{O}(1)\right).$$

(b) (Strong contraction). *The r_1-component of $\Pi_1^{(\alpha)}$ is a strong contraction with respect to r_1. More precisely,*

$$\frac{\partial \Pi_{1,r_1}^{(\alpha)}}{\partial r_1}(r_1, \theta_1, \varepsilon_1) = \mathcal{O}\left(e^{-\tilde{\varrho}/\varepsilon_1^3}\right).$$

The image $\Pi_1^{(\alpha)}(\Sigma_1^{\text{in}}) \subset \Sigma_1^{\text{out}}$ is a wedge-like region about the intersection $M_1^{\text{a}} \cap \Sigma_1^{\text{out}}$.

Proof Consider an initial condition $(r_1, \theta_1, R, \varepsilon_1) \in \Sigma_1^{\text{in}}$. The form of the map $\Pi_1^{(\alpha)}(r_1, \theta_1, R, \varepsilon_1)$ follows immediately after evaluating the solutions for $\theta_1(t_1)$, $\rho_1(t_1)$, and $\varepsilon_1(t_1)$ at $t_1 = T_1$ using Lemma 4.8 and defining $h_{\theta_1}^{(\alpha)}(r_1, \theta_1, \varepsilon_1) = \theta_1(T_1)$. The expression for $r_1(T_1) = \Pi_{1,r_1}^{(\alpha)}(r_1, \theta_1, \varepsilon_1)$ follows from Lemma 4.6. Specifically, choosing E, R sufficiently small ensures that the initial condition $(r_1, \theta_1, R, \varepsilon_1)$ is contained in a fast fiber of M_1^{a}. It follows that

$$\left\|r_1(T_1) - h_{r_1}^{(\alpha)}(\theta_1(T_1), \rho_1(T_1), E)\right\| = \mathcal{O}(e^{-\varrho T_1})$$

for the constant ϱ of Lemma 4.6. Thus $r_1(T_1) = h_{r_1}^{(\alpha)}(\theta_1(T_1), \rho_1(T_1), E) + \mathcal{O}(e^{-\varrho T_1})$, which yields the expression in Assertion (a) after substituting the expression for T_1 in Lemma 4.8.

Assertion (b) follows by direct differentiation. The estimate follows since $h_{r_1}^{(\alpha)}(\theta_1, \rho_1, \varepsilon_1)$ does not depend on r_1. $\qquad\square$

Remark 4.10 Strictly speaking, the arguments above only guarantee that $\Pi_1^{(\alpha)}$ is well-defined for initial conditions with $\varepsilon_1 \in (0, E]$. This is not problematic since we aim to derive results for $\varepsilon > 0$.

4.3 Dynamics in the Rescaling Chart K_2

In chart K_2 we study solutions close to the extension of the centre manifold $M_2^{\text{a}} = \kappa_{12}(M_1^{\text{a}})$.

Lemma 4.11 *Following the singular time rescaling $\rho_2 dt = dt_2$ or equivalently, $\rho_2 t = t_2$, the desingularised equations in chart K_2 are given by*

$$
\begin{aligned}
r_2' &= -a(\theta_2)y_2 + b(\theta_2)r_2^2 + \mathcal{O}(\rho_2), \\
\theta_2' &= \rho_2^{\alpha-1}, \\
y_2' &= -c(\theta_2) + \mathcal{O}(\rho_2), \\
\rho_2' &= 0,
\end{aligned}
\tag{39}
$$

where by a slight abuse of notation we now write $(\cdot)' = d/dt_2$. Since $0 < \rho_2 = \varepsilon \ll 1$, system (39) can also be viewed as a perturbation problem in (r_2, θ_2, y_2)-space as $\rho_2 \to 0$.

Proof This follows immediately after differentiating the defining expressions for local K_2 coordinates in (31) and applying $\rho_2 t = t_2$. □

In order to understand system (39), we first consider the limiting system as $\rho_2 \to 0$, i.e.

$$
\begin{aligned}
r_2' &= -a(\theta_2)y_2 + b(\theta_2)r_2^2, \\
\theta_2' &= 0^{\alpha-1}, \\
y_2' &= -c(\theta_2).
\end{aligned}
\tag{40}
$$

There are two possibilities for the angular dynamics, depending on α, since

$$
\theta_2' = \begin{cases} 1, & \alpha = 1, \\ 0, & \alpha = 2. \end{cases}
$$

We start with the case $\alpha = 2$. In this case, we obtain a θ_2-family of planar systems

$$
\begin{aligned}
r_2' &= -ay_2 + br_2^2, \\
y_2' &= -c,
\end{aligned}
\tag{41}
$$

where $a = a(\theta_2)$, $b = b(\theta_2)$ and $c = c(\theta_2)$ define (parameter dependent) positive constants. The transformation

$$
t_2 = (abc)^{-1/3}T_2, \qquad r_2 = \left(\frac{ac}{b^2}\right)^{1/3} R_2, \qquad y_2 = \left(\frac{c^2}{ab}\right)^{1/3} Y_2,
\tag{42}
$$

leads to

$$
\begin{aligned}
\frac{dR_2}{dT_2} &= -Y_2 + R_2^2, \\
\frac{dY_2}{dT_2} &= -1,
\end{aligned}
\tag{43}
$$

which is precisely the Riccati-type equation which arises within the K_2 chart in the analysis of the regular fold point in Krupa and Szmolyan (2001a). For each fixed $\theta \in \mathbb{R}/\mathbb{Z}$, solutions to system (43) (and therefore also (41)) can be written in terms of Airy functions, whose asymptotic properties are known (Grasman 1987; Mishchenko et al. 1975). The properties that are relevant for our purposes are collected in Mishchenko et al. (1975) and reformulated in a notation similar to ours in Krupa and Szmolyan (2001a). The following result is a direct extension of the latter formulation; we simply append the existing result with the decoupled angular dynamics induced by the equation for θ_2.

Proposition 4.12 *Fix $\alpha = 2$ and consider the restricted system (39) $|_{\rho_2=0}$ or, equivalently, the limiting system (40). The following assertions are true:*

(a) *Every orbit approaches a two-dimensional horizontal asymptote/plane $y_2 = y_r$ from $y_2 > y_r$ as $r_2 \to \infty$. The value of y_r depends on the initial conditions.*

(b) *There exists a unique, invariant two-dimensional surface*

$$\gamma_2 := \left\{ \left(r_2, \theta_2, h_{y_2}^{(2)}(r_2), 0 \right) : r_2 \in \mathbb{R}, \ \theta_2 \in \mathbb{R}/\mathbb{Z} \right\}, \tag{44}$$

where $h_{y_2}^{(2)}(r_2)$ is smooth with asymptotics

$$h_{y_2}^{(2)}(r_2) = \frac{b}{a} r_2^2 + \frac{c}{2b} \frac{1}{r_2} + \mathcal{O}\left(\frac{1}{r_2^4} \right) \qquad \text{as } r_2 \to -\infty,$$

$$h_{y_2}^{(2)}(r_2) = -\left(\frac{c^2}{ab} \right)^{1/3} \Omega_0 + \frac{c}{b} \frac{1}{r_2} + \mathcal{O}\left(\frac{1}{r_2^3} \right) \quad \text{as } r_2 \to \infty,$$

and Ω_0 is the constant defined in Theorem 3.2.

(c) *All orbits with initial conditions to the right of γ_2 in the (r_2, y_2)-plane are backwards asymptotic to the paraboloid $\{(r_2, \theta_2, (b/a)r_2^2, 0) : r_2 \geq 0, \theta_2 \in \mathbb{R}/\mathbb{Z}\}$.*

(d) *All orbits with initial condition to the left of γ_2 in the (r_2, y_2)-plane are backwards asymptotic to a horizontal asymptote/plane $y_2 = y_l$. Specifically, $y_2(t_2) \to y_l$ from below and $r_2(t_2) \to -\infty$ as $t_2 \to -\infty$. The value of y_l depends on the initial conditions, but satisfies $y_l > y_r$ for each fixed orbit.*

(e) *The unique centre manifold N_1^a described in Lemma 4.6 coincides with the surface γ_2 where K_1 and K_2 overlap, i.e. $\kappa_{12}(N_1^a) = \gamma_2$ on $\{y_2 > 0\}$.*

Proof See Mishchenko et al. (1975) and in particular (Krupa and Szmolyan 2001a, Prop. 2.3), which cover Assertions (a)–(d) in the planar case, for the transformed system (43). The corresponding statements for system (41) can be obtained directly from these results using the transformation in (42). Since the angular variable $\theta_2 = const.$ when $\alpha = 2$, Assertions (a)–(d) are obtained as higher-dimensional analogues from these results after a simple rotation through $\theta_2 \in [0, 1)$.

Assertion (e) is a straightforward adaptation of Krupa and Szmolyan (2001a, Prop. 2.6 Assertion (5)).   □

The Riccati dynamics described in Proposition 4.12 are sketched for the decoupled planar system (41) in Fig. 12, and for the three-dimensional limiting system (40) in Fig. 13.

We now consider the case $\alpha = 1$, for which system (40) can be written as the non-autonomous planar system

$$
\begin{aligned}
r_2' &= -\tilde{a}(t_2)y_2 + \tilde{b}(t_2)r_2^2, \\
y_2' &= -\tilde{c}(t_2),
\end{aligned}
\tag{45}
$$

where the functions

$$
\begin{aligned}
\tilde{a}(t_2) &:= a(\theta_2(0) + t_2 \mod 1), \quad \tilde{b}(t_2) := b(\theta_2(0) + t_2 \mod 1), \\
\tilde{c}(t_2) &:= c(\theta_2(0) + t_2 \mod 1),
\end{aligned}
$$

are smooth, positive and 1-periodic in t_2 due to the positivity and 1-periodicity of $a(\theta)$, $b(\theta)$ and $c(\theta)$; recall Proposition 2.5. Using

$$
y_2(t_2) = y_2(0) - \varphi(t_2), \qquad \varphi(t_2) := \int_0^{t_2} \tilde{c}(\xi) \, d\xi,
\tag{46}
$$

we may write (45) as a Riccati equation

$$
\frac{dr_2}{dt_2} = \tilde{a}(t_2)(\varphi(t_2) - y_2(0)) + \tilde{b}(t_2)r_2^2.
\tag{47}
$$

We now define the constants

$$
\begin{aligned}
\mathcal{A}_- &:= \inf_{t_2 \in [0,1)} \frac{\tilde{a}(t_2)}{\tilde{c}(t_2)}, \qquad \mathcal{A}_+ := \sup_{t_2 \in [0,1)} \frac{\tilde{a}(t_2)}{\tilde{c}(t_2)}, \\
\mathcal{B}_- &:= \inf_{t_2 \in [0,1)} \frac{\tilde{b}(t_2)}{\tilde{c}(t_2)}, \qquad \mathcal{B}_+ := \sup_{t_2 \in [0,1)} \frac{\tilde{b}(t_2)}{\tilde{c}(t_2)},
\end{aligned}
\tag{48}
$$

and use equation (47) in the derivation of the following result.

Proposition 4.13 *Fix $\alpha = 1$ and consider the restricted system* (39) $|_{\rho_2=0}$ *or, equivalently, the limiting system* (40). *For sufficiently small but fixed $E, R > 0$, solutions with initial conditions*

$$
(r_2(0), \theta_2(0), y(0), 0) \in \widetilde{\Sigma}_2^{\text{in}} := \left\{ \left(r_2, \theta_2, E^{-2}, 0 \right) : r_2 \in [\beta_-/ER, \beta_+/ER], \theta_2 \in \mathbb{R}/\mathbb{Z} \right\}
$$

reach the set

$$
\widetilde{\Sigma}_2^{\text{out}} := \left\{ \left(E^{-1}, \theta_2, y_2, 0 \right) : \theta_2 \in \mathbb{R}/\mathbb{Z}, y_2 \in [-\nu E^{-2}, \nu E^{-2}] \right\}
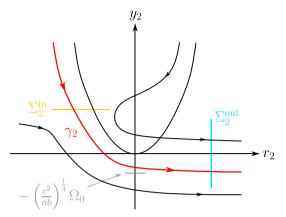$$

Fig. 12 Dynamics of the Riccati equation (41) in the (r_2, y_2)-plane for $\alpha = 2$ and a fixed choice of θ_2 (θ_2 is a parameter when $\alpha = 2$ and $\rho_2 = 0$). A qualitatively similar figure is obtained for each $\theta_2 \in \mathbb{R}/\mathbb{Z}$. The distinguished solution γ_2 with asymptotics described by Proposition 4.12 is shown in red. The parabola $y_2 = (b(\theta_2)/a(\theta_2))r_2^2$ which separates solutions with different asymptotic properties is also shown. Projections of the entry and exit sections Σ_2^{in} and Σ_2^{out} are shown in yellow and cyan, respectively (Color figure online)
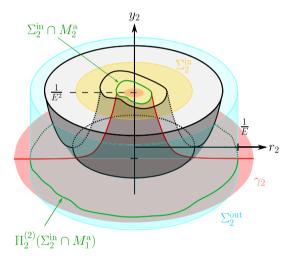

Fig. 13 Geometry and dynamics of the limiting Riccati equation $(39)|_{\rho_2=0}$ (or equivalently (40)) in (r_2, θ_2, y_2)-space. The two-dimensional surface γ_2 is shown in shaded red and coincides with the extension of the two-dimensional centre manifold N_1^{a} described in Lemma 4.6 into chart K_2 according to Proposition 4.12 Assertion (e). The evolution of initial conditions in Σ_2^{in} up to Σ_2^{out} is described by Proposition 4.16, which implies that the image $\Pi_2^{(2)}(\Sigma_2^{\mathrm{in}} \cap M_1^{\mathrm{a}}) \subset \Sigma_2^{\mathrm{out}}$, shown here in green, is contained within the surface defined by the graph $y_2 = -(c^2(\theta_2)/(a(\theta_2)b(\theta_2)))^{1/3}\Omega_0 + E$ over $\theta_2 \in \mathbb{R}/\mathbb{Z}$ (see also Lemma 4.17) (Color figure online)

in finite time, where $\nu > 0$ is a constant. In particular, we have that $\kappa_{12}(N_1^a \cap \Sigma_1^{out}) \subset \widetilde{\Sigma}_2^{in} \cap \{r_2 \in (\beta_-/ER, \beta_+/ER)\}$, where N_1^a is the unique centre manifold described in Lemma 4.6.

Proof The idea is to bound solutions to the Riccati equation (47) between upper and lower solutions with known asymptotics as $r_2 \to \infty$. Specifically, upper and lower solutions will be obtained as concatenations of solutions to Riccati equations of the form

$$\frac{dr_2}{dt_2} = \tilde{c}(t_2)\left(\lambda(\varphi(t_2) - y_2(0)) + \mu r_2^2\right), \tag{49}$$

where $\lambda, \mu \neq 0$ are suitably chosen constants. Note that it is equivalent to compare solutions of the two planar autonomous systems (45) and

$$\begin{aligned} r_2' &= \tilde{c}(t_2)(-\lambda y_2 + \mu r_2^2), \\ y_2' &= -\tilde{c}(t_2), \end{aligned} \tag{50}$$

which has asymptotic properties similar to those of system (41) with $a = \lambda$, $b = \mu$ and $c = 1$ (the factor of $\tilde{c}(t_2)$ does not effect the phase portrait since dr_2/dy_2 has no explicit time dependence).

We start by considering solutions of system (45) with initial conditions $(r_2(0), E^{-2})$ corresponding to points in $\widetilde{\Sigma}_2^{in}$ with $r_2(0) \in [\beta_-/ER, \beta_+/ER]$. Our first task is to bound the r_2-component of solutions to (45) on the interval $t_2 \in [0, T_0]$, where $T_0 > 0$ is the unique solution to $\varphi(T_0) = E^{-2}$. If a solution exists until $t_2 = T_0$ (and has not blown up in a finite time smaller than T_0), the definition of T_0 corresponds to the intersection of solutions with $\{y_2 = 0\}$ (recall that $y_2(t_2) = E^{-2} - \varphi(t_2)$, see (46)). We get a left-bound to the Riccati equation (47) by identifying a lower solution $\underline{r_2}(t_2) \leq r_2(t_2)$. This is obtained by letting $\underline{r_2}(t_2)$ be a solution of (49) with $(\underline{r_2}(0), y_2(0)) = (\beta_-/ER, E^{-2})$ and λ, μ replaced by

$$\underline{\lambda} = \mathcal{A}_+, \qquad \underline{\mu} = \mathcal{B}_-,$$

respectively. This ensures that $\underline{r_2}(0) \leq r_2(0)$ and

$$\frac{d\underline{r_2}}{dt_2} = \tilde{c}(t_2)\underline{\lambda}(\varphi(t_2) - E^{-2}) + \tilde{c}(t_2)\underline{\mu}\underline{r_2}^2 \leq \tilde{a}(t_2)(\varphi(t_2) - E^{-2}) + \tilde{b}(t_2)\underline{r_2}^2 \tag{51}$$

for all $t_2 \in [0, T_0]$, as $\varphi(t_2) - E^{-2} \leq 0$ for $t_2 \in [0, T_0]$. Solutions of equation (49) with $\lambda = \underline{\lambda}$ and $\mu = \underline{\mu}$ are described by Proposition 4.12 after a simple transformation similar to that in (42). In particular, there exists an invariant two-dimensional surface $\underline{\gamma_2}$ with properties similar to the surface γ_2, which intersects $\{y_2 = 0\}$. Choosing E and R sufficiently small guarantees that the initial condition $\underline{r_2}(0) = \beta_-/ER$ is smaller than the r_2-coordinate of the intersection $\underline{\gamma_2} \cap \{y_2 = E^{-2}\}$. This implies that the solution $(\underline{r_2}(t_2), y_2(t_2))$ also intersects $\{y_2 = 0\}$. Thus, using (47), we conclude that $\underline{r_2}(t_2)$ is a lower solution for $r_2(t_2)$, with $\underline{r_2}(t_2) \leq r_2(t_2)$ for all $t_2 \in [0, T_0]$.

An upper solution $\overline{r_2}(t_2)$ with the initial condition $(\overline{r_2}(0), y_2(0)) = (\beta_+/ER, E^{-2})$ can be constructed in a similar way, by identifying $\overline{r_2}(t_2)$ as the solution of the Riccati equation (49) with λ, μ replaced by

$$\overline{\lambda} = \mathcal{A}_-, \quad \overline{\mu} = \mathcal{B}_+,$$

respectively. We have that $\overline{r_2}(0) \geq r_2(0)$ and

$$\frac{d\overline{r_2}}{dt_2} = \tilde{c}(t_2)\overline{\lambda}(\varphi(t_2) - E^{-2}) + \tilde{c}(t_2)\overline{\mu}\overline{r_2}^2 \geq \tilde{a}(t_2)(\varphi(t_2) - E^{-2}) + \tilde{b}(t_2)\overline{r_2}^2 \quad (52)$$

for all $t_2 \in [0, T_0]$. There are now two different possibilities, depending on whether $\overline{r_2}(t_2)$ blows up in finite time for $\overline{r_2} \to \infty$ (case A), or exists up to the intersection with $\{y_2 = 0\}$, i.e. for all $t_2 \in [0, T_0]$ (case B). Blow-up for $\overline{r_2} \to -\infty$ is not possible as solutions of equation (49) with $\lambda = \overline{\lambda}$ and $\mu = \overline{\mu}$ are described by Proposition 4.12 after a simple transformation similar to that in (42). In particular, there exists an invariant two-dimensional surface $\overline{\gamma}_2$ with properties similar to the surface γ_2, which intersects $\{y_2 = 0\}$. Choosing E and R sufficiently small guarantees that the initial condition $\overline{r_2}(0) = \beta_+/ER$ is larger than the r_2-coordinate of the intersection $\overline{\gamma}_2 \cap \{y_2 = E^{-2}\}$, implying that $\overline{r_2}$ cannot blow up as $\overline{r_2} \to -\infty$. Hence it is sufficient to study case A and case B in the following.

In case A, the solution $\overline{r_2}(t_2)$ blows up in finite time $T_0^* < T_0$. The analogous statement to Proposition 4.12 for the Riccati equation with $a = \overline{\lambda}$, $b = \overline{\mu}$, $c = 1$ implies that $(\overline{r_2}(t_2), y_2(t_2))$ converges to a horizontal asymptote $y_2 = y_2^*$, therefore intersecting $\{r_2 = E^{-1}\}$ transversally (assuming $E > 0$ is small enough). Using (47), we conclude that $\overline{r_2}(t_2) \geq r_2(t_2)$ for all $t_2 \in [0, T_0^*)$. As $y_2' < 0$ it holds $y_2(t_2) \leq y_2^*$ for all $t_2 \geq T_0^*$, as long as the solution of (45) exists. We show later that $r_2(t_2)$ can also be bounded by a lower solution transversally intersecting $\{r_2 = E^{-1}\}$, such that also $r_2(t_2)$ transversally intersects $\{r_2 = E^{-1}\}$. By choosing E sufficiently small such that $y_2^* E^2 < \nu$, we can guarantee that the intersection takes place in $\{r_2 = E^{-1}, y_2 < \nu E^{-2}\}$.

In case B, $\overline{r_2}(t_2)$ exists for all $t_2 \in [0, T_0]$ and hence intersects $\{y_2 = 0\}$. Using (47), we can conclude that $\overline{r_2}(t_2) \geq r_2(t_2)$ for all $t_2 \in [0, T_0]$. Combining this with the results for the lower solution $\underline{r_2}(t_2)$, we have that

$$\underline{r_2}(t_2) \leq r_2(t_2) \leq \overline{r_2}(t_2),$$

on $t_2 \in [0, T_0]$. In particular, along $y_2 = 0$ we have

$$\underline{r_2}(T_0) \leq r_2(T_0) \leq \overline{r_2}(T_0).$$

The situation is sketched in Fig. 14 for case A and in Fig. 15 for case B.

The functions $\underline{r_2}$ and $\overline{r_2}$ (the latter only in case B) do not necessarily define lower and upper solutions when $y_2 < 0$ (i.e. when $t_2 > T_0$), since inequalities (51) and (52) may no longer be satisfied. We can, however, connect to different lower and upper solutions which we denote by $\underline{\tilde{r}_2}(t_2)$ and $\overline{\tilde{r}_2}(t_2)$, respectively, with initial conditions

$\underline{\tilde{r}_2}(T_0) = \underline{r_2}(T_0)$ and $\overline{\tilde{r}_2}(T_0) = \overline{r_2}(T_0)$, obtained as segments of solutions to (49) with λ, μ replaced by

$$\underline{\tilde{\lambda}} = \mathcal{A}_-, \qquad \underline{\tilde{\mu}} = \mathcal{B}_-,$$

and

$$\overline{\tilde{\lambda}} = \mathcal{A}_+, \qquad \overline{\tilde{\mu}} = \mathcal{B}_+,$$

respectively. This time, we may apply Proposition 4.12 for the Riccati equation with $a = \underline{\tilde{\lambda}}$, $b = \underline{\tilde{\mu}}$, $c = 1$ and $a = \overline{\tilde{\lambda}}$, $b = \overline{\tilde{\mu}}$, $c = 1$, respectively. We find that $\underline{\tilde{r}_2}(t_2)$, $\overline{\tilde{r}_2}(t_2) \to \infty$, and that orbits of the corresponding planar systems approach horizontal asymptotes $y_2 = y_{r_\pm}$ in the (r_2, y_2)-plane from above. Thus, $\underline{\tilde{r}_2}(t_2)$ and $\overline{\tilde{r}_2}(t_2)$ blow up in finite time. The relation $y_2(t_2) = E^{-2} - \varphi(t_2)$ leads to the following implicit equations for the blow-up times $t_2^\pm$:

$$\varphi(t_2^-) := E^{-2} - y_{r_-}, \qquad \varphi(t_2^+) := E^{-2} - y_{r_+}.$$

With initial conditions $\underline{\tilde{r}_2}(T_0) = \underline{r_2}(T_0)$ and $\overline{\tilde{r}_2}(T_0) = \overline{r_2}(T_0)$, the constructed upper and lower solutions guarantee that $\underline{\tilde{r}_2}(t_2) \leq r_2(t_2) \leq \overline{\tilde{r}_2}(t_2)$ for all $t_2 \in [T_0, t_2^+]$, see Fig. 15. Consequently there exists $t_2^c \in [t_2^+, t_2^-]$, such that $r_2(t_2) \to \infty$ as $t_2 \to t_2^c$ from below and $r_2(t_2)$ crosses the hyperplane $\{r_2 = E^{-1}\}$.

In case B, choosing E sufficiently small such that $\nu > |y_{r_-}|E^2$ guarantees that $\underline{\tilde{r}_2}(t_2)$ and $\overline{\tilde{r}_2}(t_2)$ and thus also $r_2(t_2)$ transversally intersect $\{r_2 = E^{-1}\}$ in the section $\widetilde{\Sigma}_2^{\text{out}}$.

In case A, choosing E sufficiently small such that such that $\nu > \max\{|y_{r_-}|, y^*\}E^2$ guarantees that $\underline{\tilde{r}_2}(t_2)$ and $\overline{r_2}(t_2)$ and thus also $r_2(t_2)$ transversally intersect $\{r_2 = E^{-1}\}$ in the section $\widetilde{\Sigma}_2^{\text{out}}$. $\qquad\qquad\qquad\qquad\qquad\qquad\qquad\qquad\qquad\square$

Remark 4.14 As pointed out by an anonymous referee, the proof of Proposition 4.13 can be simplified by fixing $\nu \geq 1$, in which case the existence of lower solutions $\underline{r_2}$ and $\underline{\tilde{r}_2}$ and the fact that $y_2' < 0$ are sufficient to show that solutions intersect $\widetilde{\Sigma}_2^{\text{in}}$. The existence of upper solutions $\overline{r_2}$ and $\overline{\tilde{r}_2}$ allows for greater control of the solutions when $\nu < 1$, but it is not strictly necessary for the proof of Theorem 3.2.

Propositions 4.12 and 4.13 can be used to describe the limiting behaviour of the y_2-component of the map $\Pi_2^{(\alpha)} : \Sigma_2^{\text{in}} \to \Sigma_2^{\text{out}}$ induced by the flow of initial conditions in

$$\Sigma_2^{\text{in}} := \left\{ \left(r_2, \theta_2, E^{-2}, \rho_2 \right) : r_2 \in [\beta_-/ER, \beta_+/ER], \theta_2 \in \mathbb{R}/\mathbb{Z}, \rho_2 \in [0, ER] \right\},$$

which is related to the exit section in chart K_1 via $\Sigma_2^{\text{in}} = \kappa_{12}(\Sigma_1^{\text{out}})$, up to the exit section

$$\Sigma_2^{\text{out}} := \left\{ \left(E^{-1}, \theta_2, y_2, \rho_2 \right) : \theta_2 \in \mathbb{R}/\mathbb{Z}, y_2 \in [-\nu E^{-2}, \nu E^{-2}], \rho_2 \in [0, ER] \right\},$$
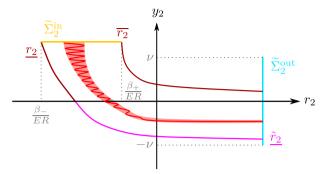
Fig. 14 Case A of the Riccati dynamics for $\alpha = 1$. The upper solution $\overline{r_2}$ does not intersect with $\{y_2 = 0\}$ and converges to a horizontal asymptote intersecting Σ_2^{out} transversally. The lower solution $\underline{r_2}$ intersects $\{y_2 = 0\}$ at $\underline{r_2}(T_0)$, where it connects to the lower solution $\tilde{r}_2$, which also converges to a horizontal asymptote intersecting Σ_2^{out} transversally. Solutions to the Riccati equation (47) with initial conditions in $\kappa_{12}(N_1^a \cap \Sigma_1^{\text{out}}) \subset \widetilde{\Sigma}_2^{\text{in}}$ are sketched in shaded red and have r_2-coordinates which are bounded between $\underline{r_2}$ and $\overline{r_2}$ ($\tilde{r}_2$ and $\overline{r_2}$) when $y_2 \geq 0$ ($y_2 \leq 0$). For fixed initial condition θ_2^*, a sample trajectory is shown in red (Color figure online)
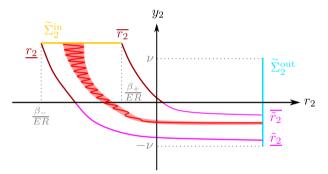

Fig. 15 Case B of the Riccati dynamics for $\alpha = 1$. The upper solution $\overline{r_2}$ intersects $\{y_2 = 0\}$ at $\overline{r_2}(T_0)$, where it connects to the upper solution $\bar{\tilde{r}}_2$, which converges to a horizontal asymptote intersecting Σ_2^{out} transversally. The lower solution $\underline{r_2}$ intersects $\{y_2 = 0\}$ at $\underline{r_2}(T_0)$, where it connects to the lower solution $\tilde{r}_2$, which also converges to a horizontal asymptote intersecting Σ_2^{out} transversally. Solutions to the Riccati equation (47) with initial conditions in $\kappa_{12}(N_1^a \cap \Sigma_1^{\text{out}}) \subset \widetilde{\Sigma}_2^{\text{in}}$ are sketched in shaded red and have r_2-coordinates which are bounded between $\underline{r_2}$ and $\overline{r_2}$ ($\tilde{r}_2$ and $\bar{\tilde{r}}_2$) when $y_2 \geq 0$ ($y_2 \leq 0$). For a fixed initial condition θ_2^*, a sample trajectory is shown in red (Color figure online)

where $\nu > 0$ is the constant in Proposition 4.13.

Similarly to the analysis in K_1, the remaining components of the image $\Pi_2^{(\alpha)}(r_2, \theta_2, E^{-2}, \rho_2)$ can be estimated directly.

Lemma 4.15 *Consider an initial condition $(r_2, \theta_2, E^{-2}, \rho_2)(0) = (r_2^*, \theta_2^*, E^{-2}, \rho_2) \in \Sigma_2^{\text{in}}$ for system* (39). *Then*

$$\theta_2(t_2) = \theta_2^* + \rho_2^{\alpha - 1} t_2 \qquad \text{mod } 1,$$

$$y_2(t_2) = \begin{cases} E^{-2} - \varphi(t_2) + \mathcal{O}(\rho_2 t_2), & \alpha = 1, \\ E^{-2} - t_2(c(\theta_2^*) + \mathcal{O}(\rho_2)), & \alpha = 2, \end{cases}$$

where $c(\theta_2^*) = const. > 0$ and $\varphi(t_2)$ is the function defined in (46).

Proof The solutions are obtained by direct integration.   □

In the following we define the function $h_{y_2}^{(\alpha)}(r_2, \theta_2)$ so that (i)

$$\Pi_2^{(1)}(\kappa_{12}(N_1^{\text{a}} \cap \Sigma_1^{\text{out}})) = (E^{-1}, \theta_2(T_2), h_{y_2}^{(1)}(E^{-1}, \theta_2), 0) \in \Sigma_2^{\text{out}},$$

(Proposition 4.13 guarantees the existence of this intersection), and (ii) $h_{y_2}^{(2)}(E^{-1}, \theta_2)$ is precisely the function $h_{y_2}^{(2)}$ defining the special Riccati solution in Proposition 4.12 (we simply suppressed the parameter dependence on θ_2 in the notation there). Combining Propositions 4.12–4.13 and Lemma 4.15, we obtain the following characterisation of the transition map $\Pi_2^{(\alpha)} : \Sigma_2^{\text{in}} \to \Sigma_2^{\text{out}}$, which summarises the dynamics in chart K_2.

Proposition 4.16 *For sufficiently small but fixed $E, R > 0$, $\Pi_2^{(\alpha)} : \Sigma_2^{\text{in}} \to \Sigma_2^{\text{out}}$ is a well-defined diffeomorphism of the form*

$$\Pi_2^{(\alpha)}\left(r_2, \theta_2, E^{-2}, \rho_2\right) = \left(E^{-1}, h_{\theta_2}^{(\alpha)}(r_2, \theta_2, \rho_2), h_{y_2}^{(\alpha)}(E^{-1}, \theta_2) + \mathcal{O}(r_2 - r_{2,c}, \rho_2), \rho_2\right),$$

where $r_{2,c}$ is the (generally θ_2-dependent) r_2-coordinate of the intersection $\kappa_{12}(N_1^{\text{a}} \cap \Sigma_1^{\text{out}}) \in \Sigma_2^{\text{in}}$, which is defined implicitly via the relation $h_{y_2}^{(\alpha)}(r_{2,c}, \theta_2) = E^{-2}$, and $h_{\theta_2}^{(\alpha)}(r_2, \theta_2, \rho_2) = \tilde{h}_{\theta_2}^{(\alpha)}(r_2, \theta_2, \rho_2) \mod 1$ where

$$\tilde{h}_{\theta_2}^{(\alpha)}(r_2, \theta_2, \rho_2) = \begin{cases} \theta_2 + \mathcal{O}(1), & \alpha = 1, \\ \theta_2 + \frac{\rho_2}{c(\theta_2)}\left(E^{-2} - h_{y_2}^{(2)}(E^{-1}, \theta_2)\right) + \rho_2\mathcal{O}(r_2 - r_{2,c}, \rho_2), & \alpha = 2. \end{cases}$$

Proof We start with the case $\alpha = 2$ and let $(r_{2,c}, \theta_2, E^{-2}, 0)$ denote the K_2 coordinates of the intersection $\gamma_2 \cap \Sigma_2^{\text{in}}$. It follows from Proposition 4.12 and Lemma 4.15 that

$$\Pi_2^{(2)}(r_{2,c}, \theta_2, E^{-2}, 0) = \left(E^{-1}, \theta_2 + \rho_2 T_2 \mod 1, h_{y_2}^{(2)}(E^{-1}, \theta_2), 0\right) \in \text{Int } \Sigma_2^{\text{out}},$$

where $T_2 > 0$ is the transition time taken from Σ_2^{in} to reach Σ_2^{out}, Int Σ_2^{out} denotes the interior of Σ_2^{out} in $\{E^{-1}\} \times \mathbb{R}/\mathbb{Z} \times \mathbb{R} \times \mathbb{R}_{\geq 0}$, and the containment in Int Σ_2^{out} follows from the asymptotics $h_{y_2}^{(2)}(\eta^{-1}, \theta_2) = -(c^2/ab)^{1/3}\Omega_0 + (c/b)\eta + \mathcal{O}(\eta^3)$ as $\eta \to 0^+$ in Proposition 4.12 Assertion (b) (note that $a = a(\theta_2)$, $b = b(\theta_2)$ and $c = c(\theta_2)$
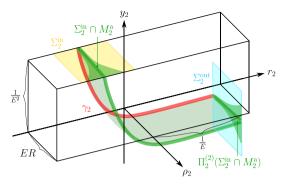
Fig. 16 Geometry and dynamics projected into (r_2, y_2, ρ_2)-space for $\alpha = 2$; c.f. Figs. 12 and 13. The extension of the (projected) three-dimensional manifold M_2^a is sketched in shaded green. The image of the wedge-shaped region $\kappa_{12}(\Pi_1^{(2)}(\Sigma_1^{in})) \subset \Sigma_2^{in}$ (recall Proposition 4.9) under $\Pi_2^{(2)}$ is also shown in shaded green (Color figure online)

are constant functions of the initial value θ_2 here). The transition time for an initial condition with $\rho_2 = 0$ can be estimated using Lemma 4.15. In particular,

$$y_2(T_2) = h_{y_2}^{(2)}(E^{-1}, \theta_2) = y_2(0) - c(\theta_2)T_2$$

$$= E^{-2} - c(\theta_2)T_2 \quad \Rightarrow \quad T_2 = \frac{E^{-2} - h_{y_2}^{(2)}(E^{-1}, \theta_2)}{c(\theta_2)},$$

which implies that

$$\Pi_2^{(2)}(r_{2,c}, \theta_2, E^{-2}, 0)$$
$$= \left(E^{-1}, \theta_2 + \frac{\rho_2}{c(\theta_2)} \left(E^{-2} - h_{y_2}^{(2)}(E^{-1}, \theta_2) \right) \mod 1, h_{y_2}^{(2)}(E^{-1}, \theta_2), 0 \right). \quad (53)$$

Since the transition time T_2 is finite and system (40) is a regular perturbation problem, a neighbourhood of $(r_{2,c}, \theta_2, E^{-2}, 0) \in \Sigma_2^{in}$ is mapped diffeomorphically to a neighbourhood of $\gamma_2 \cap \Sigma_2^{out}$ in Σ_2^{out}. The form of the map in Proposition 4.16 follows.

Now fix $\alpha = 1$. In this case the transition time T_2 satisfies $0 < T_2^- \le T_2 \le T_2^+ < \infty$, where $T_2^{\pm}$ are the transition times associated to the lower/upper solutions used in the proof of Proposition 4.13. The result from here follows similarly to the case $\alpha = 2$, using the fact that T_2 is finite and that system (40) is a regular perturbation problem. $\qquad \square$

The extension of M_2^a up to Σ_2^{out}, as described by Proposition 4.16, is shown in projections onto (r_2, θ_2, y_2)- and (r_2, y_2, ρ_2)-space for $\alpha = 2$ in Figs. 13 and 16, respectively.

Finally we note that if $\alpha = 2$, then the expression for $h_{y_2}^{(2)}(E^{-1}, \theta_2)$ (and therefore the map $\Pi_2^{(2)}$) can be simplified using the following result, which can be found in Krupa and Szmolyan (2001a).

Lemma 4.17 *For $\alpha = 2$, the Riccati function $h_{y_2}^{(2)}$ defined in Proposition* 4.12 *satisfies*

$$h_{y_2}^{(2)}\left(E^{-1}, \theta_2\right) = -\left(\frac{c^2}{ab}\right)^{1/3}\Omega_0 + E,$$

where $a = a(\theta_2)$, $b = b(\theta_2)$ and $c = c(\theta_2)$.

Proof This can be proven using the asymptotic properties of the decoupled Riccati equation (41) described in Proposition 4.12. Since the proof does not depend on the angular dynamics ($\theta_2 = const.$ when $\rho_2 = 0$ and $\alpha = 2$), we refer to Krupa and Szmolyan (2001a, Rem. 2.10 and Prop. 2.11). □

4.4 Dynamics in the Exit Chart K_3

In chart K_3 we study solutions close to the extension of the manifold $M_3^a = \kappa_{23}(M_2^a)$ as it leaves a neighbourhood of the singular cycle S_0^c.

Lemma 4.18 *Following the positive transformation of time $\rho_3 dt = dt_3$, the desingularised equations in chart K_3 are given by*

$$\begin{aligned}
\rho_3' &= \rho_3 F(\rho_3, \theta_3, y_3, \varepsilon_3), \\
\theta_3' &= \rho_3^{\alpha-1}\varepsilon_3^{\alpha}, \\
y_3' &= -2y_3 F(\rho_3, \theta_3, y_3, \varepsilon_3) + \varepsilon_3^3(-c(\theta) + \mathcal{O}(\rho_3)), \\
\varepsilon_3' &= -\varepsilon_3 F(\rho_3, \theta_3, y_3, \varepsilon_3),
\end{aligned}$$

(54)

where $F(\rho_3, \theta_3, y_3, \varepsilon_3) = b(\theta) - a(\theta)y_3 + \mathcal{O}(\rho_3)$.

Proof This follows after direct differentiation of the local coordinate expressions in (31) and subsequent application of the desingularisation $\rho_3 dt = dt_3$. □

Except for the angular coordinate θ_3, the analysis in K_3 is entirely local. Specifically, we focus on dynamics within the set

$$\mathcal{D}_3 := \{(\rho_3, \theta_3, y_3, \varepsilon_3) : \rho_3 \in [0, R], \theta_3 \in \mathbb{R}/\mathbb{Z}, y_3 \in [-\nu, \nu], \varepsilon_3 \in [0, E]\},$$

where E, R and ν are the same positive constants used to define the entry and exit sections in charts K_1 and K_2. System (54) has a circular critical manifold

$$Q := \{(0, \theta_3, 0, 0) : \theta_3 \in \mathbb{R}/\mathbb{Z}\},$$

with the following properties.

Lemma 4.19 *Consider system* (54)*. Q is normally hyperbolic and saddle type. More precisely, the linearisation along Q has eigenvalues*

$$\lambda_1 = b(\theta), \quad \lambda_2 = 0, \quad \lambda_3 = -2b(\theta), \quad \lambda_4 = -b(\theta),$$
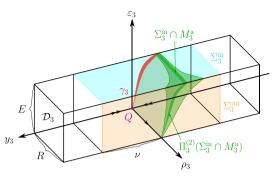
Fig. 17 Geometry and dynamics within $\mathcal{D}_3$, shown in $(r_3, \rho_3, \varepsilon_3)$-space for $\alpha = 2$. The (projection of the) two-dimensional surface $\gamma_3 = \kappa_{23}(\gamma_2)$ shown in red connects to the circular saddle-type critical manifold Q, which is indicated by the purple dot at the origin. Entry and exit sections Σ_3^{in} and Σ_3^{out} are shown in shaded cyan and orange, respectively. The wedge-shaped region within Σ_2^{out} (shown in shaded green in Fig. 16) is shown here in Σ_3^{in} (again in shaded green), along with its image in Σ_3^{out} under $\Pi_3^{(2)}$. The projection of the three-dimensional manifold M_3^a with base along $\gamma_3 \cup \{y_3 = \varepsilon_3 = 0, \rho_3 \geq 0\}$ is also shown (Color figure online)

and corresponding eigenvectors $(1, 0, 0, 0)$, $(0, 1, 0, 0)$, $(0, 0, 1, 0)$ and $(0, -\alpha \rho_3^{\alpha-1} \varepsilon_3^{\alpha-1}/b(\theta), 0, 1)$, respectively.

Proof Direct calculation. $\qquad\qquad\qquad\qquad\qquad\qquad\qquad\qquad\qquad\qquad\qquad\square$

Lemma 4.19 implies the existence of local centre, stable and unstable manifolds at Q. Specifically, there is a one-dimensional centre manifold $W_3^c(Q)$, a two-dimensional stable manifold $W_3^s(Q)$, and a one-dimensional unstable manifold $W_3^u(Q)$. The geometry is sketched in different three-dimensional subspaces and projections in Figs. 17, 18 and 19.

If $\alpha = 2$, we can show that the extension of the surface γ_2 connects to the critical manifold Q tangentially to the cylinder spanned by the centre and weakly stable eigenvectors.

Lemma 4.20 *Fix $\alpha = 2$. Then the extension of γ_2 under system* (54)*, i.e. $\gamma_3 = \kappa_{23}(\gamma_2)$, connects to Q tangentially to the cylinder segment* $\{(0, \theta_3, 0, \varepsilon_3) \in \mathcal{D}_3\}$.

Proof Applying the change of coordinates formula in (32) together with the Riccati asymptotics as $r_2 \to \infty$ in Proposition 4.12 Assertion (b), we obtain

$$\kappa_{23}(\gamma_2) \cap \mathcal{D}_3$$
$$= \left\{ \left(0, \theta_3, \varepsilon_3^2 \left(-\left(\frac{c^2}{ab}\right)^{1/3} \Omega_0 + \frac{c}{b}\varepsilon_3 + \mathcal{O}(\varepsilon_3^3) \right), \varepsilon_3 \right) : \theta_3 \in \mathbb{R}/\mathbb{Z}, \varepsilon_3 \in [0, E] \right\},$$

where $a = a(\theta_3)$, $b = b(\theta_3)$ and $c = c(\theta_3)$ are constant ($\theta_3' = 0$ in $\{\rho_3 = 0\}$), which converges to the critical manifold Q tangentially to $\{(0, \theta_3, 0, \varepsilon_3) \in \mathcal{D}_3\}$ as $\varepsilon_3 \to 0$. $\qquad\square$

Having described the geometry for $\alpha = 2$, we turn our attention to the characteristics of the map $\Pi_3^{(\alpha)} : \Sigma_3^{\text{in}} \to \Sigma_3^{\text{out}}$ induced by the flow of initial conditions in

$$\Sigma_3^{\text{in}} := \{(\rho_3, \theta_3, y_3, E) \in \mathcal{D}_3\},$$

which corresponds to the exit section Σ_2^{out} in chart K_2 via $\Sigma_3^{\text{in}} = \kappa_{23}(\Sigma_2^{\text{out}})$, up to the exit section

$$\Sigma_3^{\text{out}} := \{(R, \theta_3, y_3, \varepsilon_3) \in \mathcal{D}_3\},$$

which is precisely the representation of the exit section $\Delta_\varepsilon^{\text{out}}$ defined in (29) after blow-up in chart K_3 if we set $y_0 = R^2 \nu$. Similarly to the K_3 analysis for the regular fold point in Krupa and Szmolyan (2001a), $\Pi_3^{(\alpha)}$ can be analysed directly after a second positive transformation of time $F(\rho_3, \theta_3, y_3, \varepsilon_3)dt_3 = d\tilde{t}_3$, which amounts to division of the right-hand side in system (54) by $F(\rho_3, \theta_3, y_3, \varepsilon_3)$ (which is strictly positive in $\mathcal{D}_3$). This leads to the orbitally equivalent system

$$
\begin{aligned}
\rho_3' &= \rho_3, \\
\theta_3' &= \frac{\rho_3^{\alpha-1}\varepsilon_3^\alpha}{b(\theta_3) - a(\theta_3)y_3 + \mathcal{O}(\rho_3)} = \frac{\rho_3^{\alpha-1}\varepsilon_3^\alpha}{b(\theta_3)} + \mathcal{O}(\rho_3^{\alpha-1}\varepsilon_3^\alpha y_3, \rho_3^\alpha \varepsilon_3^\alpha), \\
y_3' &= -2y_3 + \frac{\varepsilon_3^3(-c(\theta_3) + \mathcal{O}(\rho_3))}{b(\theta_3) - a(\theta_3)y_3 + \mathcal{O}(\rho_3)} = -2y_3 - \varepsilon_3^3\frac{c(\theta_3)}{b(\theta_3)} + \mathcal{O}(\varepsilon_3^3 y_3, \rho_3\varepsilon_3^3), \\
\varepsilon_3' &= -\varepsilon_3,
\end{aligned}
\tag{55}
$$

where by a slight abuse of notation the prime notation now refers to differentiation with respect to $\tilde{t}_3$.

System (55) is used to obtain the following result.

Proposition 4.21 *Fix $\nu > 0$ and $E, R > 0$ sufficiently small. Then the map $\Pi_3^{(\alpha)} : \Sigma_3^{\text{in}} \to \Sigma_3^{\text{out}}$ is well-defined and given by*

$$\Pi_3^{(\alpha)}(\rho_3, \theta_3, y_3, E) = \left(R, h_{\theta_3}^{(2)}(\rho_3, \theta_3, y_3), h_{y_3}^{(\alpha)}(\rho_3, \theta_3, y_3), \frac{E}{R}\rho_3\right).$$

We have that $h_{\theta_3}^{(\alpha)}(\rho_3, \theta_3, y_3) = \tilde{h}_{\theta_3}^{(\alpha)}(\rho_3, \theta_3, y_3) \mod 1$, where

$$\tilde{h}_{\theta_3}^{(\alpha)}(\rho_3, \theta_3, y_3) = \begin{cases} \theta_3 + \mathcal{O}\left(\ln\left(\rho_3^{-1}\right)\right), & \alpha = 1, \\ \theta_3 + \mathcal{O}\left(\rho_3 \ln\left(\rho_3^{-1}\right)\right), & \alpha = 2. \end{cases}$$
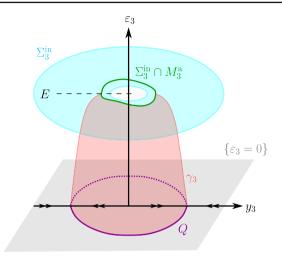
Fig. 18 Geometry and dynamics within the invariant hyperplane $\{\rho_3 = 0\}$ with $\alpha = 2$, projected into $(y_3, \theta_3, \varepsilon_3)$-space; c.f. Fig. 17 (Color figure online)
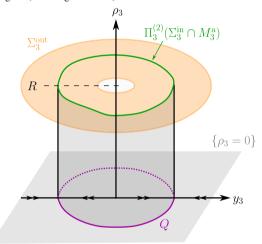

Fig. 19 Geometry and dynamics within the invariant hyperplane $\{\varepsilon_3 = 0\}$ with $\alpha = 2$, projected into (y_3, θ_3, ρ_3)-space; c.f. Figs. 17 and 18 (Color figure online)

Moreover, there exist constants $\sigma_- < \sigma_+$ such that in case $\alpha = 1$ we have

$$\left(-\nu + \sigma_- E^3\right)(1 + \mathcal{O}(\rho_3))\left(\frac{\rho_3}{R}\right)^2 \leq h_{y_3}^{(1)}(\rho_3, \theta_3, y_3)$$
$$\leq \left(\nu + \sigma_+ E^3\right)(1 + \mathcal{O}(\rho_3))\left(\frac{\rho_3}{R}\right)^2. \quad (56)$$

In case $\alpha = 2$ we have

$$h_{y_3}^{(2)}(\rho_3, \theta_3, y_3) = \left(y_3 - E^3\right)\left(\frac{\rho_3}{R}\right)^2 + \mathcal{O}\left(\rho_3^3 \ln\left(\rho_3^{-1}\right)\right).$$

Proof. We start with the case $\alpha = 2$, and consider solutions of system (55) which satisfy $(\rho_3, \theta_3, y_3, \varepsilon_3)(0) = (\rho_3^*, \theta_3^*, y_3^*, E) \in \Sigma_3^{in}$ and $(R, \theta_3, y_3, \varepsilon_3)(T_3) \in \Sigma_3^{out}$ for some $T_3 > 0$. The equations for ρ_3 and ε_3 can be solved directly, leading to $\rho_3(\tilde{t}_3) = \rho_3^* e^{\tilde{t}_3}$ and $\varepsilon_3(\tilde{t}_3) = E e^{-\tilde{t}_3}$, and the boundary constraint $\rho_3(T_3) = R$ leads to the following expression for the transition time:

$$T_3 = \ln\left(\frac{R}{\rho_3^*}\right). \tag{57}$$

It follows that $\varepsilon_3(T_3) = E \rho_3^*/R$, as required. We need to estimate $y_3(T_3)$ and $\theta_3(T_3)$ at $\tilde{t}_3 = T_3$. Since $\alpha = 2$, we have that

$$\theta_3' = \rho_3^* \left(E^2 e^{-\tilde{t}_3} \left(b(\theta_3) - a(\theta_3) y_3 + \mathcal{O}(\rho_3) \right) \right)^{-1}.$$

One can show with direct estimates that the term in parentheses is uniformly bounded by a positive constant, which implies that

$$\rho_3^* \zeta_- \tilde{t}_3 \leq \tilde{\theta}(\tilde{t}_3) - \theta_3^* \leq \rho_3^* \zeta_+ \tilde{t}_3,$$

for all $\tilde{t}_3 \in [0, T_3]$, where $\zeta_+ \geq \zeta_- > 0$ and $\tilde{\theta}_3$ is defined via $\theta_3(\tilde{t}_3) = \tilde{\theta}_3(\tilde{t}_3) \mod 1$. Using $\rho_3(\tilde{t}_3) = \rho_3^* e^{\tilde{t}_3}$, it follows that $\tilde{\theta}_3$ can be written in terms of ρ_3; specifically, we obtain

$$\tilde{\theta}_3(\rho_3) = \theta_3^* + \mathcal{O}\left(\rho_3^* \ln\left(\frac{\rho_3}{\rho_3^*}\right) \right), \tag{58}$$

where we permit a slight abuse of notation in switching the argument from $\tilde{t}_3$ to ρ_3. Substituting $\rho_3(\tilde{t}_3) = \rho_3^* e^{\tilde{t}_3}$ and evaluating the resulting expression at $\tilde{t}_3 = T_3$ yields the desired estimate for $\theta_3(T_3) = \tilde{h}_{\theta_3}^{(2)}(\rho_3, \theta_3, y_3) \mod 1$.

It remains to estimate $y_3(T_3)$. It will be helpful to use (58) in order to write

$$a(\theta_3) = a_3 + \mathcal{O}\left(\rho_3^* \ln\left(\frac{\rho_3}{\rho_3^*}\right) \right), \quad b(\theta_3) = b_3 + \mathcal{O}\left(\rho_3^* \ln\left(\frac{\rho_3}{\rho_3^*}\right) \right),$$

$$c(\theta_3) = c_3 + \mathcal{O}\left(\rho_3^* \ln\left(\frac{\rho_3}{\rho_3^*}\right) \right), \tag{59}$$

where $a_3 = a(\theta_3^*)$, $b_3 = b(\theta_3^*)$ and $c_3 = c(\theta_3^*)$. From here, we use and adaptation of the 'partial linearisation' method used in the proof of Krupa and Szmolyan (2001a, Prop. 2.11). Define a new variable $\tilde{\varepsilon}_3 = \varepsilon_3^3$, and consider the resulting equations within the invariant hyperplane $\{\rho_3 = 0\}$:

$$\theta_3' = 0,$$
$$y_3' = -2y_3 - \frac{c_3}{b_3}\tilde{\varepsilon}_3 + \mathcal{O}(y_3\tilde{\varepsilon}_3), \tag{60}$$
$$\tilde{\varepsilon}_3' = -3\tilde{\varepsilon}_3,$$

which may be considered as a θ_3^*-family of planar systems in the $(y_3, \tilde{\varepsilon}_3)$ variables, with constants a_3, b_3 and c_3 depending on the parameter θ_3^*. Since the Jacobian at the equilibrium $(0, 0)$ is hyperbolic and non-resonant with the eigenvalues -2 and -3, there exists a parameter-dependent, near-identity transformation of the form

$$\tilde{y}_3 = \psi(y_3, \tilde{\varepsilon}_3, \theta_3^*) = y_3 + \mathcal{O}(y_3\tilde{\varepsilon}_3), \qquad y_3 = \tilde{\psi}(\tilde{y}_3, \tilde{\varepsilon}_3, \theta_3^*) = \tilde{y}_3 + \mathcal{O}(\tilde{y}_3\tilde{\varepsilon}_3), \quad (61)$$

such that the transformed system has been linearised, i.e.

$$\begin{aligned}
\tilde{y}_3' &= -2\tilde{y}_3 - \frac{c_3}{b_3}\tilde{\varepsilon}_3, \\
\tilde{\varepsilon}_3' &= -3\tilde{\varepsilon}_3,
\end{aligned} \tag{62}$$

see e.g. Il'yashenko and Yakovenko (1991, Thm. 1). Applying transformation (61) to system (55) and using (59) leads to

$$\begin{aligned}
\rho_3' &= \rho_3, \\
\theta_3' &= \frac{\rho_3\varepsilon_3^2}{b(\theta_3)} + \mathcal{O}(\rho_3\varepsilon_3^2\tilde{y}_3, \rho_3^2\varepsilon_3^2), \\
\tilde{y}_3' &= -2\tilde{y}_3 - \frac{c_3}{b_3}\varepsilon_3^3 + \varepsilon_3^3\rho_3 H(\rho_3, \theta_3, \tilde{y}_3, \varepsilon_3), \\
\varepsilon_3' &= -\varepsilon_3,
\end{aligned} \tag{63}$$

where the remainder function $H(\rho_3, \theta_3, \tilde{y}_3, \varepsilon_3)$ is smooth and uniformly bounded over $\tilde{t}_3 \in [0, T_3]$. Substituting the solutions for $\rho_3(\tilde{t}_3)$ and $\varepsilon_3(\tilde{t}_3)$ into the equations for θ_3 and $\tilde{y}_3$ in system (63) leads to the planar non-autonomous system

$$\begin{aligned}
\theta_3' &= \frac{\rho_3^*E^2}{b(\theta_3)}e^{-\tilde{t}_3} + \rho_3^*\mathcal{O}(\tilde{y}_3 e^{-\tilde{t}_3}, \rho_3^*), \\
\tilde{y}_3' &= -2\tilde{y}_3 - \frac{c_3}{b_3}E^3 e^{-3\tilde{t}_3} + \rho_3^* E^3 e^{-2\tilde{t}_3} H(\rho_3^* e^{\tilde{t}_3}, \theta_3, \tilde{y}_3, E e^{-\tilde{t}_3}).
\end{aligned}$$

Now introduce a new time-dependent variable z_3 via

$$\tilde{y}_3(\tilde{t}_3) = \left(y_3^* - E^3 + z_3(\tilde{t}_3)\right)e^{-2\tilde{t}_3} + \frac{c_3}{b_3}E^3 e^{-3\tilde{t}_3}.$$

Differentiating $\tilde{y}_3(\tilde{t}_3)$ and using $\rho_3(\tilde{t}_3) = \rho_3^* e^{\tilde{t}_3}$ leads to the following ODE in z_3:

$$z_3' = \rho_3^* E^3 \tilde{H}\left(\rho_3^*, \theta_3, y_3^*, z_3, \tilde{t}_3\right),$$

with $\tilde{H}(\rho_3^*, \theta_3, y_3^*, z_3, \tilde{t}_3) := H(\rho_3^* e^{\tilde{t}_3}, \theta_3, (y_3^* - E^3 + z_3(\tilde{t}_3))e^{-2\tilde{t}_3} + (c_3/b_3)E^3 e^{-3\tilde{t}_3}, E e^{-\tilde{t}_3})$ and initial condition $z_3(0) = 0$. One can show that $\tilde{H}\left(\rho_3^*, \theta_3, y_3^*, z_3, \tilde{t}_3\right)$ is uniformly

bounded over $\tilde{t}_3 \in [0, T_3]$, so that integration gives

$$z_3(\tilde{t}_3) = \mathcal{O}(\rho_3^* \tilde{t}_3) \implies z_3(T_3) = \mathcal{O}\left(\rho_3^* \ln\left(\frac{1}{\rho_3^*}\right)\right).$$

Changing variables back to $\tilde{y}_3$ and evaluating at $\tilde{t}_3 = T_3$ yields

$$\tilde{y}_3(T_3) = (y_3^* - E^3 + z_3(T_3))e^{-2T_3} + \frac{c_3}{b_3}E^3 e^{-3T_3}$$
$$= (y_3^* - E^3)\left(\frac{\rho_3^*}{R}\right)^2 + \mathcal{O}\left((\rho_3^*)^3 \ln\left(\frac{1}{\rho_3^*}\right)\right),$$

and therefore

$$y_3(T_3) = (y_3^* - E^3)\left(\frac{\rho_3^*}{R}\right)^2 + \mathcal{O}\left((\rho_3^*)^3 \ln\left(\frac{1}{\rho_3^*}\right)\right)$$

as required.

Now fix $\alpha = 1$. The fact that $\tilde{\theta}_3(T_3) = \mathcal{O}(\ln \rho_3^{*-1})$ follows from direct estimates using the boundedness of the right-hand side of the equation for θ_3' and the expression for the transition time T_3 in (57). It remains to bound $y_3(T_3)$. Note that we cannot apply the same partial linearisation approach as we did for $\alpha = 2$, since θ_3 is dynamic (i.e. not constant) in $\{\rho_3 = 0\}$. We can, however, obtain a coarser estimate via a more direct approach. Notice that for sufficiently small E we have $y_3'|_{y_3=-v} > 0$ and $y_3'|_{y_3=v} < 0$. It follows that $\Pi_3^{(1)}$ is well-defined, since solutions are inflowing along the faces of $\mathcal{D}_3$ defined by $\{y = \pm v\}$ for all $\tilde{t}_3 \in [0, T_3]$. Moreover, there exist constants $\sigma_- < \sigma_+$ such that

$$-2y_3 + \sigma_- \varepsilon_3^3 \le y_3' \le -2y_3 + \sigma_+ \varepsilon_3^3,$$

for all $y \in [-v, v]$ and $\varepsilon_3 \in [0, E]$. Substituting $\varepsilon_3(\tilde{t}_3) = Ee^{-\tilde{t}_3}$ and solving the first-order linear equations

$$y_3^{\pm\prime} + 2y_3^{\pm} = \sigma_{\pm} E^3 e^{-3\tilde{t}_3},$$

we obtain lower and upper solutions on $\tilde{t}_3 \in [0, T_3]$ with the property that

$$y_3^-(\tilde{t}_3) = \left(-v + \sigma_- E^3\right)e^{-2\tilde{t}_3} - \sigma_- E^3 e^{-3\tilde{t}_3} \le y_3(\tilde{t}_3) \le y_3^+(\tilde{t}_3)$$
$$= \left(v + \sigma_+ E^3\right)e^{-2\tilde{t}_3} - \sigma_+ E^3 e^{-3\tilde{t}_3}.$$

Evaluating these expressions at $\tilde{t}_3 = T_3 = \ln(R/\rho_3^*)$ yields

$$\left(-\nu + \sigma_- E^3\right)\left(1 + \mathcal{O}(\rho_3^*)\right)\left(\frac{\rho_3^*}{R}\right)^2 \leq y_3(T_3) \leq \left(\nu + \sigma_+ E^3\right)\left(1 + \mathcal{O}(\rho_3^*)\right)\left(\frac{\rho_3^*}{R}\right)^2. \quad \square$$

Note that systems (54) and (55) are orbitally equivalent. Since the result in Proposition 4.21 only depends on the initial condition in Σ_3^{in}, and not on the transition time, it holds for both systems (54) and (55).

Remark 4.22 Similarly to the arguments used to describe the map $\Pi_1^{(\alpha)}$ in proof of Proposition 4.9, the arguments used to describe the map $\Pi_3^{(\alpha)}$ in Proposition 4.21 are (strictly speaking) only valid for initial conditions with $\rho_3 \in (0, R]$. This is not problematic since we aim to derive results for $\varepsilon > 0$. Moreover, $\Pi_3^{(\alpha)}$ can be smoothly and uniquely extended to $\rho_3 = 0$.

4.5 Proof of Theorem 3.2

We now combine the results obtained in the charts K_1, K_2 and K_3 in order to prove Theorem 3.2. The idea is to describe the extended map $\pi_\varepsilon^{(\alpha)} : \Delta_\varepsilon^{\text{in}} \to \Delta_\varepsilon^{\text{out}}$ defined in Section 4.1, the first three components of which coincide with components of $\pi^{(\alpha)} : \Delta^{\text{in}} \to \Delta^{\text{out}}$, via its preimage in the blown-up space:

$$\Pi^{(\alpha)} := \Pi_3^{(\alpha)} \circ \kappa_{23} \circ \Pi_2^{(\alpha)} \circ \kappa_{12} \circ \Pi_1^{(\alpha)} : \Sigma_1^{\text{in}} \to \Sigma_3^{\text{out}}.$$

This can be done explicitly using the change of coordinate maps κ_{ij} in Lemma 4.1 and the characterisation of $\Pi_1^{(\alpha)}$, $\Pi_2^{(\alpha)}$ and $\Pi_3^{(\alpha)}$ in Propositions 4.9, 4.16 and 4.21, respectively. The geometry is sketched in Fig. 20.

In order to prove Assertions (a)–(c), we need to derive the form of the map $\Pi^{(\alpha)}$. Initial conditions $(r_1, \theta_1, R, \varepsilon_1) \in \Sigma_1^{\text{in}}$ are mapped to Σ_1^{out} under $\Pi_1^{(\alpha)}$ as described by Proposition 4.9. Since $\Sigma_2^{\text{in}} = \kappa_{12}(\Sigma_1^{\text{out}})$, we obtain the following input for the map $\Pi_2^{(\alpha)}$:

$$\begin{aligned}
(r_2, \theta_2, y_2, \rho_2) &= \kappa_{12}\left(\Pi_1^{(\alpha)}(r_1, \theta_1, R, \varepsilon_1)\right) \\
&= \left(\frac{1}{E}\left(h_{r_1}^{(\alpha)}\left(h_{\theta_1}^{(\alpha)}(r_1, \theta_1, \varepsilon_1), \frac{R}{E}\varepsilon_1, E\right)\right.\right. \\
&\quad \left.\left. + \mathcal{O}\left(e^{-\tilde{\varrho}/\varepsilon_1^3}\right)\right), h_{\theta_1}^{(\alpha)}(r_1, \theta_1, \varepsilon_1), \frac{1}{E^2}, R\varepsilon_1\right), \quad (64)
\end{aligned}$$

where we recall that $h_{\theta_1}^{(\alpha)}(r_1, \theta_1, \varepsilon_1) = \tilde{h}_{\theta_1}^{(\alpha)}(r_1, \theta_1, \varepsilon_1) \mod 1$,

$$\tilde{h}_{\theta_1}^{(\alpha)}(r_1, \theta_1, \varepsilon_1) = \theta_1 + \frac{(R\varepsilon_1)^{\alpha-1}}{c_0}\left(\frac{1}{\varepsilon_1^2} + \mathcal{O}(1)\right), \quad (65)$$

and $c_0 := \int_0^1 c(\theta_1(t_1)) \, dt_1$. Using (64), Lemma 4.1 and Proposition 4.16, we obtain an expression for the input to the map $\Pi_3^{(\alpha)}$, namely

$$
\begin{aligned}
(\rho_3, \theta_3, y_3, \varepsilon_3) &= \kappa_{23}\left(\Pi_2^{(\alpha)}(r_2, \theta_2, y_2, \rho_2)\right) \\
&= \left(\frac{R}{E}\varepsilon_1, h_{\theta_2}^{(\alpha)}(r_2, \theta_2, \rho_2), E^2 h_{y_2}^{(\alpha)}(E^{-1}, \theta_2) + \mathcal{O}(\varepsilon_1), E\right), \quad (66)
\end{aligned}
$$

where we used the fact that $r_2 - r_{2,c} = \mathcal{O}(e^{-\tilde{\varrho}/\varepsilon_1^3})$ in the derivation of the third component in the right-hand side, and $h_{\theta_2}^{(\alpha)}(r_2, \theta_2, \rho_2) = \tilde{h}_{\theta_2}^{(\alpha)}(r_2, \theta_2, \rho_2) \mod 1$ with

$$
\begin{aligned}
&\tilde{h}_{\theta_2}^{(\alpha)}(r_2, \theta_2, \rho_2) \\
&= \begin{cases}
\tilde{h}_{\theta_1}^{(1)}(r_1, \theta_1, \varepsilon_1) + \mathcal{O}(1), & \alpha = 1, \\
\tilde{h}_{\theta_1}^{(2)}(r_1, \theta_1, \varepsilon_1) + \frac{R\varepsilon_1}{c(\theta_2)}\left(E^{-2} + \left(\frac{c^2}{ab}\right)^{1/3}\Omega_0 - E\right) + \mathcal{O}(\varepsilon_1^2), & \alpha = 2,
\end{cases} (67)
\end{aligned}
$$

where $c(\theta_2) = c\left(h_{\theta_1}^{(2)}(r_1, \theta_1, \varepsilon_1)\right)$. With regards to the third component in (66), if $\alpha = 1$ then we have

$$
-\nu \le E^2 h_{y_2}^{(1)}(E^{-1}, \theta_2) \le \nu,
$$

where $\nu > 0$ is the constant appearing in the definition of Σ_2^{out} (recall Proposition 4.13). If $\alpha = 2$, then by Lemma 4.17 it holds

$$
h_{y_2}^{(2)}(E^{-1}, \theta_2) = -\left(\frac{c(\theta_2)^2}{a(\theta_2)b(\theta_2)}\right)^{1/3}\Omega_0 + E,
$$

where $a(\theta_2) = a\left(h_{\theta_1}^{(2)}(r_1, \theta_1, \varepsilon_1)\right)$, $b(\theta_2) = b\left(h_{\theta_1}^{(2)}(r_1, \theta_1, \varepsilon_1)\right)$ and $c(\theta_2) = c\left(h_{\theta_1}^{(2)}(r_1, \theta_1, \varepsilon_1)\right)$.

Substituting the right-most expression in (66) into the expression for $\Pi_3^{(\alpha)}(\rho_3, \theta_3, y_3, E)$ in Proposition 4.21 yields an expression for $\Pi^{(\alpha)}(r_1, \theta_1, R, \varepsilon_1)$. We obtain

$$
\Pi^{(\alpha)}(r_1, \theta_1, R, \varepsilon_1) = \left(R, h_{\theta_3}^{(\alpha)}(\rho_3, \theta_3, y_3), h_{y_3}^{(\alpha)}(\rho_3, \theta_3, y_3), \varepsilon_1\right), \quad (68)
$$

and specify the second and third components in the following. We have $h_{\theta_3}^{(\alpha)}(\rho_3, \theta_3, y_3) = \tilde{h}_{\theta_3}^{(\alpha)}(\rho_3, \theta_3, y_3) \mod 1$, with

$$
\begin{aligned}
&\tilde{h}_{\theta_3}^{(\alpha)}(\rho_3, \theta_3, y_3) \\
&= \begin{cases}
\tilde{h}_{\theta_2}^{(1)}(r_1, \theta_1, \varepsilon_1) + \mathcal{O}\left(\ln \rho_3^{-1}\right) = \theta_1 + \frac{1}{c_0\varepsilon_1^2} + \mathcal{O}(\ln \varepsilon_1^{-1}), & \alpha = 1, \\
\tilde{h}_{\theta_2}^{(2)}(r_1, \theta_1, \varepsilon_1) + \mathcal{O}\left(\rho_3 \ln \rho_3^{-1}\right) = \theta_1 + \frac{R}{c_0\varepsilon_1} + \mathcal{O}(\varepsilon_1 \ln \varepsilon_1^{-1}), & \alpha = 2,
\end{cases}
\end{aligned}
$$

where we used (65) and (67) in order to obtain the right-hand side. It remains to specify the third component in the right-hand side of (68). If $\alpha = 1$, we can use the bounds in (56) to estimate

$$\left(-\nu + \sigma_- E^3\right)\left(\frac{\varepsilon_1}{E}\right)^2 + \mathcal{O}\left(\varepsilon_1^3\right) \le h_{y_3}^{(1)}(\rho_3, \theta_3, y_3) \le \left(\nu + \sigma_+ E^3\right)\left(\frac{\varepsilon_1}{E}\right)^2 + \mathcal{O}\left(\varepsilon_1^3\right)$$

for constants $\nu > 0$ and $\sigma_- < \sigma_+$, such that $h_{y_3}^{(1)}(\rho_3, \theta_3, y_3) = \mathcal{O}(\varepsilon_1^2)$. If $\alpha = 2$, then

$$h_{y_3}^{(2)}(\rho_3, \theta_3, y_3) = \left(E^2 h_{y_2}^{(2)}(E^{-1}, \theta_2) - E^3\right)\left(\frac{\varepsilon_1}{E}\right)^2 + \mathcal{O}\left(\varepsilon_1^3 \ln \varepsilon_1^{-1}\right)$$

$$= -\left(\frac{c(\theta_3)^2}{a(\theta_3)b(\theta_3)}\right)^{1/3}\Omega_0\varepsilon_1^2 + \mathcal{O}\left(\varepsilon_1^3 \ln \varepsilon_1^{-1}\right),$$

where

$$a(\theta_3) = a\left(h_{\theta_3}^{(2)}(\rho_3, \theta_3, y_3)\right) = a(\theta_2) + \mathcal{O}(\varepsilon_1 \ln \varepsilon_1^{-1}),$$

$$b(\theta_3) = b\left(h_{\theta_3}^{(2)}(\rho_3, \theta_3, y_3)\right) = b(\theta_2) + \mathcal{O}(\varepsilon_1 \ln \varepsilon_1^{-1}),$$

$$c(\theta_3) = c\left(h_{\theta_3}^{(2)}(\rho_3, \theta_3, y_3)\right) = c(\theta_2) + \mathcal{O}(\varepsilon_1 \ln \varepsilon_1^{-1}),$$

which follows from $a(\theta_2) = a(h_{\theta_1}^{(2)}(r_1, \theta_1, \varepsilon_1))$, $b(\theta_2) = b(h_{\theta_1}^{(2)}(r_1, \theta_1, \varepsilon_1))$, $c(\theta_2) = c(h_{\theta_1}^{(2)}(r_1, \theta_1, \varepsilon_1))$ together with $\tilde{h}_{\theta_3}^{(2)}(\rho_3, \theta_3, y_3) = \tilde{h}_{\theta_1}^{(2)}(r_1, \theta_1, \varepsilon_1) + \mathcal{O}(\varepsilon_1 \ln \varepsilon_1^{-1})$.

Applying the blow-down transformations defined by the local coordinate formulae in (31) to (68) yields the map

$$\pi_\varepsilon^{(\alpha)}(r, \theta, R^2, \varepsilon) = \left(R, h_\theta^{(\alpha)}(r, \theta, \varepsilon), h_y^{(\alpha)}(r, \theta, \varepsilon), \varepsilon\right), \tag{69}$$

for all $\varepsilon \in (0, \varepsilon_0]$ (the limiting value $\varepsilon = 0$ is omitted because the blow-down transformation is only defined for $\varepsilon > 0$). The estimates above 'blow-down' to those given in Assertion (b) in Theorem 3.2, since the map π is identified with π_ε after omitting the trivial component $\varepsilon \mapsto \varepsilon$. Assertion (a) is a direct consequence of Assertion (b).

It remains to prove the strong contraction property in Assertion (c). This can be done by differentiating the expression for $\Pi^{(\alpha)}$. Letting $\mathcal{Q}^{(\alpha)} := \Pi_3^{(\alpha)} \circ \kappa_{23} \circ \Pi_2^{(\alpha)} \circ \kappa_{12}$, we obtain

$$\frac{\partial \Pi^{(\alpha)}}{\partial r_1}(r_1, \theta_1, R, \varepsilon_1) = \frac{\partial \mathcal{Q}^{(\alpha)}}{\partial r_1}\left(\Pi_1^{(\alpha)}(r_1, \theta_1, R, \varepsilon_1)\right)\frac{\partial \Pi_1^{(\alpha)}}{\partial r_1}(r_1, \theta_1, R, \varepsilon_1),$$

after applying the chain rule. Direct calculations using Lemma 4.1, Propositions 4.16 and 4.21 show that $(\partial \mathcal{Q}^{(\alpha)}/\partial r_1)(\Pi_1^{(\alpha)}(r_1, \theta_1, R, \varepsilon_1))$ is (at worst) algebraically growing in r_1 and ε_1. Since the second term $(\partial \Pi_1^{(\alpha)}/\partial r_1)(r_1, \theta_1, R, \varepsilon_1)$ is exponentially
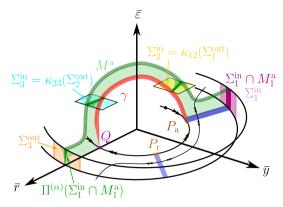
Fig. 20 Global geometry and dynamics in the blown-up space projected into $(\bar{r}, \bar{y}, \bar{\varepsilon})$-space. The three-dimensional manifold M^{a} which extends from $\Delta_{\varepsilon}^{\mathrm{in}}$ up to $\Delta_{\varepsilon}^{\mathrm{out}}$ (which are identified with Σ_1^{in} and Σ_3^{out}, respectively) is shown again in shaded green. Theorem 3.2 is proven by combining results obtained in charts K_1, K_2 and K_3: The flow from Σ_1^{in} to Σ_1^{out} is described by Proposition 4.9, the flow from Σ_2^{in} to Σ_2^{out} is described by Proposition 4.16, and the flow from Σ_3^{in} to Σ_3^{out} is described by Proposition 4.21 (Color figure online)

small due to the strong contraction in K_1, recall Proposition 4.9 Assertion (b), it follows that

$$\frac{\partial \Pi^{(\alpha)}}{\partial r_1}(r_1, \theta_1, R, \varepsilon_1) = \mathcal{O}\left(\mathrm{e}^{-\tilde{\varrho}/\varepsilon_1^3}\right),$$

for a constant $\tilde{\varrho} > 0$, assuming the constant E bounding ε_1 is sufficiently small. Assertion (c) in Theorem 3.2 follows for all $\varepsilon \in (0, \varepsilon_0]$ with ε_0 sufficiently small after applying the blow-down transformation (in particular $\varepsilon_1 = \varepsilon/R$).   □

5 Applications

In this section we consider semi-oscillatory dynamics near folded limit cycle manifolds in two different applications. Specifically, we consider

1. Periodically forced oscillators of Liénard type;
2. A toy model 'normal form' for the study of tipping phenomena in climate systems proposed in Zhu et al. (2015).

The first of these will allow us to illustrate the application of the main results in Sect. 3. The second is an example of a model exhibiting a folded limit cycle bifurcation in the partial singular limit $\varepsilon_1 > 0$, $\varepsilon_2 \to 0$ (recall system (5)), which violates both Assumptions 1–2.

5.1 Periodically Forced Oscillators

Periodically forced oscillators in mechanical and electrical engineering can often be modelled using Liénard equations of the form

$$x'' + \mu f(x)x' + g(x) = A(\omega t), \tag{70}$$

where $A(\omega t) = A(\omega t + 1)$ for all $t \in \mathbb{R}$, the friction/resistance function $f(x)$ is smooth, and the parameters μ and ω determine the magnitude of the friction/resistance and the frequency of the (periodic) forcing term A, respectively.

Remark 5.1 A very well-known and historically important example of a Liénard equation is the van der Pol equation (van der Pol 1920, 1926). We refer to Burke et al. (2016), Guckenheimer et al. (2003), Haiduc (2008) for detailed geometric studies of the (local and global) dynamics of the periodically forced van der Pol equation in a number of frequency regimes.

We recast equation (70) as an autonomous dynamical system by (i) rescaling time via $\tau = \mu^{-1}t$, and (ii) introducing new variables via the *Liénard transformation*

$$y := -\mu^{-1}x' + K(x), \qquad s = \omega\mu\tau,$$

where $K(x) = -\int_0^x f(\xi)\,d\xi$. This leads to

$$\dot{x} = \mu^2 \left(-y + K(x)\right),$$
$$\dot{s} = \mu\omega,$$
$$\dot{y} = g(x) - A(s),$$

where the overdot denotes now differentiation with respect to τ. Exploiting the periodicity property $A(s + 1) = A(s)$ in order to replace s with an angular variable $\theta \in \mathbb{R}/\mathbb{Z}$ and rewriting the system on the (new) fast time-scale defined by $\tilde{t} = \mu^2\tau$ leads to

$$x' = -y + K(x),$$
$$\theta' = \mu^{-1}\omega,$$
$$y' = \mu^{-2}\left(g(x) - A(\theta)\right),$$

where by a slight abuse of notation, we allow the dash to denote differentiation with respect to the new time $\tilde{t}$. Our analysis applies in particular scaling regimes with $0 < \mu^{-1}\omega, \mu^{-2} \ll 1$. Specifically, we derive results for scaling regimes defined by

$$\varepsilon^\alpha = \mu^{-1}\omega\vartheta^{-1}, \qquad \varepsilon^3 = \mu^{-2}, \tag{71}$$

where $\alpha \in \mathbb{N}_+$ and $\vartheta > 0$ is a parameter such that $\vartheta = \mathcal{O}(1)$ as $\varepsilon \to 0$. Note that this is equivalent to considering the scaling regimes defined by

$$\omega = \vartheta\mu^{1 - \frac{2}{3}\alpha}, \qquad \alpha = 1, 2, \ldots, \qquad 0 < \mu^{-1} \ll 1. \tag{72}$$

After one more change of time-scale $\hat{t} = \vartheta \tilde{t}$, our system becomes

$$
\begin{aligned}
x' &= -\vartheta^{-1}y + \vartheta^{-1}K(x), \\
\theta' &= \varepsilon^{\alpha}, \\
y' &= \varepsilon^3 \left(\vartheta^{-1}g(x) - \vartheta^{-1}A(\theta) \right),
\end{aligned}
$$

where by a slight abuse of notation, we now allow the dash to denote differentiation with respect to the time $\hat{t}$. Finally, we assume the following properties of the functions K, g and A.

Assumption 3 There exists a point x_F such that

$$
\frac{\partial K}{\partial x}(x_F) = 0, \qquad \frac{\partial^2 K}{\partial x^2}(x_F) > 0, \qquad g(x_F) - A(\theta) < 0,
$$

for all $\theta \in \mathbb{R}/\mathbb{Z}$.

Assumption 3 implies that the critical manifold, given by $S_0 = \{(x, \theta, K(x)) : x \in \mathbb{R}, \theta \in \mathbb{R}/\mathbb{Z}\}$, contains a regular folded cycle $S_0^c = \{(x_F, \theta, K(x_F)) : \theta \in \mathbb{R}/\mathbb{Z}\}$. The set S_0^c can be moved to the 'origin' via the coordinate translation $(\tilde{x}, \tilde{y}) = (x - x_F, y - K(x_F))$, which yields the system

$$
\begin{aligned}
\tilde{x}' &= -a(\theta)\tilde{y} + b(\theta)\tilde{x}^2 + \mathcal{O}(\tilde{x}^3), \\
\theta' &= \varepsilon^{\alpha}, \\
\tilde{y}' &= \varepsilon^3 \left(-c(\theta) + \mathcal{O}(\tilde{x}) \right),
\end{aligned} \tag{73}
$$

which is—up to relabelling $(\tilde{x}, \tilde{y}) \leftrightarrow (r, y)$—in general form (22) with

$$
\begin{aligned}
a(\theta) &\equiv \vartheta^{-1}, \qquad b(\theta) \equiv \vartheta^{-1}\frac{1}{2}\frac{\partial^2 K}{\partial x^2}(x_F) =: \vartheta^{-1}\frac{1}{2}K''(x_F), \\
c(\theta) &= -\vartheta^{-1}\left(g(x_F) - A(\theta)\right),
\end{aligned} \tag{74}
$$

all of which are strictly positive due to Assumption 3. Using the same relabelling, we define entry and exit sections Δ^{in} and Δ^{out} analogously to those in (23) and (24), respectively, and let $\pi^{(\alpha)} : \Delta^{\text{in}} \to \Delta^{\text{out}}$ denote the transition map induced by the forward flow of system (73) for a given $\alpha \in \mathbb{N}_+$.

Theorem 5.2 *Consider system* (73) *with fixed* $\alpha \in \mathbb{N}_+$. *There exists an* $\varepsilon_0 > 0$ *such that for all* $\varepsilon \in (0, \varepsilon_0]$, *the map* $\pi^{(\alpha)} : \Delta^{\text{in}} \to \Delta^{\text{out}}$ *is described by Theorem* 3.2 *after relabelling* $(\tilde{x}, \tilde{y}) \leftrightarrow (r, y)$. *In particular, we have*

$$
\tilde{h}_{\theta}^{(\alpha)}(\tilde{x}, \theta, \varepsilon) = \begin{cases} \theta + \frac{R^2}{c_0}\varepsilon^{-2} + \mathcal{O}(\ln \varepsilon), & \alpha = 1, \\ \theta + \frac{R^2}{c_0}\varepsilon^{-1} + \mathcal{O}(\varepsilon \ln \varepsilon), & \alpha = 2, \\ \psi(\theta) + \mathcal{O}(\varepsilon^3 \ln \varepsilon), & \alpha = 3, \\ \theta + \mathcal{O}(\varepsilon^3 \ln \varepsilon), & \alpha \geq 4, \end{cases}
$$

where

$$c_0 = -\vartheta^{-1} g(x_F) + \vartheta^{-1} \int_0^1 A(\theta) \mathrm{d}\theta, \qquad \psi(\theta) = \theta + \frac{1}{2} \vartheta \frac{K''(x_F)}{A(\theta) - g(x_F)} R + \mathcal{O}(R^2),$$

and

$$h_{\tilde{y}}^{(\alpha)}(\tilde{\theta}, \varepsilon) = \begin{cases} \mathcal{O}(\varepsilon^2), & \alpha = 1, \\ -\left(\frac{2(g(x_F) - A(\tilde{\theta}))^2}{K''(x_F)} \right)^{1/3} \Omega_0 \varepsilon^2 + \mathcal{O}(\varepsilon^3 \ln \varepsilon), & \alpha \geq 2. \end{cases}$$

Proof This is a direct application of Theorem 3.2, using the notation of (73) and the identities in (74). □

Note that via (71), the results in Theorem 5.2 can be reformulated and restated for the scaling regimes defined by (72). As for our main results in Sect. 3, the results for scalings corresponding to semi-oscillatory dynamics ($\alpha \in \{1, 2\}$) cannot be obtained using established theory for two time-scale systems. These results are new, to the best of our knowledge, even for the forced van der Pol example (the intermediate frequency regime considered in Burke et al. (2016) covers the case $\alpha = 3/2$).

5.2 Tipping Phenomena in Climate Systems

The authors in Zhu et al. (2015) proposed the following simple normal form for studying early warning signs for saddle-node induced tipping in climate systems:

$$z'(t) = \tilde{a}(t) - z^2 - \mathcal{A}\sin(2\pi\omega t), \qquad \tilde{a}(t) = \tilde{a}(0) - \tilde{\delta}t,$$

where $0 < \tilde{\delta} \ll 1$ and the parameters $\mathcal{A}, \omega > 0$ determine the amplitude, frequency of the sinusoidal periodic forcing term, respectively. This can recast as an autonomous system of the form

$$\begin{aligned} z' &= \tilde{a} - z^2 - \mathcal{A}\sin(2\pi\theta), \\ \theta' &= \omega, \\ \tilde{a}' &= -\tilde{\delta}, \end{aligned} \tag{75}$$

where $\theta \in \mathbb{R}/\mathbb{Z}$. We shall be interested in the dynamics when $0 < \tilde{\delta}, \omega \ll 1$, and in particular the semi-oscillatory case $0 < \tilde{\delta} \ll \omega \ll 1$. In this case, system (75) is oscillatory with respect to the partial singular limit $\omega > 0, \tilde{\delta} \to 0$, but stationary with respect to the double singular limit $(\omega, \tilde{\delta}) \to (0, 0)$.

We are particularly interested in system (75) as a model example of a system which violates Assumptions 1–2.

Proposition 5.3 *Consider system (75) with $\omega > 0$ fixed and $0 < \tilde{\delta} \ll 1$. This system has a regular fold of limit cycles at $z = \tilde{a} = 0$. In particular, the necessary*

and sufficient conditions on the Poincaré map in (9) *and* (10) *are satisfied; however, Assumptions* 1 *and* 2 *are not.*

Proof The fact that Assumptions 1–2 are violated follows from direct calculations on the system obtained from (75) in the partial singular limit $\omega > 0$, $\tilde{\delta} \to 0$. The details are omitted for brevity.

In order to verify the existence of a regular fold of cycles, we derive an expression for the Poincaré map P induced on a section contained in the plane $\{\theta = 0\}$. Using the fact that

$$\frac{\mathrm{d}z}{\mathrm{d}\theta} = \omega^{-1}\left(\tilde{a} - z^2 - \mathcal{A}\sin(2\pi\theta)\right), \qquad \frac{\mathrm{d}\tilde{a}}{\mathrm{d}\theta} = -\omega^{-1}\tilde{\delta},$$

we obtain

$$P(z, \tilde{a}, \omega, \tilde{\delta}) = \begin{pmatrix} P_z(z, \tilde{a}, \omega, \tilde{\delta}) \\ P_{\tilde{a}}(z, \tilde{a}, \omega, \tilde{\delta}) \end{pmatrix} = \begin{pmatrix} z \\ \tilde{a} \end{pmatrix} + \omega^{-1}\begin{pmatrix} \int_0^1 \left(\tilde{a}(\theta) - z(\theta)^2\right)\mathrm{d}\theta \\ -\tilde{\delta} \end{pmatrix}.$$

This expression can be used to check the necessary and sufficient conditions in (9) and (10) for a regular fold of cycles directly. $\qquad\square$

Our aim in what follows is to demonstrate that problems of this kind can (to a large extent) be analysed with existing theory for two time-scale systems. We shall restrict attention to scaling regimes defined by

$$\tilde{\delta} = \varepsilon^3 \nu, \qquad \omega = \varepsilon^\alpha,$$

where $\nu = \mathcal{O}(1)$ as $\varepsilon \to 0$ and $\alpha \in \mathbb{N}_+$. We shall also simplify the fast equation by defining a new variable $a := \tilde{a} - \mathcal{A}\sin(2\pi\theta)$. This leads to

$$\begin{aligned} z' &= a - z^2, \\ \theta' &= \varepsilon^\alpha, \\ a' &= -2\pi\varepsilon^\alpha \mathcal{A}\cos(2\pi\theta) - \varepsilon^3\nu. \end{aligned} \qquad (76)$$

The main results for this section will describe the dynamics of system (76). Letting $\varepsilon \to 0$ yields the layer problem

$$\begin{aligned} z' &= a - z^2, \\ \theta' &= 0, \\ a' &= 0. \end{aligned} \qquad (77)$$

The critical manifold is given by $S_0 = \{(z, \theta, z^2) : z \in \mathbb{R}, \theta \in \mathbb{R}/\mathbb{Z}\}$, and the non-trivial eigenvalue of the linearisation along S_0 is $\lambda = -2z$. This implies a folded critical manifold structure $S_0 = S_0^a \cup S_0^c \cup S_0^r$, where $S_0^a = S_0 \cap \{z > 0\}$ ($S_0^r = S_0 \cap \{z < 0\}$) is normally hyperbolic and attracting (repelling), and $S_0^c = \{(0, \theta, 0) : \theta \in \mathbb{R}/\mathbb{Z}\}$ is of regular fold type.

The reduced problem on S_0 will differ depending on the scaling, i.e. depending on the value of α. We are primarily interested in the cases $\alpha \in \{1, 2\}$, for which $0 < \tilde{\delta} \ll \omega \ll 1$; see however Remark 5.8 below for the cases $\alpha \geq 3$. Fixing $\alpha \in \{1, 2\}$, rewriting system (76) on the slow time-scale $\tau = \varepsilon^\alpha t$, and taking the limit $\varepsilon \to 0$ yields the reduced problem

$$
\begin{aligned}
0 &= a - z^2, \\
\dot{\theta} &= 1, \\
\dot{a} &= -2\pi \mathcal{A} \cos(2\pi\theta).
\end{aligned}
\tag{78}
$$

This leads to the following reduced vector field on S_0, expressed in the (z, θ)-coordinate chart:

$$
\begin{aligned}
\dot{z} &= -\frac{\pi \mathcal{A}}{z} \cos(2\pi\theta), \\
\dot{\theta} &= 1.
\end{aligned}
\tag{79}
$$

It is typical for problems of this kind to consider the so-called *desingularised reduced problem* (Kuehn 2015; Szmolyan and Wechselberger 2001; Wechselberger 2020). This may be obtained after a (singular) time transformation which amounts to multiplication of the vector field by z (see again Remark 2.2), leading to

$$
\begin{aligned}
\dot{z} &= -\pi \mathcal{A} \cos(2\pi\theta), \\
\dot{\theta} &= z.
\end{aligned}
\tag{80}
$$

System (80) is orbitally equivalent to system (79) on $S_0 \setminus S_0^c$, but the orientation of orbits on S_0^r (where $z < 0$) is reversed. Direct calculations reveal the presence of two equilibria along S_0^c, namely

$$
p_s : (0, 1/4), \qquad p_c : (0, 3/4),
$$

which are of neutral folded saddle and folded centre type, respectively (see Szmolyan and Wechselberger 2001 for definitions), see Fig. 21. Moreover, system (80) is Hamiltonian, with Hamiltonian function

$$
H(z, \theta) = \frac{\mathcal{A}}{2} \sin(2\pi\theta) + \frac{z^2}{2}.
$$

Except for the points p_s and p_c, there are three different types of orbits shown in Fig. 21. These are identified in the following result.

Lemma 5.4 *Consider the reduced problem* (79). *Orbits are contained within constant level sets* $H(z, \theta) = K \geq -\mathcal{A}/2$, *where*

1. $K = -\mathcal{A}/2$ *corresponds to the folded centre* p_c.
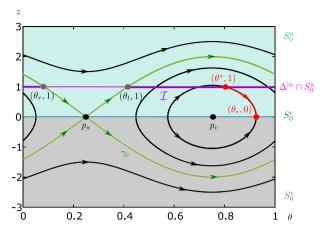
Fig. 21 Dynamics of the reduced problem (79) on S_0, projected into the (θ, z)-plane. We sketch the case with $\mathcal{A} = 2$ and $R = 1$, where we recall that $R > 0$ is the constant used to define Δ^{in}. The normally hyperbolic and attracting (repelling) branch S_0^{a} (S_0^{r}) is indicated in shaded turquoise (grey). The fold cycle S_0^{c} which separates these two branches is sketched in blue. There are two folded singularities on S_0^{c}: a neutral folded saddle p_s, and a folded centre p_c. The singular true and faux canards through p_s coincide in this case (denoted γ_c and shown in green), forming a limit cycle of period 2, and the region bounded outside of γ_c is foliated by periodic orbits of period 1. Finally, we sketch the forward evolution of an initial condition in $\Delta^{\text{in}} \cap S_0^{\text{a}}$ with initial angle $\theta^* \in \mathcal{I}$ (the interval $\mathcal{I}$ is shown in blue), i.e. inside the region bounded by γ_c. Such points reach a regular jump point on S_0^{c} with angle $\theta_e \in (3/4, 1) \cup [0, 1/4)$ in finite time. For $\mathcal{A} = 2$ and $R = 1$ we have $\theta_l = 5/12$, $\theta_r = 1/12$. The initial condition in red has angle $\theta^* = 5/6$, for which our results imply a jump angle of $\theta_e(\theta^*) = 11/12$ (Color figure online)

2. $K \in (-\mathcal{A}/2, \mathcal{A}/2)$ correspond to orbits that connect to the folded cycle S_0^{c} in both forward and backward time.
3. $K = \mathcal{A}/2$ corresponds to two saddle homoclinic orbits in the desingularised reduced problem (80), and a periodic orbit γ_c of period $\tau = 2$ along the true and faux canards through the neutral folded saddle p_s in the reduced problem (79).
4. $K > \mathcal{A}/2$ corresponds to periodic orbits of period $\tau = 1$ outside of the region bounded by γ_c.

Proof This follows from direct calculations with the desingularised reduced problem (80) and a reversal of time on S_0^{r}. □

We can use the information obtained above to describe the local dynamics near S_0^{c}. Specifically, we want to describe the transition map $\pi^{(\alpha)} : \Delta^{\text{in}} \to \Delta^{\text{out}}$ induced by the forward flow of system (76), where

$$\Delta^{\text{in}} := \left\{ (z, \theta, R^2) : |z - R| \leq \beta, \theta \in \mathbb{R}/\mathbb{Z} \right\},$$
$$\Delta^{\text{out}} := \{ (-R, \theta, a) : \theta \in \mathbb{R}/\mathbb{Z}, a \in [-a_0, a_0] \},$$

for small but fixed $R, \beta, a_0 > 0$. A *singular transition map* $\pi_0^{(\alpha)} : \Delta^{\text{in}} \to \Delta^{\text{out}}$ for $\varepsilon = 0$ can be constructed explicitly, by concatenating solutions to the layer and

reduced problems described above. If we choose $R > 0$ so that

$$R^2 < 2\mathcal{A}, \tag{81}$$

then $\Delta^{\mathrm{in}} \cap S_0^{\mathrm{a}}$ intersects the singular canard solution γ_c at the two points (R, θ_l) and (R, θ_r), where $\theta_l \in (1/4, 3/4]$ and $\theta_r \in [3/4, 0) \cup [0, 1/4)$ solve

$$\sin(2\pi\theta_{l,r}) = 1 - \frac{R^2}{\mathcal{A}},$$

see Fig. 21. Let $\mathcal{I} \subset \mathbb{R}/\mathbb{Z}$ denote the interior of the interval between θ_l and θ_r which is contained within the region bounded by γ_c. Different types of singular orbits can be constructed depending on whether or not one starts with an initial angle $\theta \in \mathcal{I}$, $\theta \in \{\theta_l, \theta_r\}$ or $\theta \notin \overline{\mathcal{I}}$.

Consider an initial condition $(z^*, \theta^*, R^2) \in \Delta^{\mathrm{in}}$ with $\theta^* \in \mathcal{I}$. This is mapped by the layer flow of system (77) to the point $(R, \theta^*, R^2) \in \Delta^{\mathrm{in}} \cap S_0^{\mathrm{a}}$. Since $\theta^* \in \mathcal{I}$, the point (R, θ^*, R^2) lies on an orbit of the desingularised reduced problem (80) which is contained within a level curve $H(z, \theta) = K \in (-\mathcal{A}/2, \mathcal{A}/2)$. In fact, one can show directly that

$$K = K(\theta^*) := \frac{\mathcal{A}}{2} \sin(2\pi\theta^*) + \frac{R^2}{2}. \tag{82}$$

Lemma 5.4 implies that the forward evolution of (R, θ^*, R^2) under the reduced problem (79) reaches S_0^{c} at a regular jump point $(0, \theta_e(\theta^*), 0)$, where $\theta_e(\theta^*) \in (3/4, 1) \cup [0, 1/4)$. In fact, the value of θ_e can be calculated explicitly using

$$H(0, \theta_e) = \frac{\mathcal{A}}{2} \sin(2\pi\theta_e) = K(\theta^*), \qquad \theta_e(\theta^*) \in (3/4, 1) \cup [0, 1/4). \tag{83}$$

Note that the containment condition on the right ensures that $\theta_e(\theta^*)$ is uniquely determined, i.e. that the function $\theta_e : \mathcal{I} \to (3/4, 1) \cup [0, 1/4)$ is well-defined. Since $(0, \theta_e(\theta^*), 0) \in S_0^{\mathrm{c}}$ is a (classical) regular jump point, we can connect to the layer flow of system (77) and map it to the point $(-R, \theta_e(\theta^*), 0) \in \Delta^{\mathrm{out}}$. Thus we have shown that for all initial conditions with (z^*, θ^*, R^2) with $\theta^* \in \mathcal{I}$, the singular transition map is

$$\pi_0^{(\alpha)}(z^*, \theta^*, R^2) = \left(-R, \theta_e(\theta^*), 0\right),$$

where $\theta_e(\theta^*)$ is uniquely determined by expressions (82) and (83).

Now consider an initial condition $(z^*, \theta^*, R^2) \in \Delta^{\mathrm{in}}$ with $\theta^* \notin \mathcal{I}$. In this case the point (z^*, θ^*, R^2) is mapped via the layer flow to $(R, \theta^*, R^2) \in S_0^{\mathrm{a}}$, but this point lies on an orbit of the reduced problem with $H(z, \theta) \geq \mathcal{A}/2$. Specifically, if $\theta^* \in \{\theta_l, \theta_r\}$, then $(R, \theta^*, R^2) \in \gamma_c$. The map $\pi_0^{(\alpha)}$ is multi-valued in this case, since every point on $\gamma_c \cap S_0^{\mathrm{r}}$ can be concatenated with an orbit segment of the layer problem. In particular,

$$\pi_0^{(\alpha)}(z^*, \theta_{l,r}, R^2) = \{(-R, \theta, \mathcal{A}(1 - \sin(2\pi\theta))) : \theta \in \mathbb{R}/\mathbb{Z}\}.$$

If $\theta^* \notin \overline{\mathcal{I}}$, then (R, θ^*, R^2) lies on a periodic orbit of the reduced problem which is bounded above γ_c. In this case solutions never leave S_0^a, and the map $\pi_0^{(\alpha)}$ is not defined.

The following result describes the perturbation of singular orbits with initial conditions in the sector defined by requiring that $\theta \in \mathcal{I}$.

Proposition 5.5 *Consider system* (76) *with* $\alpha \in \{1, 2\}$, *assume the constant R which defines* Δ^{in} *satisfies* (81), *and let*

$$\tilde{\Delta}^{\mathrm{in}} := \{(z, \theta, R^2) \in \Delta^{\mathrm{in}} : \theta \in \mathcal{J}_1\},$$

for a closed interval $\mathcal{J}_1 \subset \mathcal{I}$. *There exists an* $\varepsilon_0 > 0$ *such that for all* $\varepsilon \in (0, \varepsilon_0)$, *the restricted map* $\tilde{\pi}^{(\alpha)} := \pi^{(\alpha)}|_{\tilde{\Delta}^{\mathrm{in}}} : \tilde{\Delta}^{\mathrm{in}} \to \Delta^{\mathrm{out}}$ *is well-defined and given by*

$$\tilde{\pi}^{(\alpha)}(z, \theta, R^2) = \left(-R, \tilde{\pi}_\theta^{(\alpha)}(z, \theta, \varepsilon), \tilde{\pi}_a^{(\alpha)}(z, \theta, \varepsilon)\right),$$

where

$$\tilde{\pi}_\theta^{(\alpha)}(z, \theta, \varepsilon) = \theta_e(\theta) + \mathcal{O}(\varepsilon^\alpha \ln \varepsilon), \qquad \tilde{\pi}_a^{(\alpha)}(z, \theta, \varepsilon) = \mathcal{O}(\varepsilon^{2\alpha/3}),$$

$\tilde{\pi}^{(\alpha)} \to \pi_0^{(\alpha)}|_{\tilde{\Delta}^{\mathrm{in}}}$ *as* $\varepsilon \to 0$, *and* $\theta_e(\theta)$ *is uniquely determined by equations* (82) *and* (83). *Explicitly,*

$$\theta_e(\theta) = \frac{1}{2\pi} \arcsin\left(\sin(2\pi\theta) + \frac{R^2}{\mathcal{A}}\right), \qquad \theta \in (3/4, 1) \cup [0, 1/4). \qquad (84)$$

Proof Consider the forward evolution of initial conditions $(z^*, \theta^*, R^2) \in \tilde{\Delta}^{\mathrm{in}}$ under system (76). By Fenichel theory, such solutions are initially attracted at an exponential rate to the Fenichel slow manifold S_ε^a which perturbs from S_0^a, after which they remain $\mathcal{O}(\varepsilon^\alpha)$-close to solutions of the reduced vector field induced by system (78) until reaching a neighbourhood of the regular jump point $(-R, \theta_e(\theta^*), 0)$. The local dynamics near $(-R, \theta_e(\theta^*), 0)$ are governed by the system

$$\begin{aligned}
z' &= a - z^2, \\
\theta' &= \varepsilon^\alpha, \\
a' &= \varepsilon^\alpha \left(-2\pi \mathcal{A} \cos(2\pi\theta_e(\theta^*)) + \mathcal{O}((\theta - \theta_e(\theta^*))^2, \varepsilon^{3-\alpha})\right),
\end{aligned}$$

where $\cos(2\pi\theta_e(\theta^*)) > 0$ since $\theta_e(\theta^*) \in (3/4, 1) \cup [0, 1/4)$. Direct calculations verify that this is a stationary two time-scale problem with a regular fold curve passing through the point $(0, \theta^*, 0)$. This observation allows for a derivation of the desired result using a slight adaptation of the well-known result in Szmolyan and Wechselberger (2004). □

Proposition 5.5 describes regular jump-type dynamics for solutions with initial conditions in $\widetilde{\Delta}^{\text{in}}$, which can be chosen arbitrarily close to $\Delta^{\text{in}}|_{\theta \in \mathcal{I}}$ by decreasing ε_0 if necessary. It is worthy to note that the leading-order approximation for the 'jump angle' $\tilde{\pi}_\theta^{(\alpha)}(z, \theta, \varepsilon) \sim \theta_e(\theta)$ can be calculated explicitly as a function of the initial angle using (84). It is also worthy to note that for $\alpha \in \{1, 2\}$ we have $\tilde{\pi}_a^{(\alpha)}(z, \theta, \varepsilon) = \mathcal{O}(\varepsilon^{2\alpha/3})$, in contrast to the $\mathcal{O}(\varepsilon^2)$ estimates for the parameter drift in Theorem 3.2. This is a consequence of the fact that the 'parameter drift' in system (76) in a occurs on the intermediate, rotational time-scale. This is not the case for systems satisfying Assumptions 1–2.

We may also consider the case in which initial conditions are chosen 'higher up', in an annular section

$$\Sigma^{\text{in}} := \left\{ (z, \theta, \rho^2) : |z - R| \leq \beta, \theta \in \mathbb{R}/\mathbb{Z} \right\}$$

where the constant $\rho > 0$ satisfies

$$\rho^2 > 2\mathcal{A} > R^2, \tag{85}$$

c.f. equation (81). A subset of solutions with initial conditions in Σ^{in} are described by the following result. We formulate it in terms of the transition map $\Pi^{(\alpha)} : \Sigma^{\text{in}} \to \Delta^{\text{out}}$.

Proposition 5.6 *Consider system* (76) *with* $\alpha \in \{1, 2\}$, *assume the constant* ρ *which defines* Σ^{in} *satisfies* (85), *and let*

$$\widetilde{\Sigma}^{\text{in}} := \{(z, \theta, \rho^2) \in \Sigma^{\text{in}} : \theta \in \mathcal{J}_2\},$$

where $\mathcal{J}_2 := \{\theta \in \mathbb{R}/\mathbb{Z} : T(\theta, \varepsilon) \in \mathcal{J}_1\}$, *where* $\mathcal{J}_1 \subset \mathcal{I}$ *is the interval from Proposition* 5.5, *and* $T(\theta, \varepsilon)$ *is the minimal positive solution of the transcendental equation*

$$\rho^2 + \mathcal{A}\sin(2\pi\theta) - R^2 = \varepsilon^3 \nu T + \mathcal{A}\sin(2\pi(\theta + \varepsilon^\alpha T)). \tag{86}$$

Then there exists an $\varepsilon_0 > 0$ *such that for all* $\varepsilon \in (0, \varepsilon_0)$, *the restricted transition map* $\widetilde{\Pi}^{(\alpha)} := \Pi^{(\alpha)}|_{\widetilde{\Sigma}^{\text{in}}} : \widetilde{\Sigma}^{\text{in}} \to \Delta^{\text{out}}$ *is given by*

$$\widetilde{\Pi}^{(\alpha)}(z, \theta, \rho^2) = \left(-R, \theta_e(\theta + \varepsilon^\alpha T(\theta, \varepsilon) \mod 1) + \mathcal{O}(\varepsilon^\alpha \ln \varepsilon), \mathcal{O}(\varepsilon^{2\alpha/3})\right). \tag{87}$$

Proof The idea is to consider $\widetilde{\Pi}^{(\alpha)}$ as a composition $\widetilde{\Pi}^{(\alpha)} = \tilde{\pi}^{(\alpha)} \circ \hat{\pi}^{(\alpha)}$, where $\tilde{\pi}^{(\alpha)}$ is the local transition map described in Proposition 5.5 above and $\hat{\pi}^{(\alpha)} : \widetilde{\Sigma}^{\text{in}} \to \widetilde{\Delta}^{\text{in}}$. The (θ', a') system decouples from system (76), and can be solved directly. We obtain

$$\theta(t) = \theta^* + \varepsilon^\alpha t \mod 1, \quad a(t) = \rho^2 + \mathcal{A}\left(\sin(2\pi\theta^*) - \sin(2\pi(\theta^* + \varepsilon^\alpha t))\right) - \varepsilon^3 \nu t,$$

for all $t \in \mathbb{R}$, where $\theta^* = \theta(0)$. The transition time $T = T(\theta^*, \varepsilon) > 0$ is determined implicitly as the first positive solution of $a(T) = R^2$, i.e. of the transcendental equation (86). The estimate for $z(T)$ follows from Fenichel theory, which implies that the

attracting slow manifold S_ε^a which perturbs from S_0^a can be written as a graph $z = \varphi_\varepsilon(\theta, a) = \sqrt{a} + \mathcal{O}(\varepsilon^\alpha)$ in this regime (normal hyperbolicity is guaranteed by the fact that $a(t) \geq R^2 > 0$ for all $t \in [0, T(\theta, \varepsilon)]$).

The preceding arguments imply that

$$\hat{\pi}^{(\alpha)}(z, \theta, \rho^2) = \left(\varphi_\varepsilon(\theta(T), R^2) + \mathcal{O}(e^{-\kappa/\varepsilon^\alpha}), \theta(T), R^2 \right).$$

Since the domain of $\hat{\pi}^{(\alpha)}$ is $\widetilde{\Sigma}^{\text{in}}$, we have that $\theta(T) = \theta(T(\theta^*, \varepsilon)) \in \mathcal{J}_1$, where $\mathcal{J}_1 \subset \mathcal{I}$ is the interval from Proposition 5.5. Thus the composition $\widetilde{\Pi}^{(\alpha)} = \tilde{\pi}^{(\alpha)} \circ \hat{\pi}^{(\alpha)}$ is well-defined and, using Proposition 5.5, given by (87). □

Remark 5.7 Due to the transcendental nature of equation (86), a closed-form expression for the function $T = T(\theta, \varepsilon)$ can only be given in terms of special functions. Nevertheless, for any given θ, $T(\theta, \varepsilon)$ be calculated to arbitrary precision with standard numerical methods (e.g. Newton or bisection methods).

Propositions 5.5 and 5.6 describe solutions of 'regular jump type', but they do not explain what happens to solutions with initial conditions in $\Delta^{\text{in}} \backslash \mathcal{J}_1$. This corresponds to a set of initial conditions that is 'small' in these sense that the diameter of the interval $[0, 1) \setminus \overline{\mathcal{I}}$ tends to zero as $R \to 0$, but for fixed $R > 0$ it is still $\mathcal{O}(1)$ with respect to $\varepsilon \to 0$. Moreover, this set contains solutions close to the singular canard γ_c, which are expected to play an important role in determining the qualitative dynamics (Szmolyan and Wechselberger 2001). A detailed description of the dynamics in this case is left for future work.

Remark 5.8 For $\alpha \geq 3$, the dynamics can be analysed and understood entirely with established theory for two time-scale systems. The case $\alpha = 3$ is non-trivial, and features a degenerate bifurcation in the desingularised reduced problem as the folded saddle p_s and neutral folded centre p_c collide and annihilate at a particular value of the forcing $\mathcal{A} = \mathcal{A}_c > 0$. For $\mathcal{A} < \mathcal{A}_c$, the folded cycle S_0^c is regular, i.e. there are no folded singularities. For $\alpha \geq 4$, S_0^c is always regular. A direct application of the results in Szmolyan and Wechselberger (2004) in this case yields an explicit expression for the transition map:

$$\pi^{(\alpha)}\left(z, \theta, R^2\right) = \left(-R, \theta + \mathcal{O}(\varepsilon^\alpha \ln \varepsilon), \mathcal{O}(\varepsilon^{2\alpha/3}) \right), \qquad \alpha \geq 4.$$

Remark 5.9 The local geometry and dynamics near the fold lines/circles in the forced van der Pol system considered in e.g. Burke et al. (2016), Guckenheimer et al. (2003), Haiduc (2008) are characterised by alternation of folded saddles and folded focus singularities, in contrast to the alternation of folded saddle and folded centre singularities in Fig. 21. Nevertheless, there are many similarities, including the fact that the image of S_ε^a on Δ^{out} is non-circular as $\varepsilon \to 0$, due to the folded saddles. This feature, which is not present for the systems described by Theorem 3.2, is utilised in the construction of horseshoes in the forced van der Pol system (Haiduc 2008).

6 Summary and Outlook

GSPT is an established and powerful tool for the analysis of stationary fast–slow systems, particularly when combined with the blow-up method. The corresponding theory for oscillatory fast–slow systems which possess a limit cycle manifold instead of (or in addition to) a critical manifold is less developed, despite the fact that oscillatory systems are common in applications. One reason for this appears to be that the theory for stationary fast–slow systems, notably Fenichel–Tikhonov theory and the blow-up method, depend on quasi-equilibrium properties possessed by stationary but not oscillatory fast–slow systems. The main purpose of this article has been to show that both Fenichel–Tikhonov theory and the blow-up method can be applied to study the dynamics of a class of multiple time-scale systems with three or more time-scales, as long as the angular/rotational dynamics are sufficiently slow relative to the radial dynamics. The class of systems considered, namely those in general form (4), contains a 'semi-oscillatory' class of systems that are oscillatory with respect to the partial singular limit $\varepsilon_1 > 0$, $\varepsilon_2 \to 0$, but stationary with respect to the double singular limit $(\varepsilon_1, \varepsilon_2) \to (0, 0)$. Although our approach is not applicable in the purely oscillatory case, our analysis showed that Fenichel–Tikhonov theory and the blow-up method can be applied directly in the semi-oscillatory case.

More concretely, we focused on the dynamics near a (three time-scale) global singularity corresponding to a kind of folded cycle bifurcation in the layer problem obtained in the partial singular limit. In order to do so we derived a prototypical system for the three time-scale global singularity near the non-hyperbolic cycle S_0^c, recall Proposition 2.5, and studied the transition map induced by the flow. Our main result is Theorem 3.2, which is stated for system (22), which provides a rigorous characterisation of the asymptotic and strong contraction properties of the flow near S_0^c. The asymptotics $h_y^{(\alpha)}(\theta, \varepsilon) = \mathcal{O}(\varepsilon^2)$ and the strong contraction property are the same as for the stationary regular fold point studied in Krupa and Szmolyan (2001a), Mishchenko et al. (1975), Szmolyan and Wechselberger (2004), not only in the semi-oscillatory cases $\alpha \in \{1, 2\}$ considered herein in detail, but for all $\alpha \in \mathbb{N}_+$. The semi-oscillatory cases $\alpha \in \{1, 2\}$ are distinguished from the cases $\alpha \geq 3$ by the fact that the leading-order estimates for $h_y^{(\alpha)}(\theta, \varepsilon)$ are, in general, non-constant functions of θ. We derived an explicit expression for the leading-order estimate in terms of the functions $a(\theta)$, $b(\theta)$ and $c(\theta)$ appearing in system (22) when $\alpha = 2$ in particular. In addition, we provided detailed estimates for the exit angle, recall (25), as well as estimates for the total number of rotations about the y-axis as solutions traverse the region between Δ^{in} and Δ^{out}, recall Corollary 3.3. Theorem 3.2 is proved using the blow-up method in Sect. 4, thereby demonstrating the applicability of geometric blow-up techniques to study global singularities of limit cycle type in suitable classes of three time-scale systems. We focused on a detailed presentation of the proof in the semi-oscillatory cases $\alpha \in \{1, 2\}$. The proof for $\alpha \geq 3$ can be obtained either via straightforward adaptations of the proof for $\alpha = 2$, or via straightforward adaptations of the proof of the established results for two time-scale systems in Krupa and Szmolyan (2001a), Mishchenko et al. (1975), Szmolyan and Wechselberger (2004). The primary complication in cases $\alpha \in \{1, 2\}$ stems from the fact that the dynamics remain 'global' in θ after blow-up

near S_0^c. Consequently, one has to consider a blow-up of the entire cycle (as opposed to a local blow-up about a point on S_0^c). We also demonstrated the applicability of our results by using them to derive detailed geometric and asymptotic information about the passage through a folded cycle singularity in a class of periodically forced Liénard equations; recall Sect. 5.1 and in particular Theorem 5.2. Finally, in Sect. 5.2, we considered a toy model for the study of tipping phenomena. Due to the periodic forcing in the fast equation, this model violates both of our primary Assumptions 1–2. The partial geometric analysis presented herein provides reason to argue that cases of this kind can for the most part be analysed using classical two time-scale theory.

In summary, the current manuscript provides a precedent for the effectiveness of stationary methods including Fenichel–Tikhonov theory and the blow-up method in semi-oscillatory multiple time-scale systems with at least three time-scales. There are many interesting directions which one might take from here. Our analysis of the toy model for tipping considered in Sect. 5.2 is incomplete and motivates the analysis of a more general class of systems with regular folded cycle manifolds which violate our main Assumptions 1–2. One might also consider the applicability of the methods developed herein for other global cycle singularities for which there is no direct and lower-dimensional analogue in stationary fast–slow systems, e.g. near a non-hyperbolic flip/period-doubling-type cycle in three time-scale systems of form (4). We also expect the detailed estimates on the local dynamics near regular folded cycles in Theorem 3.2 to play an important role in the description of multi-scale oscillations which involve regular folded cycles as a key ingredient. In Szmolyan and Wechsel-berger (2004), the authors derive a detailed characterisation of the local dynamics near a regular fold curve using geometric blow-up and combine it with Fenichel theory in order to derive the form of the Poincaré map associated to prototypical 1-fast 2-slow systems with an S-shaped critical manifold. These results were used to prove the existence of an invariant torus for a certain parameter regime in the forced van der Pol equation, which contains an attracting relaxation oscillation if a particular circle map induced on the angular variable is contracting. We conjecture that similar constructions could be applied to the three time-scale semi-oscillatory systems considered herein, under suitable assumptions on the global geometry. The details of these and other related problems are left for future work.

Data Availability No datasets were generated or analysed during the current study.

Declarations

Conflict of interest The authors have no competing interests.

References

Anosova, O.D.: On invariant manifolds in singularly perturbed systems. J. Dyn. Control Syst. **5**, 501–507 (1999)

Anosova, O.D.: Invariant manifolds in singularly perturbed systems. Trudy Matematicheskogo Instituta Imeni VA Steklova **236**, 27–32 (2002)

Baesens, C.: Slow sweep through a period-doubling cascade: delayed bifurcations and renormalisation. Phys. D **53**, 319–375 (1991)

Baesens, C.: Gevrey series and dynamic bifurcations for analytic slow–fast mappings. Nonlinearity **8**, 179 (1995)

Baspinar, E., Avitabile, D., Desroches, M.: Canonical models for torus canards in elliptic bursters. Chaos Interdiscip. J. Nonlinear Sci. **31**, 063129 (2021)

Benes, G.N., Barry, A.M., Kaper, T.J., Kramer, M.A., Burke, J.: An elementary model of torus canards. Chaos Interdiscip. J. Nonlinear Sci. **21**, 023131 (2011)

Bertram, R., Butte, M.J., Kiemel, T., Sherman, A.: Topological and phenomenological classification of bursting oscillations. Bull. Math. Biol. **57**, 413–439 (1995)

Burke, J., Desroches, M., Granados, A., Kaper, T.J., Krupa, M., Vo, T.: From canards of folded singularities to torus canards in a forced van der Pol equation. J. Nonlinear Sci. **26**, 405–451 (2016)

Cardin, P., da Silva, P., Teixeira, M.: Three time scale singular perturbation problems and nonsmooth dynamical systems. Q. Appl. Math. **72**, 673–687 (2014)

Cardin, P.T., Teixeira, M.A.: Fenichel theory for multiple time scale singular perturbation problems. SIAM J. Appl. Dyn. Syst. **16**, 1425–1452 (2017)

Cartwright, M.L., Littlewood, J.E.: On non-linear differential equations of the second order II. Ann. Math. pp. 472–492 (1947)

De Maesschalck, P., Kutafina, E., Popović, N.: Three time-scales in an extended Bonhoeffer–van der Pol oscillator. J. Dyn. Differ. Equ. **26**, 955–987 (2014)

Desroches, M., Burke, J., Kaper, T.J., Kramer, M.A.: Canards of mixed type in a neural burster. Phys. Rev. E **85**, 021920 (2012)

Desroches, M., Kirk, V.: Spike-adding in a canonical three-time-scale model: superslow explosion and folded-saddle canards. SIAM J. Appl. Dyn. Syst. **17**, 1989–2017 (2018)

Dumortier, F., Roussarie, R.: Canard cycles and center manifolds, no. 577 in Memoirs of the American Mathematical Society, American Mathematical Society (1996)

Ermentrout, B., Terman, D.H.: Mathematical Foundations of Neuroscience, vol. 35. Springer, Berlin (2010)

Fenichel, N.: Geometric singular perturbation theory for ordinary differential equations. J. Differ. Equ. **31**, 53–98 (1979)

Fruchard, A., Schäfke, R.: A survey of some results on overstability and bifurcation delay. Discrete Contin. Dyn. Syst. S **2**, 931 (2009)

Grasman, J.: Asymptotic Methods for Relaxation Oscillations and Applications. Springer, Berlin (1987)

Guckenheimer, J.: Towards a global theory of singularly perturbed dynamical systems. In: Nonlinear Dynamical Systems and Chaos. Springer, pp. 213–225 (1996)

Guckenheimer, J., Hoffman, K., Weckesser, W.: The forced forced van der Pol equation i: the slow flow and its bifurcations. SIAM J. Appl. Dyn. Syst. **2**, 1–35 (2003)

Guckenheimer, J., Tien, J.H., Willms, A.R.: Bifurcations in the fast dynamics of neurons: implications for bursting. In: Bursting: The Genesis of Rhythm in the Nervous System. World Scientific, pp. 89–122 (2005)

Haiduc, R.: Horseshoes in the forced van der pol system. Nonlinearity **22**, 213 (2008)

Il'yashenko, Y.: Embedding theorems for local maps, slow–fast systems and bifurcation from Morse-Smale to Smale-Williams. Transl. Am. Math. Soc. Ser. **2**(180), 127–140 (1997)

Il'yashenko, Y.S., Yakovenko, S.Y.: Finitely-smooth normal forms of local families of diffeomorphisms and vector fields. Russ. Math. Surv. **46**, 1 (1991)

Jalics, J., Krupa, M., Rotstein, H.G.: Mixed-mode oscillations in a three time-scale system of ODEs motivated by a neuronal model. Dyn. Syst. **25**, 445–482 (2010)

Jardón-Kojakhmetov, H., Kuehn, C.: A survey on the blow-up method for fast–slow systems. Contemp. Math. **775**, 115–160 (2021)

Jelbart, S., Kuehn, C.: Discrete geometric singular perturbation theory. Discrete Contin. Dyn. Syst. **43**, 57–120 (2023)

Jelbart, S., Kuehn, C.: Extending discrete geometric singular perturbation theory to non-hyperbolic points, arXiv preprint arXiv:2308.06141 (2023)

Jones, C.K.: Geometric singular perturbation theory. In: Dynamical systems, vol. 1609 of Lecture Notes in Mathematics. Springer, pp. 44–118 (1995)

Kaklamanos, P., Popović, N.: Complex oscillatory dynamics in a three-timescale El Niño southern oscillation model, arXiv preprint arXiv:2207.03230 (2022)

Kaklamanos, P., Popović, N., Kristiansen, K.U.: Bifurcations of mixed-mode oscillations in three-timescale systems: an extended prototypical example. Chaos Interdiscip. J. Nonlinear Sci. **32**, 013108 (2022)

Kaklamanos, P., Popović, N., Kristiansen, K.U.: Geometric singular perturbation analysis of the multiple-timescale Hodgkin–Huxley equations. SIAM J. Appl. Dyn. Syst. **22**, 1552–1589 (2023)

Kirillov, S.Y., Nekorkin, V.: Dynamic saddle-node bifurcation of the limit cycles in the model of neuronal excitability. Radiophys. Quantum Electron. **57**, 837–847 (2015)

Kosiuk, I., Szmolyan, P.: Geometric singular perturbation analysis of an Autocatalator model. Discrete Contin. Dyn. Syst. **2**, 783–806 (2009)

Kosiuk, I., Szmolyan, P.: Scaling in singular perturbation problems: blowing up a relaxation oscillator. SIAM J. Appl. Dyn. Syst. **10**, 1307–1343 (2011)

Kosiuk, I., Szmolyan, P.: Geometric analysis of the Goldbeter minimal model for the embryonic cell cycle. J. Math. Biol. **72**, 1337–1368 (2016)

Kramer, M.A., Traub, R.D., Kopell, N.J.: New dynamics in cerebellar purkinje cells: torus canards. Phys. Rev. Lett. **101**, 068103 (2008)

Kristiansen, K.U., Szmolyan, P.: Relaxation oscillations in substrate-depletion oscillators close to the non-smooth limit. Nonlinearity **34**, 1030 (2021)

Kruff, N., Walcher, S.: Coordinate–independent singular perturbation reduction for systems with three time scales. Math. Biosci. Eng. **16**, 5062–5091 (2019)

Krupa, M., Popović, N., Kopell, N.: Mixed-mode oscillations in three time-scale systems: a prototypical example. SIAM J. Appl. Dyn. Syst. **7**, 361–420 (2008)

Krupa, M., Szmolyan, P.: Extending geometric singular perturbation theory to nonhyperbolic points–fold and canard points in two dimensions. SIAM J. Math. Anal. **33**, 286–314 (2001)

Krupa, M., Szmolyan, P.: Extending slow manifolds near transcritical and pitchfork singularities. Nonlinearity **14**, 1473 (2001)

Krupa, M., Szmolyan, P.: Relaxation oscillation and canard explosion. J. Differ. Equ. **174**, 312–368 (2001)

Kuehn, C.: Multiple Time Scale Dynamics, vol. 191 of Applied Mathematical Sciences. Springer (2015)

Kuehn, C., Berglund, N., Bick, C., Engel, M., Hurth, T., Iuorio, A., Soresina, C.: A general view on double limits in differential equations. Phys. D **431**, 133105 (2022)

Kuehn, C., Szmolyan, P.: Multiscale geometry of the Olsen model and non-classical relaxation oscillations. J. Nonlinear Sci. **25**, 583–629 (2015)

Kuznetsov, Y.A.: Elements of Applied Bifurcation Theory, vol. 112 of Applied Mathematical Sciences. Springer (2013)

Letson, B., Rubin, J.E., Vo, T.: Analysis of interacting local oscillation mechanisms in three-timescale systems. SIAM J. Appl. Math. **77**, 1020–1046 (2017)

Lizarraga, I., Rink, B., Wechselberger, M.: Multiple timescales and the parametrisation method in geometric singular perturbation theory. Nonlinearity **34**, 4163 (2021)

Mishchenko, E., Rozov, N.K.H.: Differential equations with small parameters and relaxation oscillations, Nauka, Moscow (transl.: Plenum Press, New York, 1980) (1975)

Nan, P., Wang, Y., Kirk, V., Rubin, J.E.: Understanding and distinguishing three-time-scale oscillations: case study in a coupled Morris–Lecar system. SIAM J. Appl. Dyn. Syst. **14**, 1518–1557 (2015)

Nipp, K., Stoffer, D.: Invariant manifolds in discrete and continuous dynamical systems, vol. 21 of EMS Tracts in Mathematics, European Mathematical Society (2013)

Nipp, K., Stoffer, D., Szmolyan, P.: Graph transform and blow-up in singular perturbations. In: AIP Conference Proceedings, American Institute of Physics, pp. 861–868 (2009)

Pontryagin, L.S., Rodygin, L.V.: Approximate solution of a system of ordinary differential equations involving a small parameter in the derivatives. In: Doklady Akademii Nauk, vol. 131(2). Russian Academy of Sciences, pp. 255–258 (1960)

Rinzel, J.: A formal classification of bursting mechanisms in excitable systems. In: Mathematical Topics in Population Biology, Morphogenesis and Neurosciences, pp. 267–281. Springer (1987)

Roberts, K.-L., Rubin, J.E., Wechselberger, M.: Averaging, folded singularities, and torus canards: explaining transitions between bursting and spiking in a coupled neuron model. SIAM J. Appl. Dyn. Syst. **14**, 1808–1844 (2015)

Szmolyan, P., Wechselberger, M.: Canards in $\mathbb{R}^3$. J. Differ. Equ. **177**, 419–453 (2001)

Szmolyan, P., Wechselberger, M.: Relaxation oscillations in $\mathbb{R}^3$. J. Differ. Equ. **200**, 69–104 (2004)

Tikhonov, A.N.: Systems of differential equations containing small parameters in the derivatives. Matematicheskii Sbornik **73**, 575–586 (1952)

van der Pol, B.: A theory of the amplitude of free and forced triode vibrations. Radio Rev. **1**, 701–710 (1920)

van der Pol, B.: On "relaxation-oscillations". Lon. Edinb. Dublin Philos. Mag. J. Sci. **2**, 978–992 (1926)

Vo, T.: Generic torus canards. Phys. D **356**, 37–64 (2017)

Wechselberger, M.: Geometric singular perturbation theory beyond the standard form. In: Frontiers in Applied Dynamical Systems: Reviews and Tutorials. Springer (2020)

Wiggins, S.: Normally Hyperbolic Invariant Manifolds in Dynamical Systems, vol. 105. Springer, Berlin (1994)

Zhu, J., Kuske, R., Erneux, T.: Tipping points near a delayed saddle node bifurcation with periodic forcing. SIAM J. Appl. Dyn. Syst. **14**, 2030–2068 (2015)